See Pocket 5 for end

WM DOCKET CONTROL CENTER

~~83 DEC 34~~ A10:43
1/3/84

Department of Energy
Richland Operations Office
P.O. Box 550
Richland, Washington 99352

~~WM Record File~~ 101.2
WM Project 10
Docket No.
PDR ✓
LPDR ✓
Distribution:
RWright
(Return to WM, 623-SS) C2

DEC 23 1983

Dr. Robert J. Wright
Senior Technical Advisor
High Level Waste Technical
Development Branch
U. S. Nuclear Regulatory Commission
Washington, DC 20555

Dear Dr. Wright:

NRC REQUEST FOR CASE HISTORIES

As you requested during the BWIP/NRC Underground Test Workshop held on November 29-December 2, 1983, at Richland, enclosed is one copy each of six case histories of mining through rock showing disking in exploratory boreholes.

If you have any questions covering this material, please contact J. E. Mecca (FTS 444-5038) or D. J. Squires (FTS 444-7240) of my staff.

Very truly yours,

James E. Mecca

for O. L. Olson, Project Manager
Basalt Waste Isolation Project Office

BWI:DJS

Enclosures

cc, w/o encl: M. W. Frei, DOE-HQ

638

see ltr to Wright
from Olson
12/23/83

CASE HISTORIES INVOLVING CORE DISKING AND OPENING INSTABILITY (*)

1. Carlisle, S (1983) personal communication
Boreholes drilled horizontally from the main drive, in order to locate the position of the ore vein, encountered disking. There was a close correlation between the location of disking and the occurrence of spalling of cross cuts eventually excavated.

Scott Carlisle
Mining Engineer
Hecla Mining Co.
Lucky Friday Mine
Mullan, Idaho 98873

2. Saito, T., Tsukada, K., Inami, E., Inoma, H. and Ito, Y. (1983), "Study on Rockburst at the Face of a Deep Tunnel, The Kan-Etsu Tunnel in Japan Being an Example", Proc. 5th Congr. Int. Soc. Rock Mech., Melbourne, Australia.

3. Bai, S., Zhu, W. and Wang, K. (1983), "Some Rock Mechanics Problems Related to a Large Underground Power Station in a Region With High Rock Stress", Proc. 5th Congr. Int. Soc. Rock Mech., Melbourne, Australia.

4. Aggson, J. R. (1978), "Coal Mine Floor Heave in the Beckley Coalbed, An Analysis", U.S. Bureau of Mines Report of Investigations 8274.

5. Turchaninov, I.A., Iofis, M. A. and Kasparyan, E. V. (1979), Principles of Rock Mechanics, first published in Russian by Nedra Press, Leningrad; translation edited by W. A. Hustrulid, translated edition published by Terraspace, Inc., Rockville, MD. (**)

6. Beus, M. J. and Chan, S. M. (1980), "Shaft Design in the Coeur d'Alene Mining District, Idaho - Results of In Situ Stress and Physical Property Measurements", U.S. Bureau of Mines Report of Investigations 8435.

(*) The above references represent case histories where the core disking phenomenon was observed in the same vicinity that spalling or related stress - induced instabilities were encountered in full scale openings (shafts, tunnels or mine rooms).

(**) While BWIP does not currently have the complete reference No. 5, a description of its contents has been prepared and included herein. The description was prepared by BWIP contractor Lachel Hansen and Associates Inc. and appears in an internal report which has not been formally reviewed by BWIP.

ISRM 5th Congress on Rock Mechanics
Melbourne 1983

STUDY ON ROCKBURSTS AT THE FACE OF A DEEP TUNNEL, THE KAN-ETSU TUNNEL IN JAPAN BEING AN EXAMPLE

Etude de la chute de roches sur le front de taille d'un tunnel profond – cas du tunnel de Kan-Etsu, Japon –

Untersuchung über Gebirgsschläge and der Ortsbrust eines tiefliegenden Tunnels, dargestellt am Beispiel des Kan-Etsu Tunnels in Japan

T. Saito
K. Tsukada
Dept. of Mineral Science and Technology, Kyoto University, Kyoto, Japan

E. Inami
H. Inoma
Y. Ito
Japan Highway Public Corporation, Tokyo, Japan

SYNOPSIS

In the Kan-Etsu Tunnel, which is one of the deepest expressway tunnels in Japan, rockbursts occurred mostly at the tunnel face. In order to prevent them, the authors carried out several investigations, including the measurements of initial rock stresses and the change of rock stress ahead of the advancing face. It was found that the areas of the core disking, observed at the coreboring before the excavation, fairly corresponded to those of rockbursts. Through these investigations and observations, the mechanism of rockbursts at the tunnel face is discussed.

RESUME

Dans le tunnel Kan-Etsu, l'un des tunnels d'autoroute les plus profonds, des chutes de roches ont eu lieu en particulier au front de la taille. Afin d'éviter ce phénomène, certaines investigations telles que mesures de contrainte initiale de roches et mesures de changement de contrainte de roches en avant du front, ont été faites. Il s'est avéré que les zones de disquage de carotte observées lors due carottage réalisé avant l'excavation correspondent bien a celles des chutes de roches. En se basant sur ces investigations et observations, on examine le mécanisme de chute des roches sur le front de taille.

ZUSAMMENFASSUNG

Im Kan-Etsu Tunnel, der einer der tiefsten Autobahntunnel in Japan ist, traten Gebirgsschläge zumeist an der Tunnelortsbrust auf. Um dieses Phänomen zu verhindern, wurden mehrere Untersuchungen durchgeführt, einschließlich Messung der geologischen Spannungen und der Spannungsänderungen vor der Ortsbrust. Hierbei wurde festgestellt, daß Bereiche, in denen der Bohrkern diskenförmig zerbrach, ziemlich genau denen der Gebirgsschläge entsprechen. Anhand dieser Untersuchungen und Beobachtungen wird der Mechanismus von Gebirgsschlägen an der Tunnelfront erörtert.

1. Introduction

Kan-Etsu Tunnel is 10,885m-long expressway tunnel, under the heavy overburden over 1000m in height, located at the place where Kan-Etsu Expressway passes throgh Tanigawa-Range which is one of the steepest mountain ranges in Japan. The construction of this tunnel started in summer, 1977. The excavation of the sub-tunnel ($20m^2$ section) and the main tunnel ($86m^2$ section), which are parallel each other at a distance of 30m, were finished in Feb. 1981 and in Feb. 1982, respectively.

Under Tanigawa-Range there are three railway tunnels in operation already (Dai-shimizu Tunnel, New Shimizu Tunnel and Shimizu Tunnel). In the excavation of every tunnel, they experienced the occurrence of rocknoises and rockbursts. Therefore it had been expected that rockbursts would occur at the excavation of Kan-Etsu Tunnel. As expected, over the area of 1100m length rockbursts occurred intermittently. Most of them were not so large in fracture zones, the same as a spalling. However they occurred mostly at the tunnel face rather than at the side wall, which is different from past experiences, and were very serious for the excavation works. Fortunately they caused no severe accident but interrupted construction work frequently.

In order to prevent the rockbursts and to secure the safty working, the authors carried out some investigations in the field. Through these results, the mechanism of rockbursts and the countermeasures against them are discussed from the point of view of rock mechanics.

2. Features of Rockbursts in Kan-Etsu Tunnel

The rock masses surrounding Kan-Etsu Tunnel are mainly consist of quartz diorite and hornfels (See in Fig.3), and include no apparent faults. In the region of quartz diorite, the part containing the regular joints and the relatively massive part appear alternately at the intervals varied from about 20m to 130m, while hornfels contains many fine joints. The average uniaxial compressive strength of quartz diorite is 230MPa

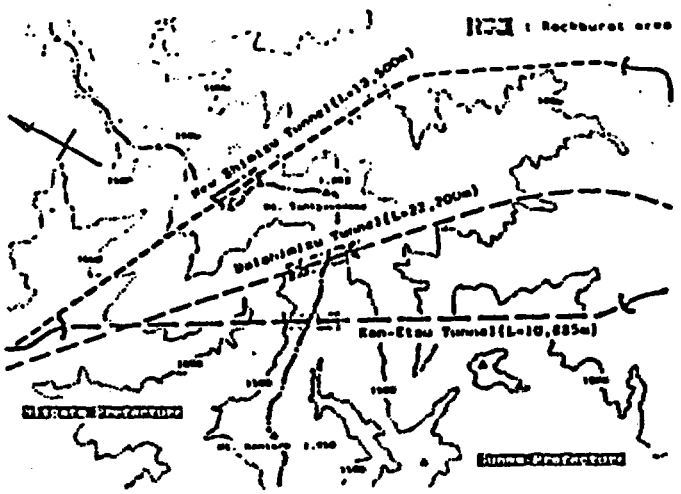

Fig. 1 Rockburst area of three tunnels under the Tanigawa-Range

and that of hornfels is 310MPa. Kan-Etsu Tunnel had been excavated at the rate of about 100m per month by the full face method. The largest rockburst in this tunnel occurred in quartz diorite at a distance of 4,327m from the north entrance. Thereafter the intermittent occurrence of rockbursts had been observed until the bed rock changed into hornfels completely.

Fig.1 shows the region in which rockbursts occurred frequently in the three neighboring tunnels. The fact that every region lies under the same ridge is interested, suggesting that the area under this ridge has the potentiality causing the rockbursts. Rockbursts in Kan-Etsu Tunnel occurred mostly at the face as shown in Fig.2 which illustrates the fracture zone of the largest rockburst and can be classified into some degrees of fractures, such as bursts o spallings of rock, cracks on the face withou a spalling and only rocknoises.

Table 1 Initial rock stresses at the three points along the Kan-Etsu Tunnel
σ_1, σ_2, σ_3: principal stress
σ_v: vertical stress
σ_H: max. horizontal stress

	No.1 point	No.2 point	No.3 poin
rock	diorite	diorite	diorite & hornfel
overburden	260 m	960 m	920 m
σ_1	14.6 MPa	22.9 MPa	31.6 MPa
σ_2	6.3	10.7	22.2
σ_3	5.9	7.5	6.0
σ_v	6.2 MPa	16.4 MPa	31.3 MPa
σ_H	14.6	17.1	22.5

Some other features of rockbursts in Kan-Etsu Tunnel can be pointed out as follows.
(1) It is assumed that the occurrence is gently related with joints. The rockbursts are apt to occur in the uniform and dry rock masses which have several closed joint sets with the regular orientation, while not in the rock masses which have many fine joints, or in the massive rock which has few joints.
(2) It seems that the workings, such as blasting, chopping and drilling, provoke rockbursts at the face.
(3) The sizes of broken rock pieces are various, but the shapes of them are generally flat plate.
(4) They have experienced rockbursts in the main tunnel more frequently than in the sub-tunnel.
(5) The rockbursts occurred only in quartz diorite under the heavy overburden over 750m.

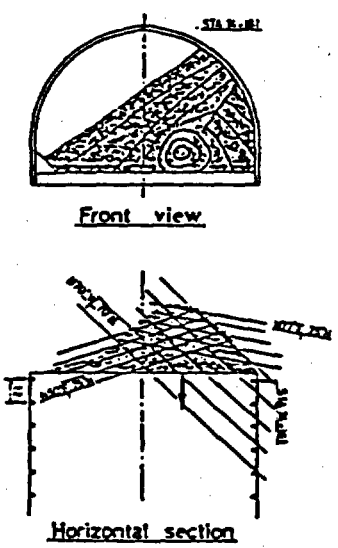

Fig. 2 Fracture zone of the rockburst at the tunnel face

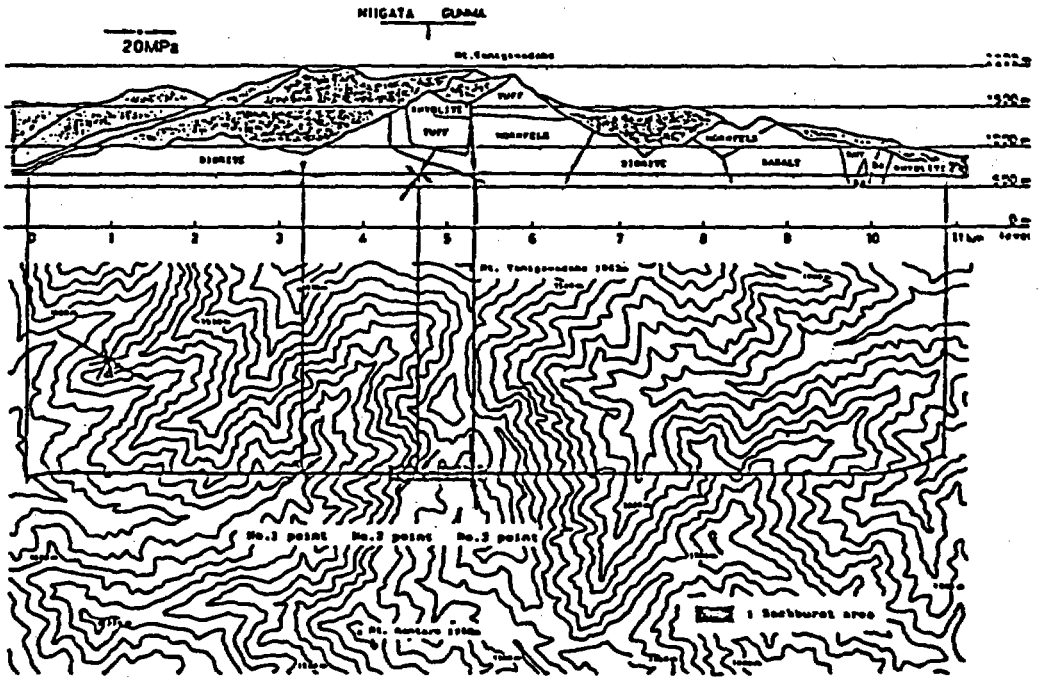

Fig. 3 Measuring points, direction and magnitude of initial rock stresses and the topography

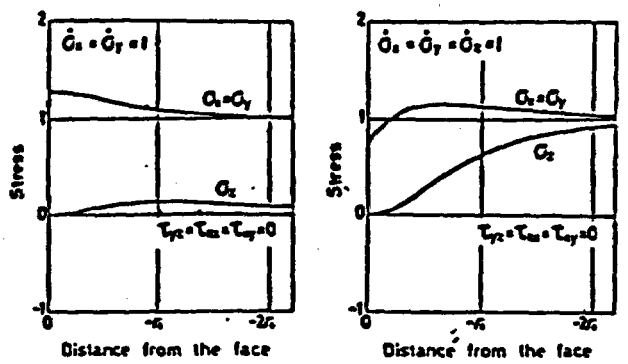

Fig. 4 Elastic stress distributions ahead of the tunnel face by unit loads
y : vertical axis, z : tunnel axis

3. Initial Rock Stresses

One of the factors which cause the rockburst seems to be the states of stress around the tunnel face. Therefore the authors tried to measure the initial rock stresses at three points along the sub-tunnel around the rockburst area.

The measuring method is a kind of the stress relief technique, using the 8 elements moulded gauge bonded on the bottom of a borehole, like the door stopper type. Table 1 shows the measured values of initial principal stresses and Fig.3 illustrates the direction and magnitude of rock stresses in the vertical and horizontal plane on the topographical map. It is found

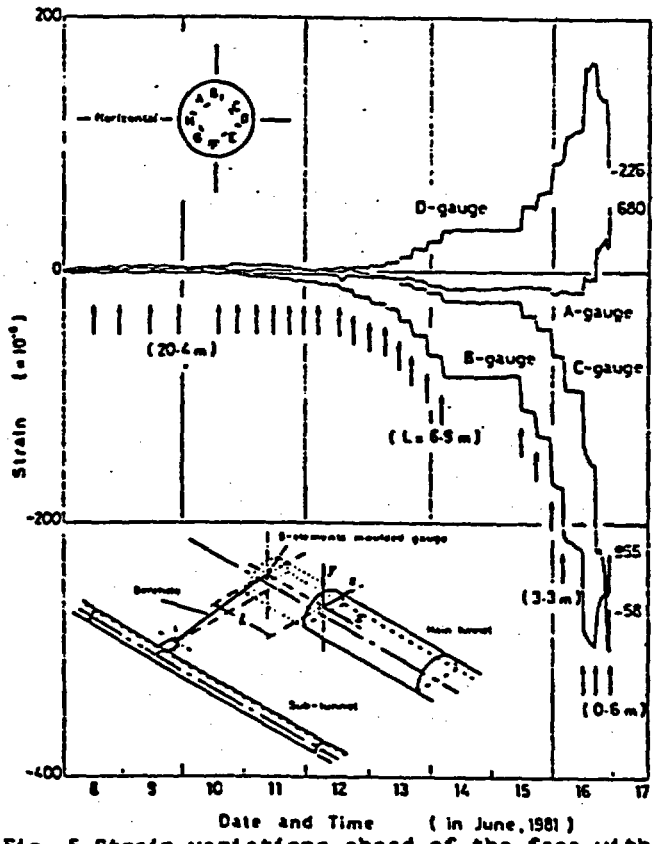

Fig. 5 Strain variations ahead of the face with the advance of the face

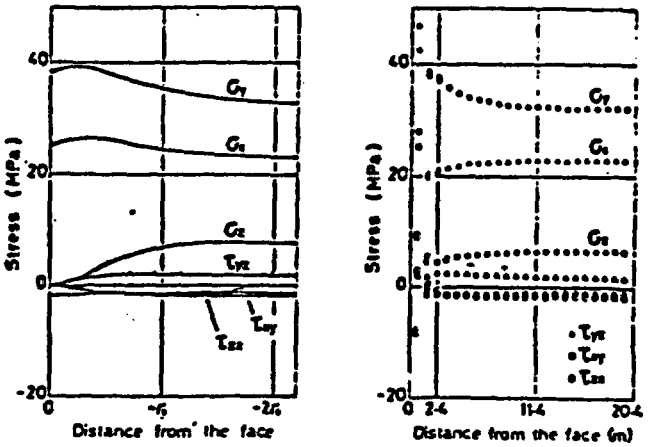

(a) (b)

Fig. 6 Stress distribution ahead of the face in the rockburst area (a) : calculated from initial rock stresses (b) : calculated from measured strain variation

that the directions of rock pressure seems to fairly correspond to ones expected by the topography. On the magnitude, the values of No.2 and No.3 point, which belong to the rockburst area, are more than that of No.1 point, and amount to about 20MPa in the horizontal. In any case, it is considered that the occurrence and the appearance of rockburst deeply depend upon the direction and magnitude of intial rock stresses.

4. Elastic Stress States around the Tunnel Face

It is important to know the states of stress around the tunnel face caused by rock pressure to consider the mechanism of rockbursts. The elastic stress states around the tunnel face were analyzed by means of FEM applied to axisymmetric elastic body under asymmetric loads, in which the tunnel structure was expressed as the corresponding cylindrical cavity.

Fig.4 shows the examples of the stress distributions ahead of the tunnel face along the tunnel axis, in case of Poisson's ratio $\nu=0.15$. At a distance of the tunnel diameter $2r_0$ away from the face, the states of stress are found to nearly come to the applied initial states. It is interested that when $\delta_z=0$, the peak of stress concentration is at the tunnel face, while, when $\delta_z=1$, it moves a little to the inner part from the face. The maximum stress concentration factor around the face is in the range of 1.16-1.32, which is generally lower than one at the side wall.

5. Stress Measurements ahead of the Face

5.1 The Stress Variation with the Advance of the Face

To clarify the actual stress states at the tunnel face in the rockburst area, the following measurements were carried out. Drilling the borehole of 40m length from the sub-tunnel which was going ahead of the main tunnel, directed to the front of the advancing face of the main tunnel, and setting the 8 elements moulded gauge on the bottom of the borehole, the changes of

the strain with the advance of the tunnel face were measured, based on the same principle as initial stress measurements.

Fig.5 shows the obtained strain variation against the time and the arrows in the figure indicate the time of blasting. The incremental strain on each time of blasting grows larger as the face approaches to the measuring point. In the same figure, the positions of 8 gauges are shown. B and C gauge are roughly directed to the vertical, therefore the strains measured by these gauges are increasing compressively, while the strain of D gauge along the tunnel axis is increasing tensionally according to the approach of the tunnel face.

Considering that the width of the tunnel is 18m, the fact that the change of strain begins to appear at a distance of 16m from the tunnel face, fairly corresponds to the results obtained by the elastic stress analysis. Futher, it is found that even at the interval between each blasting the strains increase gradually when the tunnel face approaches to the measuring within a distance of 4.2m-3.3m. It is interested that these deformations are seem to be due to the time dependent characteristics of rock or the redistribution of stresses.

5.2 The Stress States ahead of the Face in the Rockbursts Area

Fig.6(a) shows the stress distribution ahead of the face obtained from the elastic stress analysis using measured initial rock stresses, and Fig.6(b) shows the same stress distribution calculated from the measured strain variations and initial stresses. Comparing these two figures, it is found that these two results fairly coincide with each other, and therefore, the behavior of rock masses around the face is not plastic, but elastic as far as the point very close to the surface. The fact that the fracture initiated at the point more close to the face than 1.5m in this measurement, suggests that high stress concentration can appear on the surface in case of more competent rock.

The fracture of rockbursts is considered to be the brittle fracture caused by high stress concentration just ahead of the face, which value seems to be more than 40MPa, about 20% of the uniaxial compressive strength, in case of Kan-Etsu Tunnel.

6. Mechanism of Rockburst at the Tunnel Face

The correlation between occurrences of the gas and rock outburst in coal mines and the core-disking phenomena, has been pointed out. Then, the occurrences of core-disking were observed at the core boring before the excavation of the main tunnel.

Fig.7 shows these observations in comparison with the events of rockburst at the excavation of the main tunnel. Core-disking was observed at several points which fairly corresponded to the areas where rockbursts frequently occurred.

The fracture of core-disking is known to be the tensile fracture along the boring axis caused by the high compressive rock stress perpendicular to the axis, which amounts to more than about four times of the tensile strength.

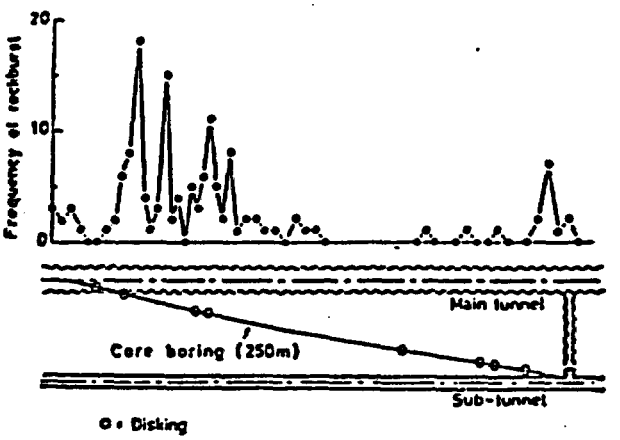

Fig. 7 Events of rockburst and core-disking

Considering the appearance of rockbursts and initial rock stresses in the rockburst area, the authors assume that both the mechanism and criterion of the rockburst at the face seem to be similar to that of core-disking.

7. The Prevention of Rockbursts by Rockbolting

The tensile fracture near the surface, mentioned above, can be prevented by a slight confining pressure, obtained with such as rockbolting or shotcrete. In fact, it seems to be due to the rockbolting that few rockbursts occurred at the side wall in Kan-Etsu Tunnel. Therefore, in this tunnel, the rockbolting on the face as well as the side wall, was adopted as the countermeasures against the rockbursts at the face.

According to the results from the stress analysis and measurements, the bolt length and the bolting pattern were fixed 3m and 2m x 2m, respectively. The effects of rockbolting can be confirmed by the fact that the occurrences of the rockbursts, especially the large scale ones, were reduced after the installation of rockbolts.

8. Conclusion

According to the results of the stress analysis, initial rock stress measurements and the stress change measurements ahead of the face, the fracture of rockbursts in Kan-Etsu Tunnel is considered to be the brittle fracture caused by high stress concentration just ahead of the face. Further, it is found that the areas of core-disking fairly corresponded to those of rockbursts. Therefore, both the mechanism and criterion of the rockburst at the face seem to be similar to those of the core-disking, that is, tensile fracture. As the prevention of rockbursts, the rockbolting is confirmed to be effective.

References

Sugawara, K., et al. (1978). A Study on Core Discing of Rock: J. Min. Metal. Inst. Japan, 94, 1089, pp797-803.

Saito, T. and Sato, K. (1981). Gas and Rock Bursts in Horonai Coal Mine: Proc. Fall Meeting of MMIJ, E2.

SOME ROCK MECHANICS PROBLEMS RELATED TO A LARGE UNDERGROUND POWER STATION IN A REGION WITH HIGH ROCK STRESS

Quelques problèmes de mécanique des roches relatifs à une centrale souterraine importante dans une région à fort niveau de contrainte des roches

Einige felsmechanische Probleme beim Bau einer Kraftwerkskaverne im Gebirge mit hohen Spannungen

Shiwei Bai
Assistant Professor

Weishen Zhu
Associate Professor

Kejun Wang
Assistant Professor
Institute of Rock and Soil Mechanics, Academia Sinica, Wuhan, China

SYNOPSIS

The phenomenon of disk-shaped fractures of cores and of rock burst are described. This is followed by a presentation of stress measurements carried out in the river bed and in galleries. Fracture mechanisms of rock and stress distributions surrounding the power house are analysed by the Finite Element Method. Furthermore there will be a report of the results of tests gained from rock samples tested in a servo-controlled press using the acoustic emission registration technique.

RESUME

On décrit respectivement les phénomènes de carottes disques et des éclatements rocheux qui ont lieu dans un site de barrage. Ensuite on présente une série de résultats de mesures de contrainte obtenus dans le lit et les galeries. Le mécanisme de la fracture de roches et la distribution de contrainte autour de l'usine souterraine sont analysés par la méthode d'élément finis. On décrit les résultats d'essais qui ont été réalisés sur certains échantillons mis en pression au moyen d'une machine rigide à l'aide de servo-asservissement et étudiés grâce à la technique d'émission acoustique.

ZUSAMMENFASSUNG

Das Auftreten scheibenförmigen Zerbrechens von Bohrkernen und Gebirgsschlägen wird beschrieben. Danach werden Ergebnisse von Spannungsmessungen, die im Flußbett und in Stollen vorgenommen wurden, präsentiert. Bruchmechanismen des Gebirges und Spannungsverteilungen um die Kraftwerkskaverne werden mit Hilfe der Finite-Element-Methode analysiert. Des weiteren werden Versuchsergebnisse mitgeteilt, die an Gesteinsproben mit einer servo-kontrollierten Prüfpresse bei Anwendung der AE-Aufzeichnungstechnik gewonnen wurden.

The Ertan Hydropower Station will be located in the remote mountain and gorge region of the lower reaches of the Yalong River in south-west China. Along the banks of the dam site are high steep mountains (about 400-500m) with an average slope of 30 to 40 degrees. An arch dam with a height of 240m will be built in this site, while a large underground power house will probably be arranged on the left bank near the dam abutment.

1. THE PHENOMENA OF THE ROCK FRACTURE OBSERVED AT THE EXPLORATON STAGE

The dam site is located on the Gonghe Fault Block. This block is situated in the west side of the middlh segment of Sichuan-Yunnan Structure Band with a south-north strike. The structure fracture inside the Fault Block is slight and the rock mass is hard and intact. The rock strata mainly consist of basalt(β) and deuterogenously intrusive syenite (ξ).
In order to make engineering geology conditions clear, nearly 100 prospecting boreholes with a total length over 10,000m are drilled. As a result, core ruptures presenting disk forms were found in many borehbles.The picture (Fig.1) shows the core failure appearance. These rock disks have even thickness with average h of $d/4 < h < d/3$(d is diameter of a core). Fracture planes are fresh and rough. The top surfaces of the disks are concave and the bottom convex. The thickness is generally proportional to the diameter. It is unexpected, that there are rock disk phenomena in 40 boreholes among 4 ones located in the river bed. Rupture phenomen took place zonally and alternatively at various depths in every borehole. The distribution probability of 332 fracture bands of 54 boreholes along the altitude of the river bed is shown in Fig.2(Shi 1979). From the figure, it can be see that the highest fracture probability appeared at the altitudes between 930-975m. This band is 20-40m just underneath the surface of rock base According to the results of a series of experiments and analyses, it can be defined that the stress concetration in bottom of core and partial unloasing during the drilling process in high level stress region are the main reason o

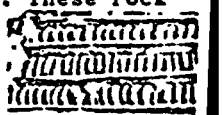

Fig.1

disk phenomena. Also from Fig.2, it can be seen clearly that greatly dense fracture bands are gathered in the stress concentration region of valley. An initial stress value of fracture rock disks was obtained successfully in later stress relief measurements of deep boreholes in the river bed. The max. and min. principal stresses were 650 and 291 kg/cm² respectively (Bai 1982). Rock burst occured many times in prospect and testing galleries on the left bank as well. Among these, the axis of branched gallery No. 3 is approximately perpendicular to the direction of max. principal stress of the stress field. It was originally planned to cut a few rock blocks with a plane of 40 X 40 cm² for shear tests. However, rock burst was occurring when the cutting depths of these blocks reached about 10cm. There were two forms of rock burst. One is scaly rock flakes with a thickness of 1-8mm bursting on the top of a block; the other is the block rooted up. The rents were fresh, fractures accompanied by noises. The edges of the flakes were thicker, the center thinner, and concave facing down. Rock disk phenomena occured many times also at the stress concentration regions, when stress relief measurements were performed in the river bed and prospective galleries of the dam area.

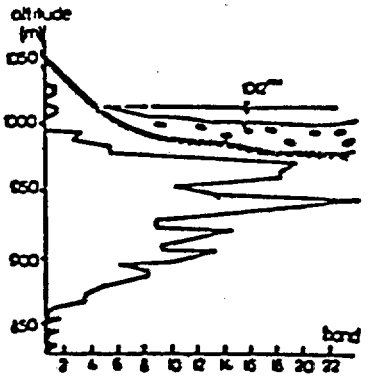

Fig.2

2. The results of stress measurements

To make a thorough investigation of the initial stress around the dam, a lot of in situ measurements has been done by means of overcoring method, including stress measurement of three dimensions and two dimensions methods at 15 points (Fig.3) as well as the measurements in the two deep perpendicular boreholes at the river bed with depths 59.4m and 53m respectively (Fig.4).

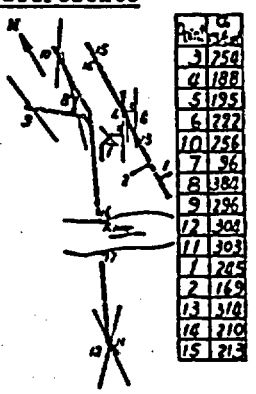

Fig.3

Fig.3 shows that the direction of max. principal stress is NE 11°-46° at most of the points except points 7 and 9, where the orientation of stress depends on local topography and change of properties of rock mass. Points 16 and 17 show the directions of max. principal stresses to be NE 12°-50° at the boreholes with a depth more than 30m. The statistical average of the above mentioned results is about NE 30°, which is just perpendicular to the direction of river with strike NE 60°. Therefore, it can be seen that the stress direction in rock mass near the slope is controlled to a great extent by topography. The stress magnitude is also shown in Fig.3. The max. principal stress in undisturbed syenite is about 200kg/cm²; but about 300kg/cm² in basalt. The main cause of the difference is due to the different rock mechanical properties at various points. The rock mass in different geological regions has different conditions of accumulating stress. In general, the rock with higher elastic modulus would have higher stress. The max. principal stress intersects horizontal plane at small angle, which shows that there is horizontal tectonic stress and its effect is much more than that of gravity.

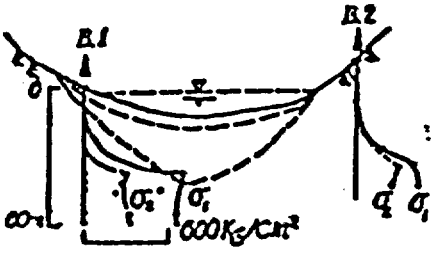

Fig.4

Fig.5

There is serious stress concentration in the bottom of river bed. The max. principal stress is over 650kg/cm². It is obviously shown in Fig.5 that stress distribution in the part of bank slopes may be divided into three areas: I, stress relaxation area, II, stress concentration area, III, stress stable area.

The plane linear elastic finite element analysis has been completed in order to form the whole outline of stress field. The calculation model is shown as Fig.6. It is a well-known fact that horizontal stress increases linearly with the depth though there has been no mature theory on the stress distribution law in surface layer of crust. Therefore effect of gravity and laterally applied triangular load increasing with depth were taken into account in the finite element analysis.

Let σx=KrH, where K is coefficient of lateral pressure for determining the grade of triangular load.

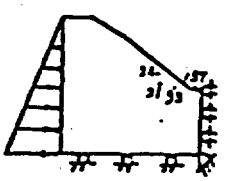
Fig.6

Table 1 shows the comparison of the calculated stresses with the corresponding measured stresses. Results of inverse calculation have good agreement with the measurement results in all four different positions. The whole outline of the stress field of dam site is delineated clearly by the analysis.


Tab.1

3. Prediction of stability of underground power station during excavation

3.1. FEM analysis

The main power house A, which is planned to have a size of about 63m.(h) X 27.5m.(w) X 240m.(l), and the main transformer chamber B and the pressure regulator chamber C are arranged as in Fig.7. Taking account of safety of the buildings in such a high stress region, at first, two dimentional FEM analyses have been done; and three dimentional nonlinear analysis will be made later. It can be considered that the results of elastic analyses are accurate to a certain degree because of higher hardness and fairly ideal elasticity of confining rock mass and high stres-

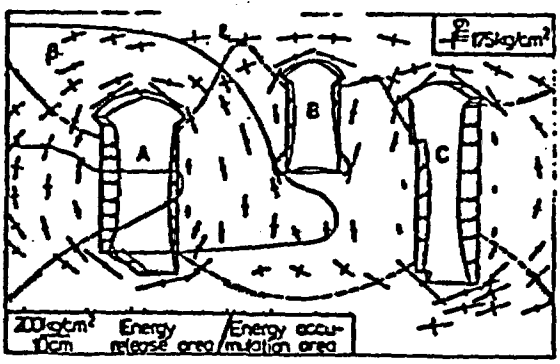

Fig.7

ses making the joints arounding caverns close tightly. The values of most redistributive stresses forming a stress-reduction region whthin the areas surrounded by three caverns are lower than the initial stresses for the horizontal stresses are higher (up to 175 kg/cm²) than vertical one. All the side walls of three houses have lager inward deformation, especially outside walls of two side ones. As shown in Fig.7, the side walls of three chambers have a large deformation inwards them. The max. displacement in the middle of the side walls of the two side chambers might reach up to 6.7cm and 7.6cm, when introducing E=20 X 10³kg/cm² for syenite(ξ) and E=16 X 10³ kg/cm² for basalt(β), while the max. periphic stress with value up to 400-500kg/cm² takes place in the vault and in the bottom parts of surrounding rock; these values of displacements are expected to be larger if the effects of joints are taken into account and stress concentration are most serious at the top and bottom parts of the regulator chamber owing to its larger ratio of height to width. It also can be seen that the elastic strain energy concentration regions are basically located also in these parts of rock; and the max. value takes place in vault and bottom of regulator room while the magnitude is over 6-7 times as large as initial one. Therefore the side walls should be protected from overdeformation and vaults and bottom parts should be protected from shear failure and rock burst. Because of increasing stress accumulation due to gradual excavation from top to bottom and because of prior supporting of the vaults in general, the probability of failure occuring in vault is expected to be lower than that occurring in bottom. In summary, more attention should be paid to the safety of bottoms.

FEM analysis was also made to rock burst phenomena occurring in cutting testing blocks in branch gallery 3 mentioned above. The results indicated that sudden rock failure had resulted from high lateral stresses with a tension stress more than 25 kg/cm² at the root of the blocks.

3.2. Research on mechanics properties of rock

A series of laboratory tests have been done to determine why rock there behave as such a marked brittle failure and almost every syenite sample made intensive burst sounds with flying out broken piece when failure occurred, in which the tests performed on a rigid machine were monitored by AE and the results are shown in Fig. 8 and 9. It can be seen that the properties of the curve of the dry sample are quite different from those of the sample saturated with water. The former has a trength about one third larger than the latter, the latter presents yield when the pressure reaches 60% of the former (beyond point p in Fig. 9). It can be seen, from these curves, that suddenness character of AE takes place for the former while the failure of latter occurs resulting from continual small fractures and AE count rates are far below the former's, which shows that rock becomes greatly softened after saturation with water to reduce suddenness of failure.

Fig.8a

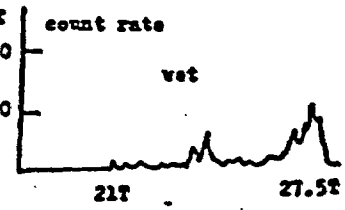

Fig.8b

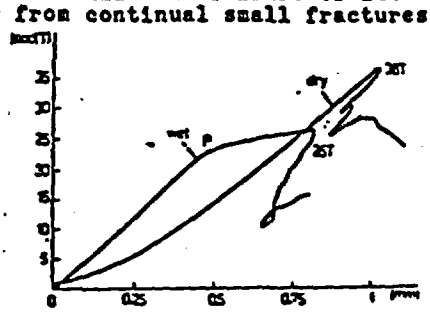

Fig.9

Conclusions

1. Phenomena of disk cores and rock bursts take place mainly at stress concentration regions; the evident brittleness of syesnite helps to form this kind of failure.

2. There exists rather high earth stress and its distribution is intensively affected by landforms.

3. The areas with great accumulation of strain energy are situated near the parts of the vaults and the bottoms of underground buildings; more attention should be focused on rock fracture at bottoms during excavation.

4. Syenite becomes evicently softened after saturation with water, with the help of which rock burst phenomena would be reduced.

Acknowledgements—Many data in situ were offered by Institute of Power Survey and Design, Chengdu. Some of tests were made by Mr. Nie Shifeng and Miss Lin Zhuoying and assistance in writing this paper was made by Mr. Zhu Zuoduo and Miss Shi Baozhen and others.

References

Bai Shiwei et al. (1982). Stress measurement of rock mass in situ and the law of stress distribution in a large dam site: 23rd U.S. Symposium on Rock Mechanics, Berkeley.

Shi Jinliang. (1979). The brittle fracture of rocks in region of high earth stress: Internal report of Institute of Power Survey and Design, Chengdu.

Report of Investigations 8274

Coal Mine Floor Heave in the Beckley Coalbed, An Analysis

By James R. Aggson

UNITED STATES DEPARTMENT OF THE INTERIOR
Cecil D. Andrus, Secretary

BUREAU OF MINES

The work upon which this report is based was done under a cooperative agreement between the Bureau of Mines, U.S. Department of the Interior, and the Pittston Co.

This publication has been cataloged as follows:

Aggson, James R

Coal mine floor heave in the Beckley coalbed, an analysis / by James R. Aggson. [Washington] : U.S. Dept. of the Interior, Bureau of Mines, 1978.

32 p. : ill., maps, diagrams ; 27 cm. (Report of investigations • Bureau of Mines ; 8274)

Bibliography: p. 31-32.

1. Coal mines and mining • West Virginia. 2. Buckling (Mechanics). 3. Structural stability. I. United States. Bureau of Mines. II. Title. III. Series: United States. Bureau of Mines. Report of investigations • Bureau of Mines ; 8274.

TN23.U7 no. 8274 622.06173

U.S. Dept. of the Int. Library

CONTENTS

ILLUSTRATIONS

TABLES

COAL MINE FLOOR HEAVE IN THE BECKLEY COALBED, AN ANALYSIS

by

James R. Aggson [1]

ABSTRACT

This Bureau of Mines report describes floor heave ground control problems that have been encountered in a new underground coal mine in West Virginia. Previous experience in the coal seam, the results of physical property investigations, and in situ rock stress determinations are discussed. The apparent cause of the ground control problems is the existence of a high, biaxial, horizontal stress field coupled with a floor member that has time-dependent deformation characteristics. A theoretical analysis of the failure process is developed. The analysis is assisted by finite element techniques. Mine design recommendations based on this analysis are presented.

INTRODUCTION

The objective of this investigation, which was conducted as part of a cooperative agreement between the Bureau of Mines, Denver Mining Research Center, and the Pittston Co., was to further the understanding of the floor heave ground control problems that have plagued underground mining of the Beckley coalbed in southern West Virginia. Floor heave is not only economically undesirable, it is also undesirable from a safety point of view. Floor heave causes a redistribution of stresses and loads that are associated with an underground opening. This redistribution of stresses may cause roof or pillar problems that otherwise would not have occurred.

The floor heave that occurs in the Beckley coalbed is not considered to be caused by "squeezing," or plastic flow of the materials involved; squeezing-type floor heave is normally associated with relatively weak floor members that contain significant amounts of clay mineralization. The floor members in the Beckley coalbed are competent, relatively strong materials that fail in a manner best described by the term "buckling." This buckling-type failure is indirectly related to the time-dependent deformation properties of the materials involved, but is considered to be more of a slender-column-type failure than a squeeze- or flow-related failure.

[1]Physicist, Denver Mining Research Center, Bureau of Mines, Denver, Colo.

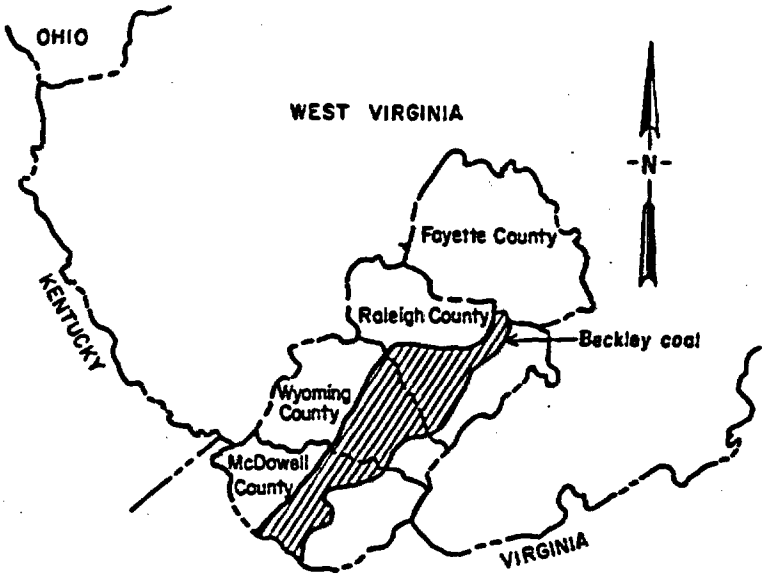

FIGURE 1. - Original minable extent of Beckley coalbed.

ACKNOWLEDGMENTS

The author wishes to express his appreciation to the Pittston Co. and to John Curran, group geotechnical engineer for the Pittston Co., for his assistance and cooperation during this investigation.

GENERALIZED ROCK SEQUENCE

Beckley Coal.--The Beckley coal is described as soft, columnar, and multibedded (9).[2] It is a low-volatile metallurgical bituminous coal. It has been shown (19) that the Beckley coalbed has a minable thickness for more than 600 square miles (fig. 1). Original minable Beckley reserves were estimated at over 2 billion tons. However, recent exploration by mining companies shows the reserves to be more extensive (24).

Draw Rock.--Immediately above the coal is a dark, fine-grained, sandy shale that is approximately 18 inches thick. This rock can be cut with continuous miners and is removed when the seam thickness is less than that required by the mining equipment.

Stack Rock.--Above the draw rock is the so-called stack rock, a laminated shale with poor lateral continuity. The thickness of this sequence is 10 to 20 feet in the area of investigation. This material is characterized by many slickensided surfaces.

Massive Sandstone.--Above the stack rock are the upper and lower Raleigh Sandstones. Approximately 200 feet above the Beckley coalbed is the Sewell coalbed.

Immediate Floor.--Beneath the coal is a black, fossiliferous shale which is typically 1 foot thick. This material is difficult to cut with a continuous miner. Thus, grading and cleanup of heaved bottom are expensive and time consuming.

Main Floor.--Beneath the immediate floor is the main floor; it is much like the stack rock but is more massive and has fewer slickensided surfaces.

[2]Underlined numbers in parentheses refer to items in the list of references at the end of the paper.

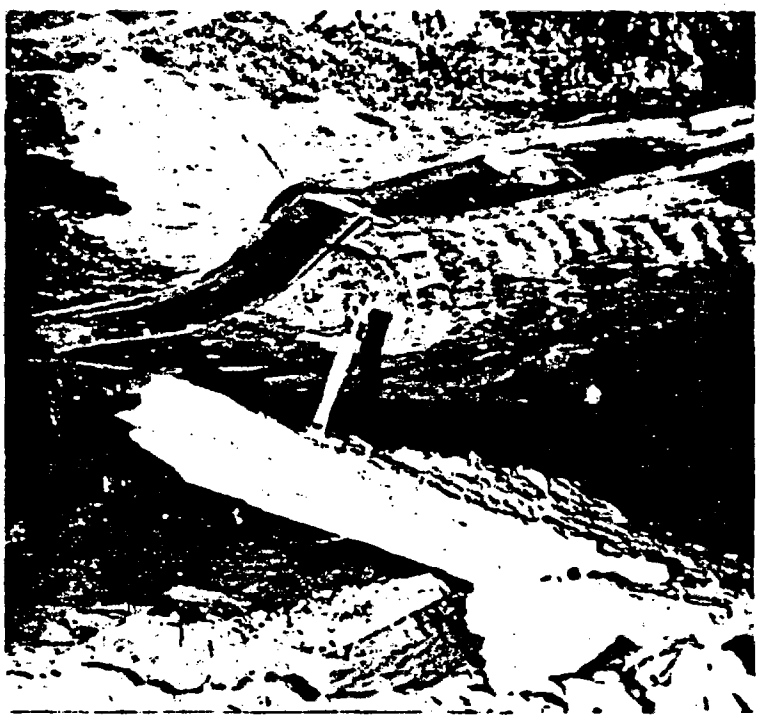

FIGURE 2. - Floor heave—immediate floor projecting up into entry.

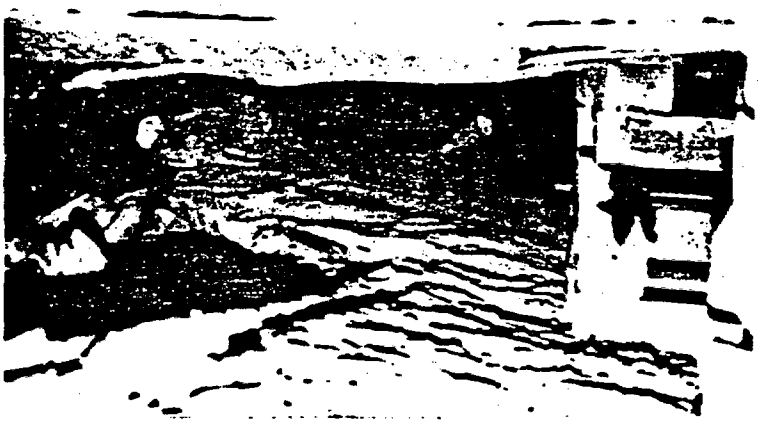

FIGURE 3. - Floor heave—the section of immediate floor in the background has failed near the pillar.

BACKGROUND

The Beckley coalbed has had a history of floor heave ground control problems. The Glen Rogers mine, which opened in the 1920's, experienced extensive floor heave. This mine was located on the Raleigh-Wyoming County line and operated by the Raleigh-Wyoming Mining Co. In a report dated April 1929, James P. Keatley of the West Virginia State Department of Mines (16) described the floor heave in the Glen Rogers mine. The following observations listed in the Glen Rogers report should be noted since they appear to be consistent with current observations:

1. Water plays no apparent part in the floor heave process.

2. No evidence of gas has been found in the floor.

3. The thickness of the overburden, which ranges from 600 to 1,300 feet, has no relationship to the floor heave.

The last of these observations is most significant and will be discussed later in this report.

In his conclusions, Keatley states, "A statement in brief as to the cause [of floor heave] would be that an undetermined natural condition doubtless augmented by former and present mining methods causes the bottom to heave." As this report will show,

Keatley's insight into the problem was most accurate. The "undetermined natural condition" is the existence of a biaxial, horizontal, compressive stress field. This stress field is in excess of that which would be expected from gravity loading. It will be shown that this stress field and the material properties of the floor rock combine to cause the floor heave that has been experienced.

The floor heave that occurs in the Beckley seam generally occurs as arching near the center of the floor span or as a break near the rib followed by vertical deflection of the floor at the rib and sloping of the floor across the entry. Examples of the floor heave are shown in figures 2, 3, and 4. It will be shown that these two types of floor heave are merely different manifestations of the same basic failure mechanism.

When the entries experiencing floor heave were identified on a map of the mine under investigation, it was apparent that there was a relationship between the floor heave and the direction of the entries. The main entries, which are used for ventilation and haulage, experienced the majority of the floor heave. This directional relationship suggested a directionally related loading mechanism, or more specifically, a biaxial, horizontal stress field

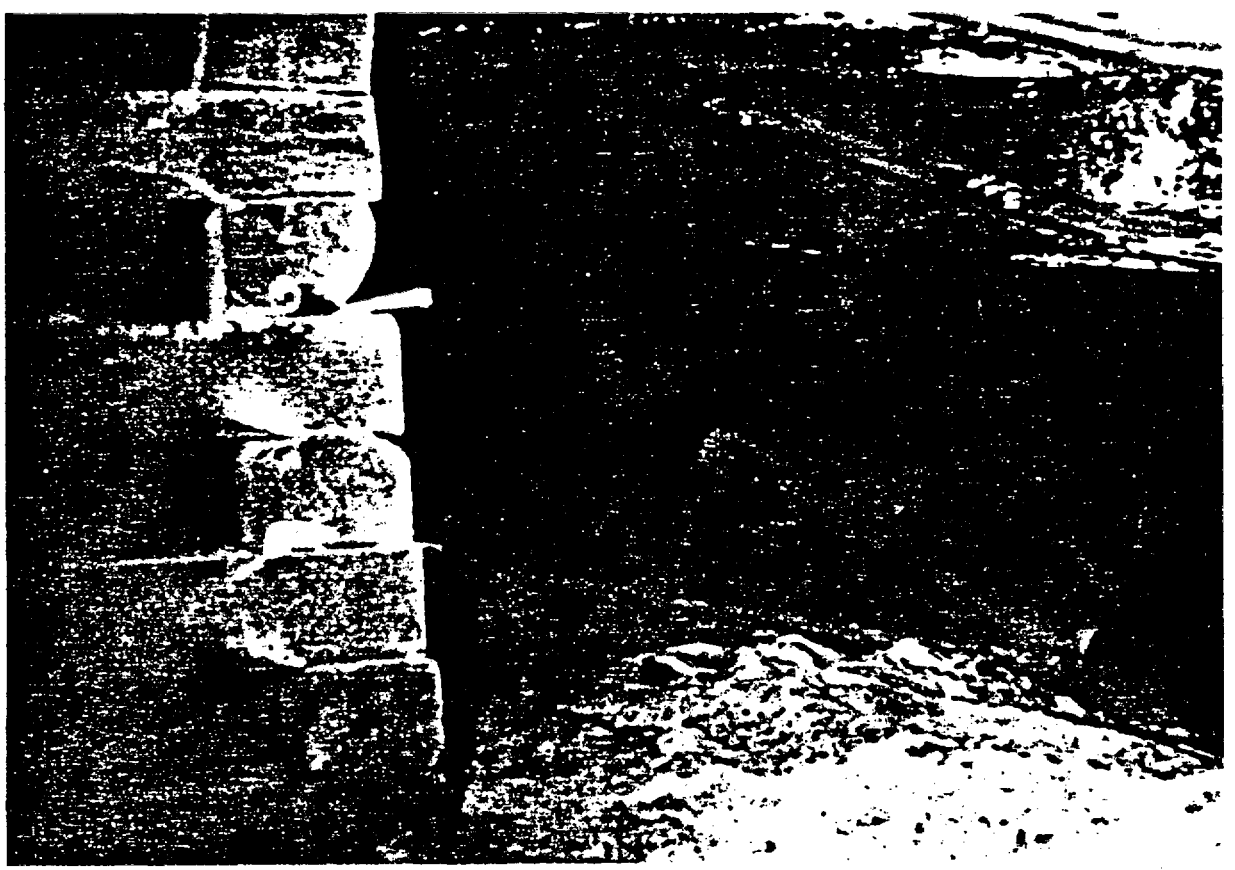

FIGURE 4. - Floor heave—a tension failure near the center of the entry can be seen in the foreground.

that exceeds what would be expected by gravity loading. Since the main entries were oriented at a bearing of N 25° W, it was hypothesized that the maximum compressive component of the horizontal stress field was at 90° to these entries or at a bearing of N 65° E. An in situ testing program was developed to test this hypothesis and investigate the floor heave problem.

MATERIAL PROPERTIES

The initial phase of the in situ investigations consisted of core-drilling the materials involved. NX (2-1/2-inch) core holes were identified by letter. The relative position of each hole can be seen in figure 5.

Hole A.--Vertical hole up through the stack rock and into the sandstone.

Hole B.--Horizontal hole into the draw rock; bearing of the hole was N 25° W.

Hole C.--Vertical hole down through the immediate floor into the main floor. The initial part of hole C was drilled 6 inches in diameter to obtain a large volume of the immediate floor. The 6-inch-diameter core was later redrilled in the laboratory into NX pieces.

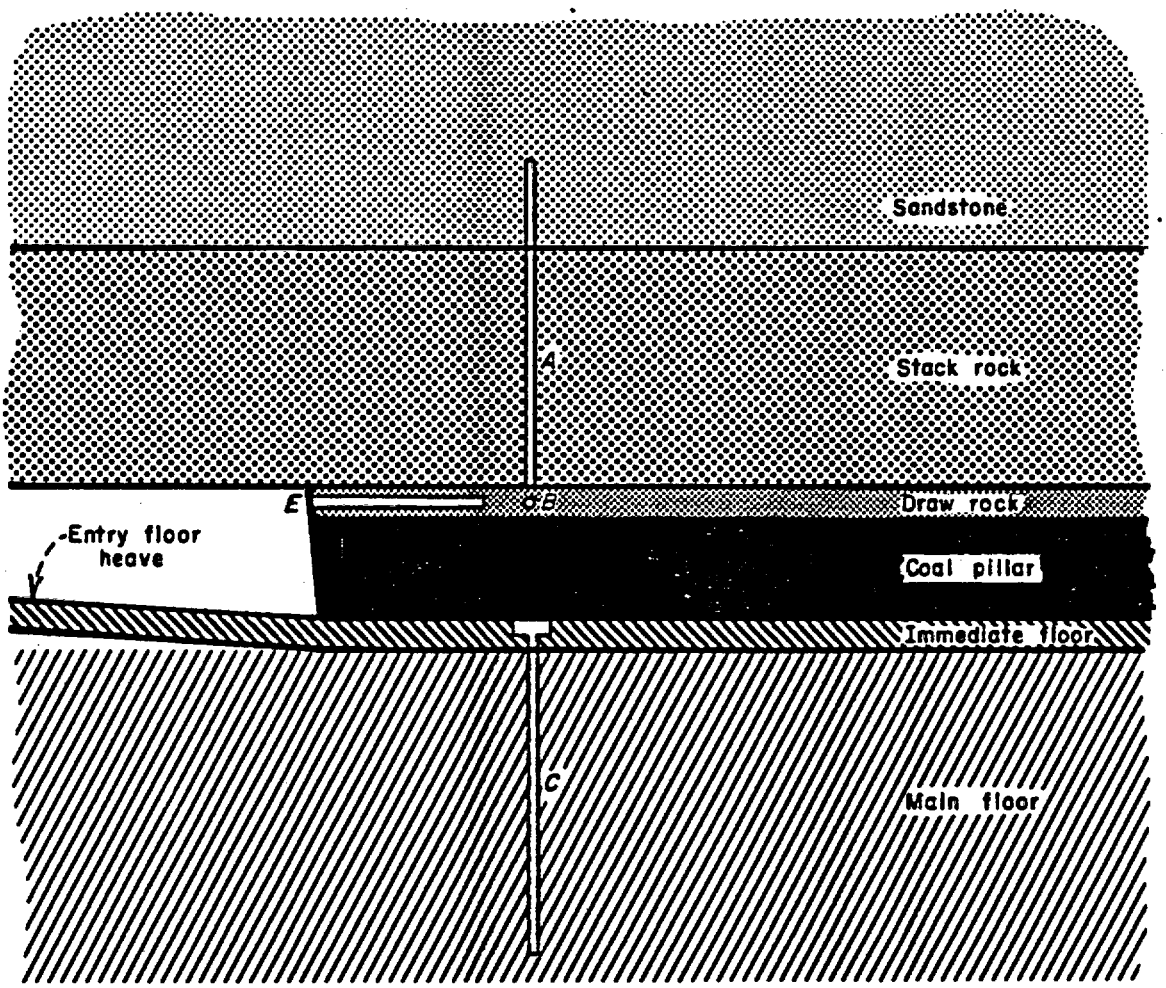

FIGURE 5. - Relative location of core holes.

Hole D.--6-inch-diameter core drilled vertically into the draw rock (not shown in fig. 5). This core was obtained in a different area of the mine in which the draw rock had not been removed.

Hole E.--Horizontal hole into the draw rock. The orientation of this hole was such that it was perpendicular to hole B.

The core samples that were obtained were tested triaxially in the laboratories of the Denver Mining Research Center. The results of the triaxial compression tests are summarized in table 1. The shear strength, coefficient of internal friction, and angle of internal friction were determined by the construction and analysis of Mohr's envelope (22, p. 286).

TABLE 1. - Triaxial compression tests

Compressive strength, psi	Lateral pressure, psi	Young's modulus, million psi		Poisson's ratio		Shear strength, psi	Internal friction	
		Sec.	Tan.	Sec.	Tan.		Coefficient	Angle
MASSIVE SANDSTONE								
17,564	0	2.47	3.85	0.09	0.16			
19,904	500	2.56	3.69	ND	ND			
26,078	1,000	2.86	4.40	ND	ND	3,325	1.119	48°13'
30,166	2,000	3.69	4.81	ND	ND			
STACK ROCK								
19,256	0	3.68	4.11	0.16	0.28			
20,355	500	4.08	3.90	ND	ND			
19,735	0	3.75	4.12	ND	ND			
21,398	1,000	4.37	4.03	ND	ND	5,879	0.510	27°0'
19,171	0	3.62	3.88	ND	ND			
25,317	2,000	4.93	4.34	ND	ND			
23,738	2,000	4.09	3.73	ND	ND			
DRAW ROCK								
6,710	0	4.34	4.81	0.37	ND			
13,674	500	4.89	4.89	ND	ND			
12,602	1,000	5.05	5.35	ND	ND	1,426	1.058	46°37'
14,660	1,500	5.43	5.43	ND	ND			
IMMEDIATE FLOOR								
16,091	0	3.87	4.32	0.19	0.28			
12,507	0	2.75	2.84	.16	.32			
14,293	500	5.96	4.16	ND	ND			
12,214	500	2.51	2.32	ND	ND			
18,307	1,000	3.86	3.86	ND	ND	3,331	0.663	33°33'
28,410	1,500	4.93	4.93	ND	ND			
17,047	1,500	3.29	2.93	ND	ND			
12,302	2,000	3.00	2.95	ND	ND			
19,713	2,000	3.31	3.21	ND	ND			
MAIN FLOOR								
31,012	0	1.91	3.10	0.03	0.09			
28,193	0	2.33	4.06	ND	ND			
29,321	500	2.53	2.96	ND	ND			
27,488	1,000	2.23	3.32	ND	ND	8,284	0.552	28°52'
33,549	1,500	2.93	3.92	ND	ND			
33,831	2,000	3.85	4.46	ND	ND			

ND--Not determined.

In addition to the triaxial compression tests shown in table 1, modulus of rupture tests were conducted (22, p. 333) to determine the outer fiber tensile strength of the horizontal cores in the draw rock (holes B and E). The average of four such tests was 828 psi with a standard deviation of 323 psi.

Also, indirect tensile strength tests, or Brazilian tests (22, p. 329), were conducted on the immediate floor. The results of three such tests gave an average tensile strength of 705 psi for the immediate floor.

The low values for the angles of internal friction of the floor rocks, shown in table 1, may be a result of the fact that not enough cores were tested to insure statistically valid results.

The core recovery in the vertical hole in the roof (hole A) was quite good. No core disking was observed in this hole. The term "disking" refers to the formation of disks, or wafers of relatively uniform thickness, which fracture or rupture on surfaces approximately normal to the axis of the core. Usually, the surfaces of the disks are concave-convex with the concave side toward the collar of the hole. When disking occurs, the relationships between the in situ stress field, the strength properties of the rock, and the stress concentrations caused by the borehole and the kerf of the drilling bit are rather complex. However, laboratory investigations (23), modeling studies (5), and field observations (13) have allowed the development of empirical relationships involving stress levels and the strength properties of the rock. One such relationship is that, providing the compressive stress in the direction of the borehole axis is relatively small, the core will disk when the average compressive stress in the plane normal to the borehole is approximately equal to one-half the unconfined compressive strength of the rock. At this threshold stress level, the thickness of the disks that are formed will be roughly one-fourth of the diameter of the core (regardless of core diameter). When the magnitude of the lateral stress field increases, the disks become thinner (shorter in the axial direction).

Core disking did occur at several locations in the vertical hole in the floor (hole C). An example of this disking that occurred in the main floor can be seen in figure 6. As can be seen in table 1, the material in the main floor is considerably stronger than the other rocks involved. The occurrence of disking in this strongest member can be explained by the fact that the entry shown in figure 5 was experiencing floor heave. Floor heave in this entry, which was approximately 7 feet from hole C, was causing a major redistribution of the stress field in the main floor. This redistribution was undoubtedly producing zones of extremely high stress concentration.

Hole B was drilled into the draw rock in order to obtain horizontal core for modulus of rupture tests. This draw rock is the immediate roof in some parts of the mine. Hole B is parallel to the entries experiencing the majority of the floor heave. A most unusual form of core disking occurred in this hole. Rather than being concave-convex as are most disks, the disks from hole B were curved in one direction only. The axial stress in the direction of the borehole was small because the disking occurred near the collar of the hole and the hole was only 8 feet deep. The vertical stress in the draw rock

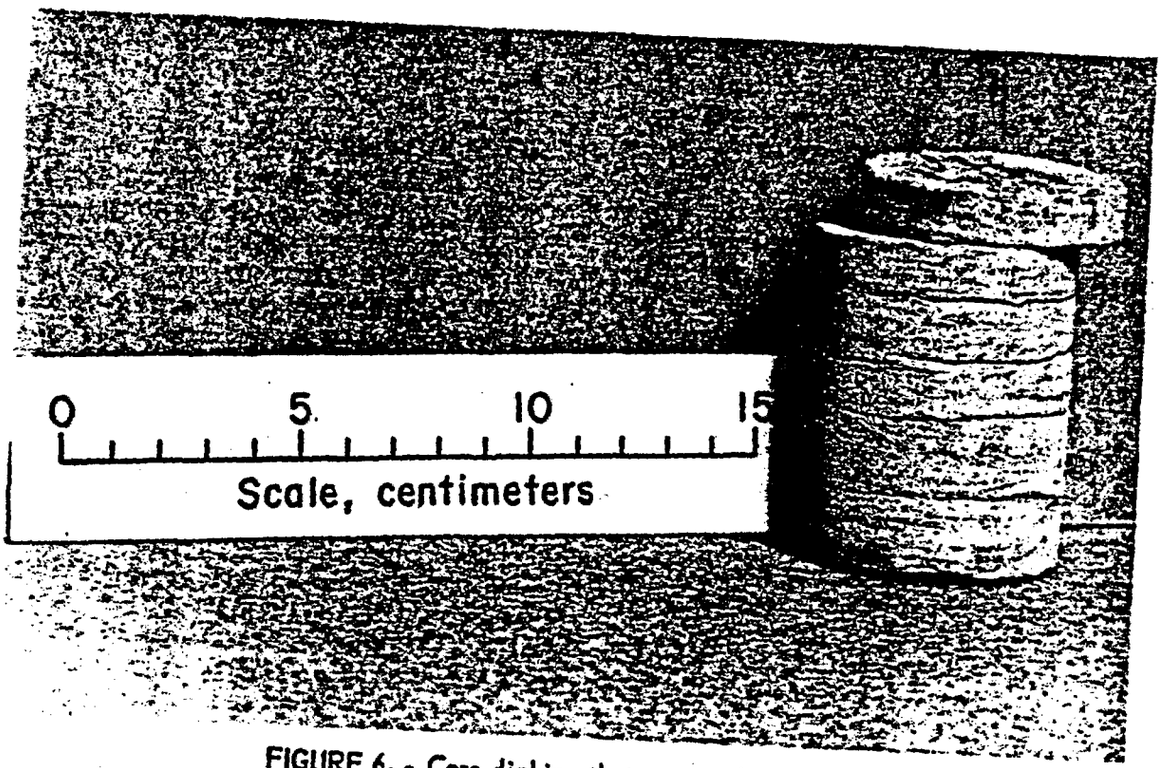

FIGURE 6. - Core disking that occurred in hole C.

near hole B was also quite small because the rib had deteriorated and the outer area of the coal pillar was not supporting a significant amount of vertical load. Thus, the unusual disking, examples of which are shown in figures 7 and 8, is due to a relatively high, nearly uniaxial stress condition. The orientation of this uniaxial horizontal compressive stress near hole B is perpendicular to the borehole and the heaving entry. This orientation would be N 65° E.

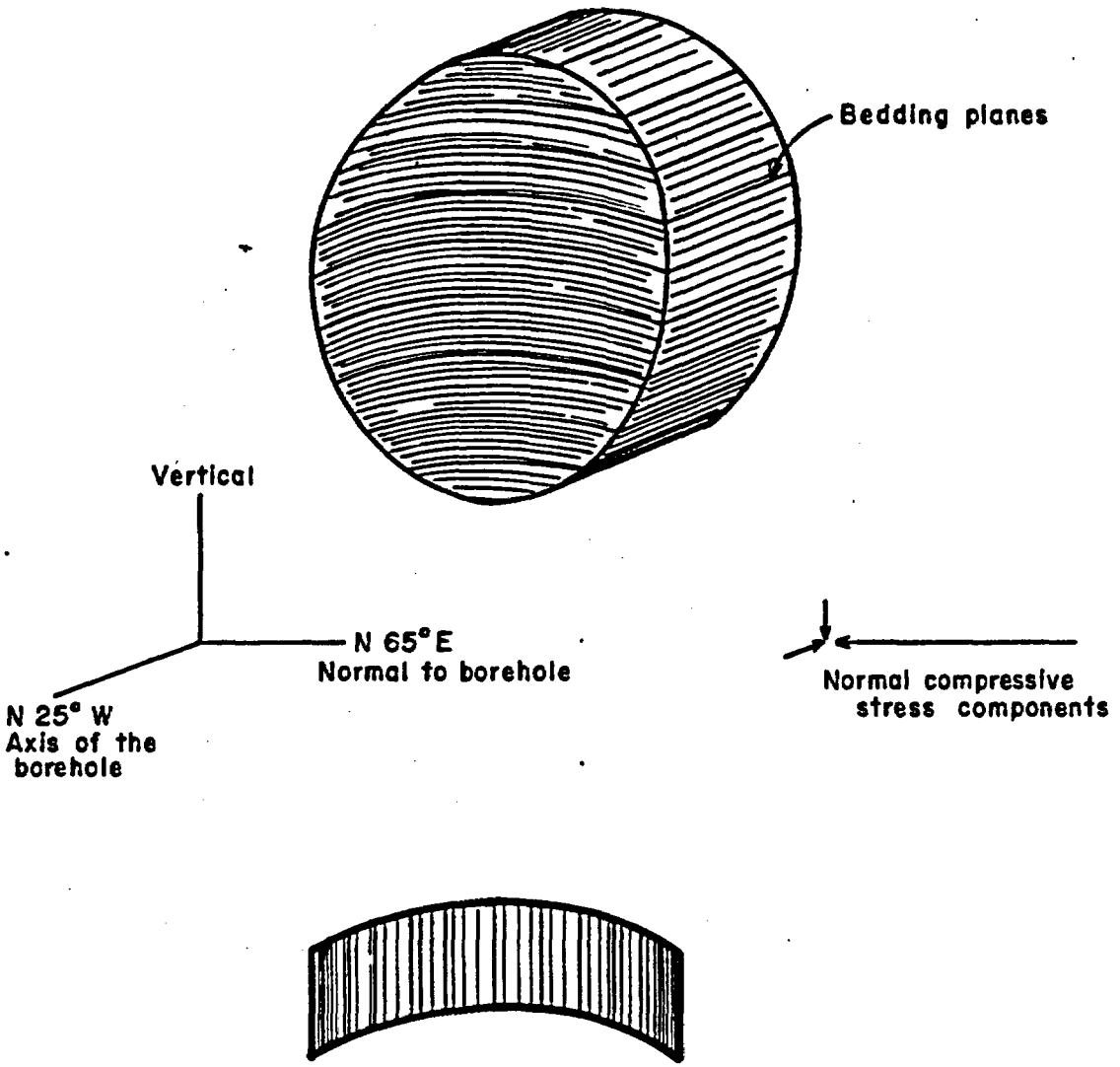

FIGURE 7. - Representation of disk caused by uniaxial compressive stress.

Hole E was drilled 90° to hole B in the draw rock to see if disking would occur in this orientation. No core disking occurred in hole E. The disking in hole B and the lack of disking in hole E provided additional information regarding the stress field. The in situ horizontal stress field was thus known to be rather biaxial in nature with the approximate orientation of the maximum compressive stress being N 65° E.

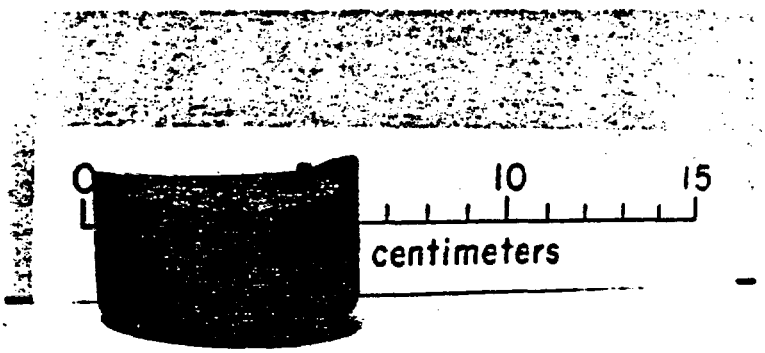

FIGURE 8. - Core disk formed by uniaxial load (looking down the vertical axis).

IN SITU STRESS DETERMINATIONS

The second phase of the in situ investigations was designed to determine the horizontal stress distribution. The stress determinations were accomplished using the borehole deformation gage and stress-relief overcoring techniques that have been developed by the Bureau of Mines (10, 12). This method of in situ rock stress determination basically consists of (1) drilling a 1.5-inch-diameter pilot borehole, (2) positioning the deformation gage in the pilot borehole, and (3) diamond-drilling a second 6-inch-diameter concentric borehole over the gage while recording the change in length of three diameters of the pilot hole. These diametral deformation measurements are then used, along with the elastic properties of the rock, to calculate the stress distribution in the plane perpendicular to the axis of the borehole.

Due to disking and poor core recovery in hole C, it was decided to overcore vertically up into the roof rather than down. Since the elastic properties of the materials in the roof and the floor were of approximately the same magnitudes, no member was significantly stiffer than any other. Thus, it was believed that stresses determined in the roof would be representative of the stresses that existed in the floor before floor heave caused a redistribution of the stress field. Overcoring proceeded quite smoothly, and an excellent set of data was obtained at hole depths great enough to insure that the presence of the opening did not influence the results.

The thick-walled cylinders obtained from overcoring were tested both biaxially (7) and triaxially (21). The cores were found to be elastically isotropic in the horizontal plane (the plane perpendicular to the axis of the core). The average elastic modulus of the 6-inch-diameter cores obtained in the stack rock was found to be 7.32×10^6 psi. The difference between this value and the elastic properties of the stack rock given in table 1 is due to the fact that the NX cores were loaded perpendicular to the sedimentary bedding while the elastic modulus of the overcores was determined parallel to the bedding. This result is not uncommon in laminated rocks. The elastic modulus that is used in the stress magnitude calculations is a secant modulus that corrects for elastic nonlinearity of the rock (2).

The secondary principal stresses in the horizontal plane were calculated from the overcoring deformation measurements and the elastic properties (3) and found to be -3,239 psi, bearing N 69° E; and -1,732 psi, bearing N 21° W. The negative sign is used to denote compression.

The gravity-induced portion of the in situ stress field can be calculated from the equations

$$\sigma_v = \gamma h, \tag{1-a}$$

and

$$\sigma_h = \left(\frac{\nu}{1-\nu}\right)\sigma_v, \tag{1-b}$$

where σ_v = vertical stress,

σ_h = horizontal stress,

γ = density of overburden,

h = depth of overburden,

and ν = Poisson's ratio.

The derivation of equations 1 is based on lateral confinement of the rock mass. Using the average specific gravity of the NX cores (2.67), the average tangent Poisson's ratio of the stack rock (0.25), and an average overburden thickness of 700 feet, the gravity-induced component of the horizontal stress field is 266 psi. The portion of the horizontal stress field that is in excess of that generated by gravity loading is described by secondary principal stresses: -2,973 psi, bearing N 69° E, and -1,466 psi, bearing N 21° W.

The measured horizontal principal compressive stresses of -3,239 psi and -1,732 psi are consistent with the hypothesized stress field in that the maximum component is within 4° of being perpendicular to the heaving entries and is biaxial in a ratio of nearly 2 to 1.

Once the horizontal stress distribution is known, it is interesting to go back and look at the stress-strength relationship between the uniaxial load and the unconfined compressive strength of the draw rock. Due to the migration of horizontal roof stress down into the draw rock, the uniaxial stress that produced the unusual disking in hole B is approximately -3,239 psi. The unconfined compressive strength of the draw rock is 6,710 psi. One-half of the compressive strength is within 116 psi of being exactly equal to the uniaxial stress that produced the unusual disking. As has been previously stated, this same 2-to-1 relationship exists between the compressive strength and the average applied stress in previously observed disking situations (13). The stress conditions and the resulting disking that occurred in hole B are admittedly quite rare. However, these results may provide a basis for analysis if disking of the type that occurred in hole B is observed in the future.

EXCESS HORIZONTAL STRESS

The horizontal stresses that exceed the expected value as predicted by equations 1 are referred to as excess horizontal stresses. Excess horizontal stress has been determined to exist at the surface of the earth as well as at depth. Experience has shown that nearly any rock mass that has extensive lateral continuity can be expected to contain horizontal compressive stresses in excess of those induced by gravity loading or temperature changes. Figure 9 is a representation of excess horizontal stress distributions that have been compiled by the Bureau of Mines. The magnitude and orientation of the

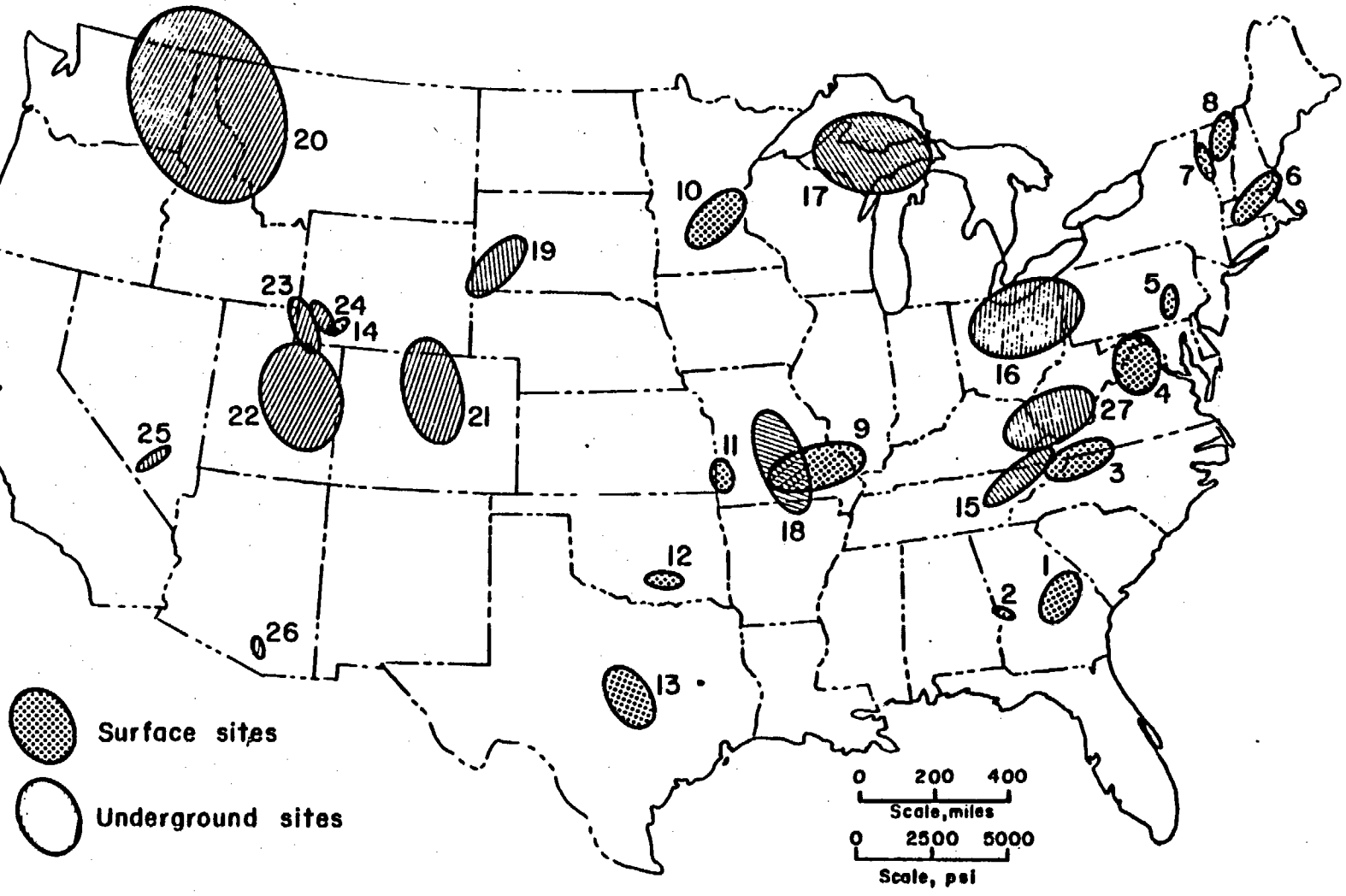

FIGURE 9. - Excess horizontal stress map.

major and minor axes of each ellipse shown in figure 9 represent the excess secondary principal stresses determined at each site. The maximum and the minimum principal stresses are referred to as P and Q, respectively. The site numbers on figure 9 correspond to tables 2 and 3.

TABLE 2. - Excess horizontal compressive stress, surface sites

Site No.	Location	Direction of P	Magnitude of P, psi	Magnitude of Q, psi	Average depth of measurement, feet	Reference
1	Lithonia, Ga.....	N 49° E	1,639	941	18.1	14
2	Douglasville, Ga....	N 64° W	512	285	1.8	14
3	Mt. Airy, N.C.....	N 87° E	2,464	1,191	33	14
4	Rapidan, Va.....	N 6° E	1,678	1,385	8.6	14
5	St. Peters, Pa.....	N 14° E	820	335	4.8	14
6	West Chelnsford, Mass.	N 56° E	2,133	1,113	61.9	14
7	Proctor, Vt.....	N 4° W	1,328	516	1.2	14
8	Barre, Vt.....	N 14° E	1,734	791	151.2	14
9	Graniteville, Mo....	N 77° E	3,190	1,397	4.7	14
10	St. Cloud, Minn.....	N 50° E	2,205	1,519	4.9	10
11	Carthage, Mo.....	N 2° E	1,066	777	4	14
12	Troy, Okla.....	N 84° W	1,075	519	4.5	14
13	Marble Falls, Tex...	N 33° W	2,219	1,491	4.7	14
14	Green River, Wyo....	N 42° E	415	171	10	Previously unpublished.

NOTE.--P and Q are the maximum and minimum secondary principal stresses.

In many of the underground sites shown in figure 9, the complete three-dimensional state of stress was determined from overcoring measurements obtained in three nonparallel boreholes. In all cases the measured vertical stress agreed with the vertical stress expected from gravity loading and given by equation 1-a.

TABLE 3. - Excess horizontal compressive stress, underground sites

Site No.	Location	Direction of P	Magnitude of P, psi	Magnitude of Q, psi	Depth of overburden, feet	Reference
15	Immel mine, Knoxville, Tenn.	N 58° E	3,007	551	925	Previously unpublished.
16	Limestone mine, Barberton, Ohio.	N 77° E	4,000	2,500	2,300	20
17	Mather mine, Ishpeming, Mich.	N 82° W	3,822	2,937	3,200	1
18	Fletcher mine, Bunker, Mo.	N 17° W	3,682	1,595	1,000	15
19	Homestake mine, Lead, S. Dak.	N 38° E	2,778	1,053	6,200	Previously unpublished.
20	Crescent mine, Wallace, Idaho.	N 27° W	6,258	4,966	5,300	25
21	Henderson mine, Empire, Colo.	N 15° W	3,398	2,283	3,127	13
22	Sunnyside mine, Sunnyside, Utah.	N 31° W	3,718	2,898	1,060	Previously unpublished
23	Allied Chemical mine, Green River, Wyo.	N 23° W	1,781	404	1,600	Do.
24	Big Island mine, Green River, Wyo.	N 38° W	1,054	705	850	Do.
25	Rainier Mesa Nevada test site.	N 46° W	972	345	1,250	11
26	Lakeshore mine, Casa Grande, Ariz.	N 69° E	502	160	1,570	4
27	Beckley No. 1 mine, Bolt, W. Va.	N 69° E	2,973	1,466	700	Previously unpublished

NOTE.--P and Q are the maximum and minimum secondary principal stresses.

At any particular site, the in situ stress field is a function of regional structure, the local geometry of the materials involved, the material properties of these materials, and the far-field applied boundary stresses. The far-field forces may be the same forces associated with the plate tectonics model of the earth. Accurate prediction, without measurement, of in situ stress fields may never be possible. However, three generalities from figure 9 can be stated: (1) Near the eastern coast of the United States the maximum compressive component of the horizontal stress field tends to be parallel to the Appalachian mountain chain; (2) near the Great Lakes, the maximum compressive stress tends to be tangential to the Michigan basin; and (3) in the Rocky Mountain States, the maximum compressive stress is parallel to the Rocky Mountains.

The apparent conflict between data points 9 and 18 is explained by the fact that the data for site 18 were obtained in an underground borehole that was drilled vertically into the extremely irregular surface of the Precambrian

igneous basement rock that underlies the mine under investigation. This basement rock was exposed in the mine. The determined orientation of the horizontal stresses in an underground outcrop of this material may have been a function of the site that was selected and its relationship to the surface contours of the igneous basement rock. The orientation of stresses at site 18 was also controlled by local structure.

The structural geology of the area shown in figure 1 has been studied extensively. In the literature (18) it is stated, "there appears to be a complete absence of faults, as nothing even approaching a break in the strata was observed in either Wyoming or McDowell County. Just across the State line, however, a great thrust fault develops along the northwest flank of the Abbs Valley Anticline, in the vicinity of Borssevian, 3 miles southwest of Pocahontas. It bears south 55 to 60 degrees west, roughly parallel to the State line, and, at the point where it intersects Jacob Fork of Dry Fork, misses the southeastern edge of McDowell County [by] less than 2000 feet. Hence, it is quite evident that the territory of this report [Wyoming and McDowell Counties] is barely west of the great series of faults associated with the formation of the Appalachian mountain system." This series of thrust faults is shown in figure 10 (17). The thrust fault system is believed to be the dominant feature that is influencing the in situ stress field of this region. A portion of the area of influence of this thrust fault system can be seen in figure 9. Data points 3, 15, and 27 are within the area of influence of the system of thrust faults shown in figure 10.

The manner in which the thrust fault system influences the existing stress field is not exactly known. The two leading possibilities are outlined as follows:

The first possibility is that the major forces that formed the Appalachian mountains and the thrust fault system in southwestern Virginia were acting in a direction that was basically northwest-southwest in this area. The formation of the mountains and the thrust faults relieved these major forces, leaving the northeast-southwest component of the stress field as the largest component. It would be this remaining component that we have determined to be the maximum existing compressive stress.

The second possibility is that the existing stress field is only indirectly related to the forces that created the mountains and the thrust faults. This can be explained by the argument that the existing stresses are the result of the far-field, possible tectonic, boundary stresses acting on a structure that is least rigid or stiff in the northeast-southwest directions. The result of such a situation could also produce the in situ stress field that has been found to exist in this area.

Whichever of these possibilities is more nearly correct, or if yet another explanation exists, the fact remains that the maximum compressive component of the existing horizontal stress field in this area is in the northeast-southwest direction.

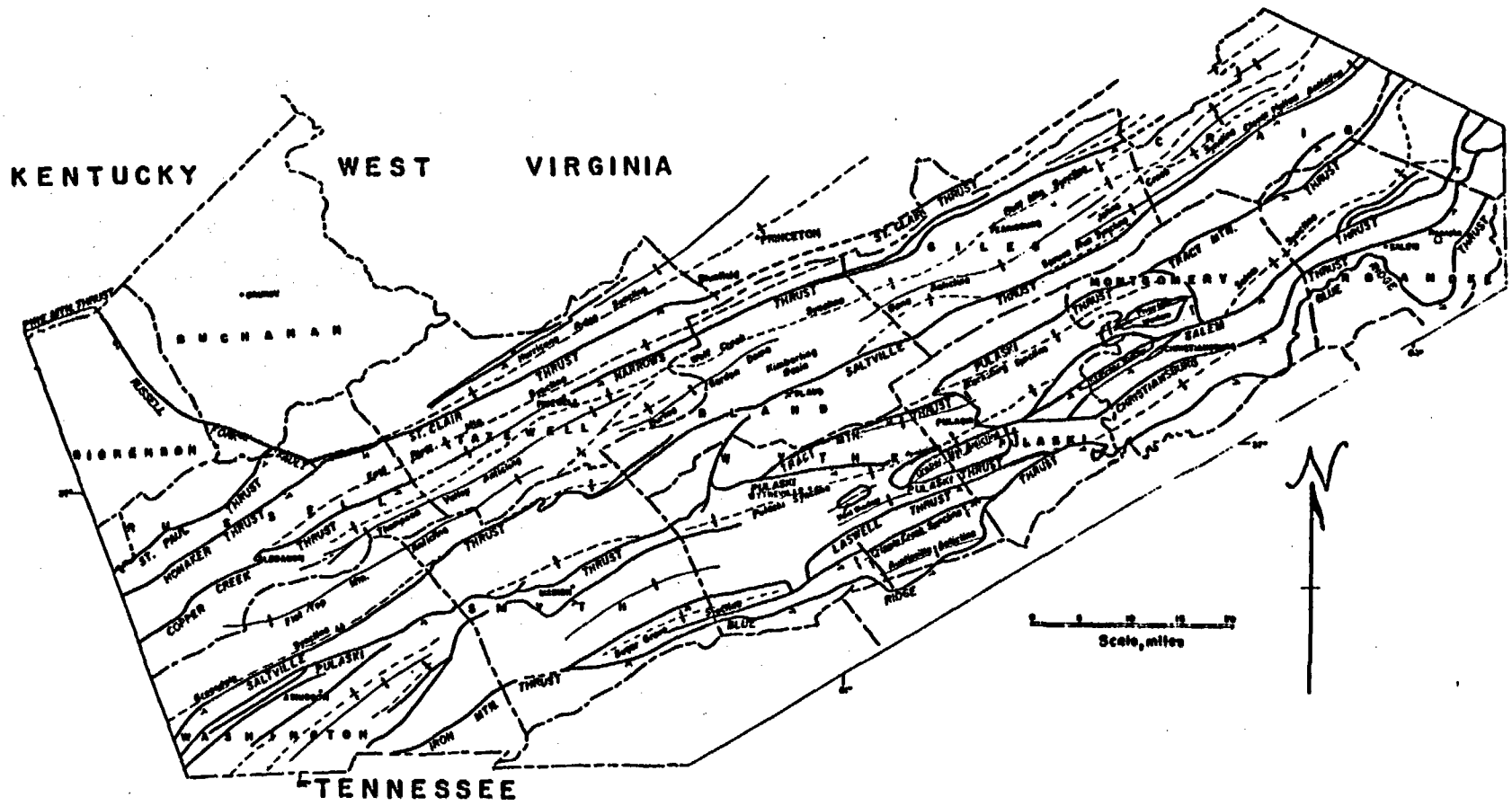

FIGURE 10. - Thrust fault system in Virginia.

FLOOR HEAVE FAILURE MECHANISM

When both the strength properties of the rock involved and the in situ stress distribution have been obtained, one important fact is immediately obvious. This fact is that all rocks involved are sufficiently strong when compared with the in situ stress levels. On the basis of the material presented thus far, a theoretical or numerical analysis of the failing entries, including stress concentration factors due to the geometry of the openings, would predict a totally stable situation. This, however, was not the case. Thus, additional investigations were required. Since the floor heave sometimes occurred many months after an entry was developed, it was decided to look at the time-dependent characteristics of the rocks involved.

Samples of the materials involved were each loaded at approximately one-half of the previously determined unconfined compressive strength as shown in table 1. The deformation of the sample was then recorded as a function of time. The results of two such tests are shown in figures 11 and 12. Figure 11 shows that all time-dependent deformation of a sample from the main floor occurred during the first 20 days and that no additional creep occurred in the final 25 days of the test. In contrast to this, figure 12 shows the time-dependent deformation curve, at a lower stress level, for a sample from the immediate floor. As can be seen, this material deformed, or crept, at a constant rate of 11.3 μin/in/day for the last 27 days of the test. The observed differences between the time-dependent deformation characteristics of the immediate floor and the main floor are key factors in the floor heave process.

The immediate floor member was deposited as a flat sediment and was not cut or broken when the entry was mined with a continuous miner. When the entry is mined, there is an associated vertical strain relief in the floor material directly below the entry. This vertical strain relief is due to the

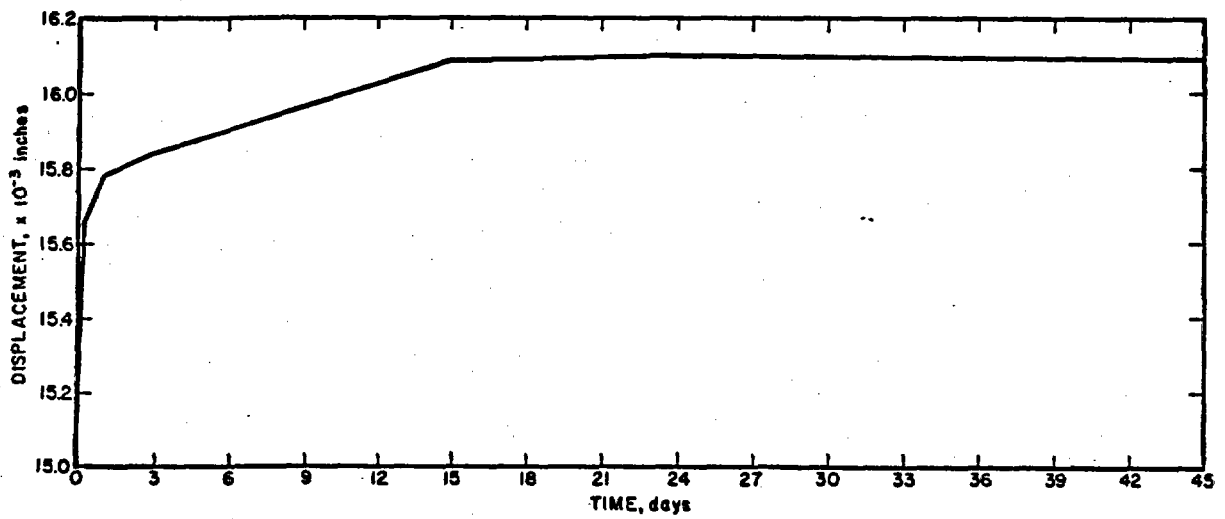

FIGURE 11. - Creep curve for main floor material.

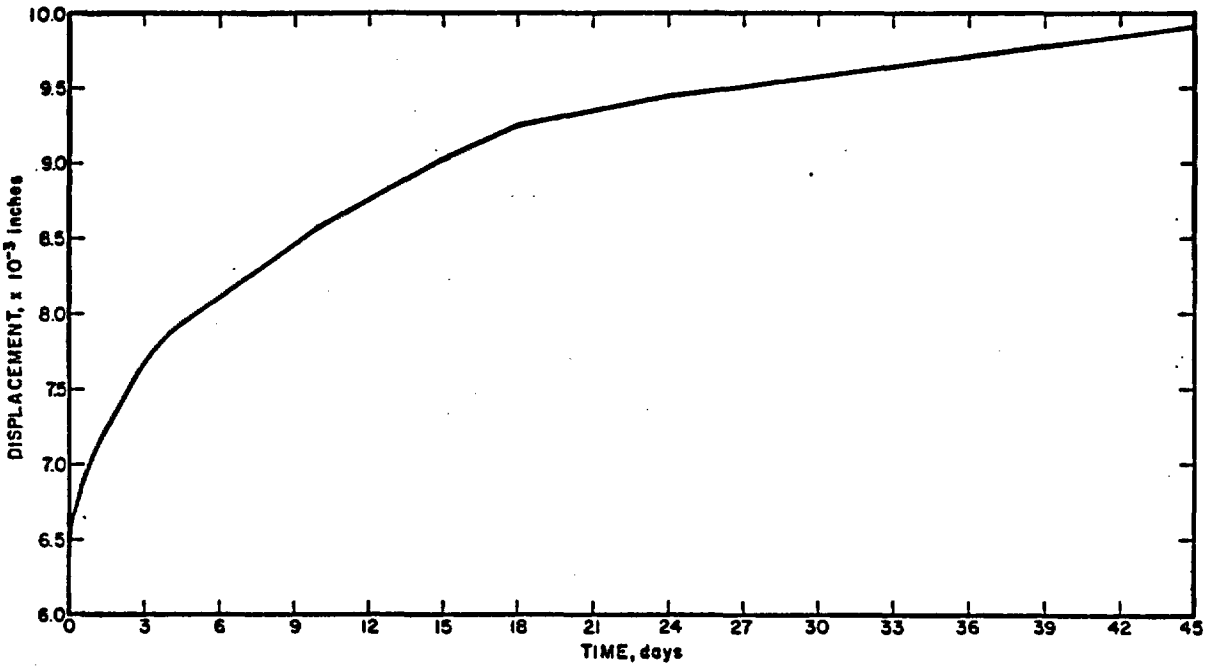

FIGURE 12. - Creep curve for immediate floor material.

creation of a vertical stress envelope, the shape of which is dependent on the geometry of the opening. The vertical strain relief in the material below the entry causes upward displacement of the immediate floor. The magnitude of this vertical displacement is a function of the stored vertical strain and the depth to which the vertical stress is relieved by the creation of the vertical stress envelope. A finite element model of an entry was created to obtain the magnitude of the initial vertical displacement of the immediate floor and an estimation of the zone of influence of the opening.

Figure 13 is a representation of the modeled entry. The model was loaded with the overburden vertical stress predicted by equation 1 and the measured maximum horizontal compressive stress. These values were -800 psi and -3,200 psi, respectively. Average elastic properties from table 1 were used for each material involved. The finite element analysis was conducted in two steps. The first step was to load the model without the entry. The results of this run were taken to be the zero displacement field that existed before mining the entry. The next step was to remove those elements that formed the entry and rerun the program. The displacement differences between the two finite element models are the displacements due to the creation of the opening. The results of this procedure indicate that the immediate floor is deflected upwards 0.07 inch at the center (point A, fig. 13) owing to the creation of the opening. This vertical deflection can be used to calculate the effective area of influence of the opening. The elastic vertical deflection (η) of the immediate floor at point A can be set equal to the stored vertical strain due to gravity loading (ϵ_v) multiplied by the effective depth of the vertical stress relief (d):

$$\eta = \epsilon_v d. \qquad (2)$$

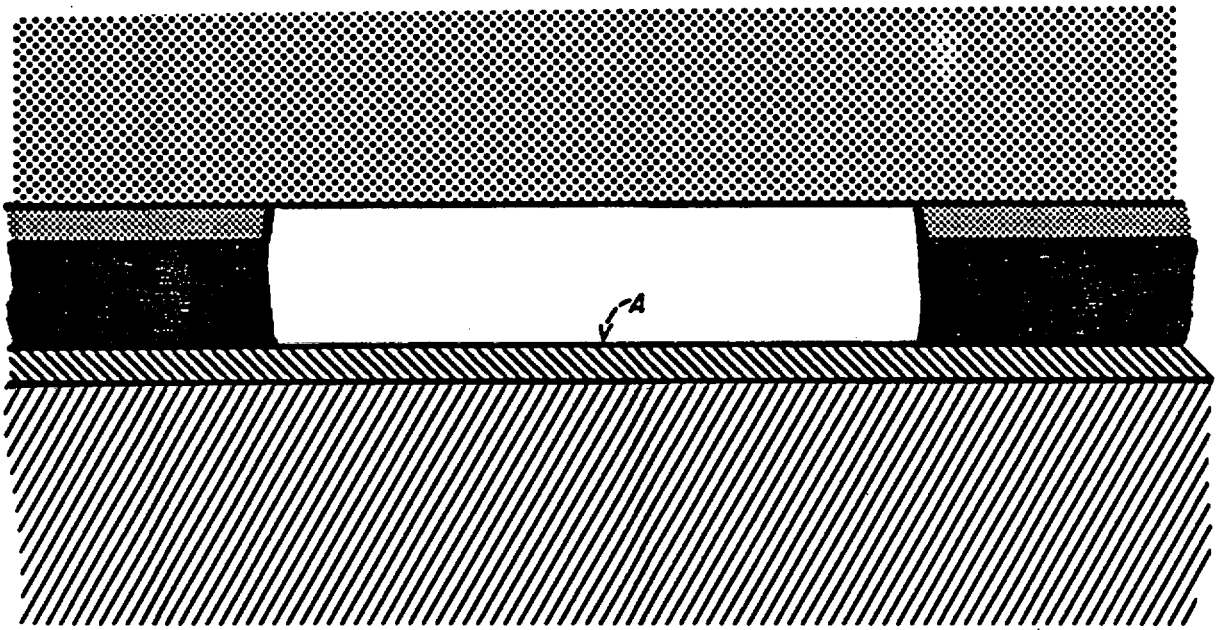

FIGURE 13. - Mined entry.

Since the elastic vertical deflection is known (0.07 inch) and the stored vertical strain can be calculated from the vertical stress (800 psi) and an average elastic modulus (2.96×10^6 psi), equation 2 can be solved for the effective depth of stress relief. Substitution of these values produces the result that the effective depth of vertical stress relief is 21 feet 7 inches directly below point A.

The release of vertical strain below the entry imparts a bending moment into the immediate floor.

It should be pointed out that the creation of the opening only relieves the vertical stress under the entry and that horizontal stress still exists in both the immediate floor and the main floor. Both members are loaded to significant stress levels by the horizontal in situ stress distribution. Due to stress concentrations around the opening, the stress magnitudes in the immediate floor and the main floor may not be the same. The immediate floor is no longer contained in all directions. The presence of the opening will allow the immediate floor to deform with time in a manner similar to that demonstrated in figure 12. The time-dependent deformation of the immediate floor, in addition to the bending moment in the immediate floor, will cause shear stress to develop along the sedimentary bedding planes. The shear strength of such bedding planes is usually quite low. Thus, after some time, the continuing time-dependent deformation of the immediate floor causes a shear failure of the bond between the immediate floor and the material below. Once this bond is broken, the immediate floor can act independently of the material below.

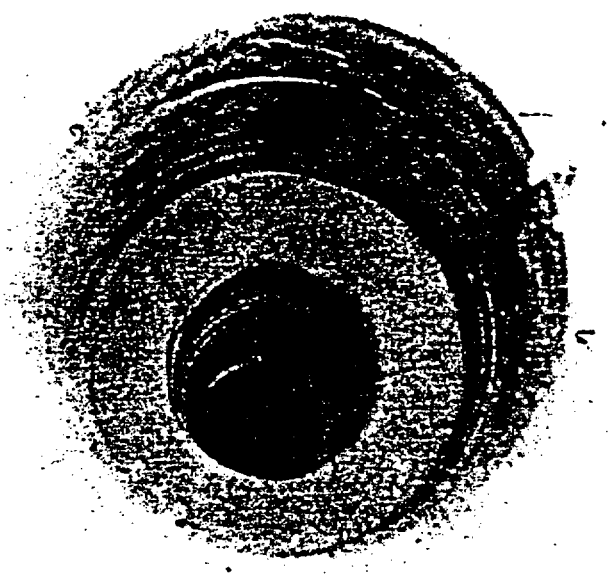

FIGURE 14. - Sedimentary bedding plane failure--the failure surface can be seen in the NX portion of the hole.

Evidence of shear failure along the bedding planes can be seen in figure 14, which is a photograph of borehole C which was drilled in the floor. The first 6-inch portion of this hole was drilled with a 6-inch-diameter bit. The remainder of the hole (22 feet) was drilled with an NX bit. After approximately 2 months, shear failure occurred along a bedding plane. Failure of the bedding plane bond caused the axis of the hole to offset at the plane of failure. The offset in the NX portion of the hole can be seen in figure 14.

The immediate floor is now a curved beam, with a bending moment, which is made of a material that has time-dependent deformation characteristics. This beam contains stored axial strain due to the horizontal stress. The stored axial strain will be relieved by continued bending into the entry. This situation is similar to a long coiled spring in axial compression. Without lateral restrictions, the spring will bend and elongate to its uncompressed length with the application of the slightest bending moment.

The stored axial strain in the immediate floor is

$$\epsilon = \frac{\sigma_h}{E} = \frac{-3{,}239 \text{ psi}}{3.31 \times 10^6 \text{ psi}} = -979 \ \mu\text{in/in.} \qquad (3)$$

The change in axial length of the immediate floor due to bending and the release of this stored strain is

$$\Delta L = \epsilon L = 0.211 \text{ inch}, \qquad (4)$$

where L is the length of the beam (18 feet). From this change in length of the immediate floor, the approximate deflection at the center of the span can be calculated by assuming a displacement distribution. A representation of the curved beam is shown in figure 15. The boundary conditions that must be satisfied by the displacement distribution function are (1) the ends of the beam are clamped by the pillar, thus letting η represent vertical deflection;

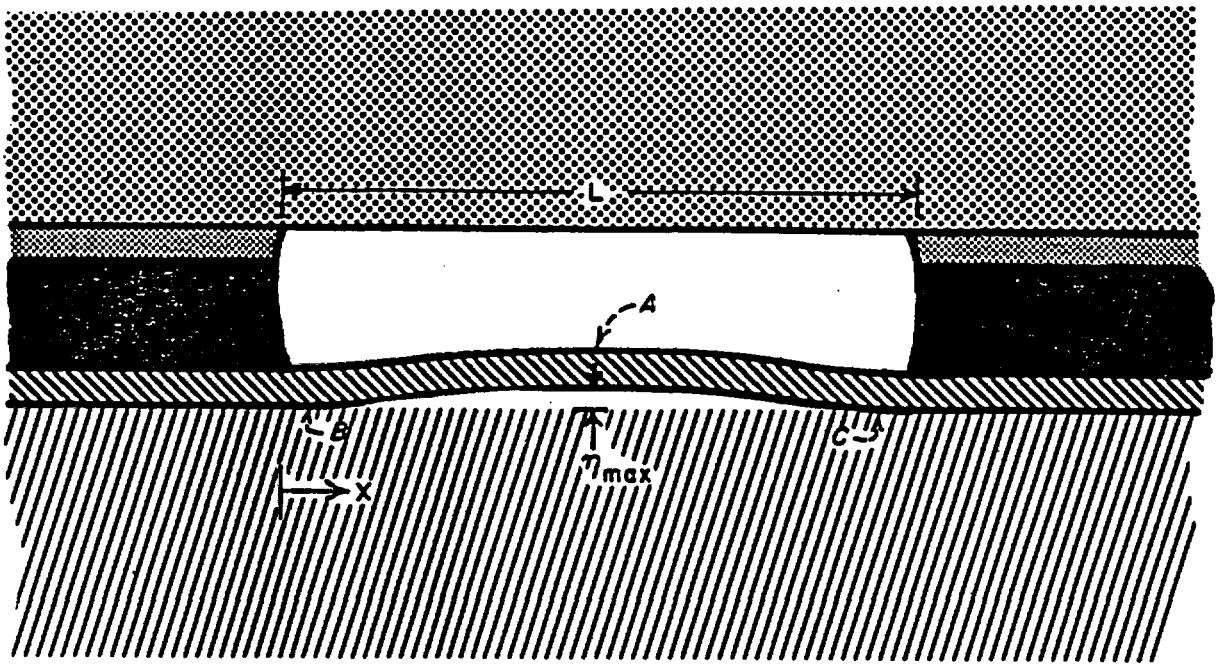

FIGURE 15. - Elastic vertical deflection of the immediate floor.

(2) $\eta = 0$ at $x = 0$ and $x = L$; (3) $\frac{d\eta}{dx} = 0$ at $x = 0$ and $x = L$; and (4) from symmetry η is a maximum at $x = L/2$ (call this maximum displacement A). The most simplified distribution function that satisfies the boundary conditions is

$$F(x) = \frac{A}{2}\left(1 - \cos\frac{2\pi x}{L}\right) = \frac{A}{2}(1 - \cos ax) \tag{5}$$

where

$$a = \frac{2\pi}{L}.$$

The length of the curved beam (call it L′) is now given by

$$L' = \int_0^L \sqrt{1 + (dF(x)/dx)^2}\, dx, \tag{6}$$

$$= \int_0^L \sqrt{1 + (A^2a^2/4)\sin^2 ax}\, dx. \tag{7}$$

The solution of equation 7 is an expression that relates the curved-beam length to the maximum deflection. The initial distance across the opening was 18 feet. The curved-beam length is the original length plus the change due to the release of stored axial strain that is given by equation 4. Thus,

$$L' = L + \Delta L = 216.211 \text{ inches}. \tag{8}$$

Integrating equation 7 and substituting equation 8 into the resulting expression gives the result that the maximum deflection in the center of the entry is 4.305 inches.

The immediate floor can now be analyzed as a loaded column with an initial curvature according to established procedures (8). To account for load eccentricity or initial curvature in a column, it is necessary to determine the maximum moment generated by the end loads or the deflection. This moment depends on the end support conditions, eccentricity of loading, and initial curvature. A separate analysis, based on beam theory, is required for each set of conditions. From such an analysis, moment and deflection distribution can be plotted as a function of axial load. The bending moment distribution for a column which has both ends clamped is shown in figure 16. After the maximum bending moment caused by the initial curvature is determined from figure 16, the maximum stresses (σ_{max}) are calculated from the equation

$$\sigma_{max} = -\left(\frac{P}{A} \pm \frac{Mc}{I}\right). \qquad (9)$$

In equation 9 and figure 16,

A = cross-section area of column,

c = distance from neutral axis to outermost fiber of the column,

E = modulus of elasticity,

I = minimum moment of inertia of column cross section,

L = length of column,

M = maximum bending moment caused by load eccentricity or initial curvature,

P = axial column load,

η = eccentricity of loading or amplitude of initial curvature,

and λ_ℓ = load parameter, $L(P/EI)^{1/2}$.

In equation 9, the first negative sign on the right side appears because compressive stresses are negative in this paper. The choice of the + or - sign before the last term depends on that portion of the beam under investigation. The + sign is used for the fibers in which the direct stress (P/A) and the bending stress (Mc/I) are alike (compression-compression or tension-tension). The - sign applies to fibers in which direct and bending stresses are opposite. Compression bending stresses will be induced at points on the column that are opposite points A, B, and C in figure 15. Tension bending stresses will be induced at points A, B, and C in figure 15. In fact, the maximum tension will occur at points B and C, and one-half that value will occur at point A (22, p. 149).

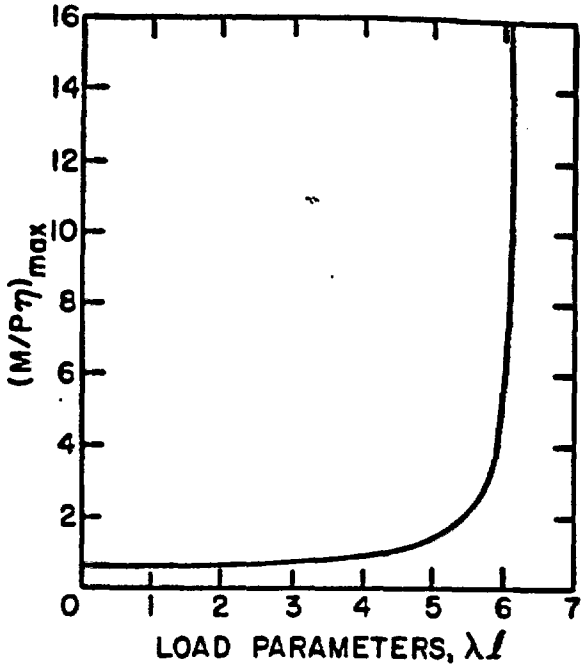

FIGURE 16. - Maximum bending moment curve.

For a 1-foot-thick column of unit depth, length (L) = 216 inches, elastic modulus (E) = 3.3 x 10^6 psi, load (P) = (3,239 psi) x (144 in^2) = 466,000 pounds, and moment of inertia (I) = 1/12 dt^3 = 1,728 in^4, the load parameter $\lambda\ell$, is 1.95. From figure 16,

$$(M/P\eta)_{max} = 0.8. \tag{10}$$

Substituting the column load and the maximum deflection, which has been determined to be 4.305 inches, into equation 10 gives

$$M = 1.6 \times 10^8 \text{ in-lb.}$$

From equation 9, the maximum outer fiber stress is

$$\sigma_{max} = - (3,239 \pm 5,555) \text{ psi.} \tag{11}$$

The maximum compressive stress is -8,794 psi. This value is less than the unconfined compressive strength of the immediate floor as shown in table 1. Therefore, compressive failure will not occur. However, the maximum tensile stress is 2,316 psi. This value far exceeds the tensile strength of the immediate floor, which has been determined to be 705 psi. Thus, tensile failure will occur at point B and/or point C (fig. 15).

The tensile failure at points B or C will occur long before the deflection of the immediate floor reaches the calculated maximum bending deflection of 4.305 inches. The magnitude of the deflection for which the initial

failure occurs can be calculated by reversing the above procedure and solving for the deflection. Failure will occur when the maximum outer fiber stress reaches 700 psi. So,

$$\sigma_{max} = 700 = -\left(3{,}239 - \frac{MC}{I}\right). \quad (12)$$

Solving for M gives

$$M = 1.13 \times 10^6 \text{ in-lb.}$$

Substituting this value into equation 10 gives

$$\eta = 3.03 \text{ inches.}$$

Thus, when the vertical deflection of the immediate floor at point A reaches 3 inches, the tensile stress at point B or C (or both) will exceed the tensile strength of the immediate floor.

The vertical deflection of 3 inches at failure corresponds to a release of stored axial strain of 489 με. Strain release of this magnitude is 50 percent of the available stored axial strain in the immediate floor.

After the initial failure has occurred, the column can behave as if it has pinned or free ends. If the failure occurs at point B and the end of the column is free to move upward, the slab of immediate floor can move vertically until the free end is in the upper corner of the entry. If the failed end is not free to move upward, then further deflection of the column will cause another tensile failure at point A. The driving force for motion or additional failure is the release of stored horizontal energy in the floor under the pillar. As this stored strain is released, sedimentary bed separation similar to that shown in figure 14 may occur. Representations of these two types of failure are shown in figure 17. The similarity between the types of failure shown in figure 17 and figures 2 and 3 should be noted.

The foregoing analysis applies to those entries that are experiencing the majority of floor heave (bearing N 25° W). If the same analysis is applied to the entries that are at 90° to the main entries (N 65° E), the result would indicate that these entries should also be experiencing a great deal of floor heave. This, however, is not the case. The N 65° E entries are experiencing some floor heave, but only about 10 percent of the total. This apparent contradiction can be explained by the argument that the N 65° E entries are not subjected to sufficient normal stress perpendicular to the axis of the opening to cause sufficient differential creep between the immediate floor and the main floor. If the differential creep does not cause shear failure of the bedding plane between the two members, the immediate floor cannot act independently and the preceding analysis would not apply. If, however, the immediate floor becomes separated from the main floor and reacts independently, floor heave does occur and would be predicted by equation 12.

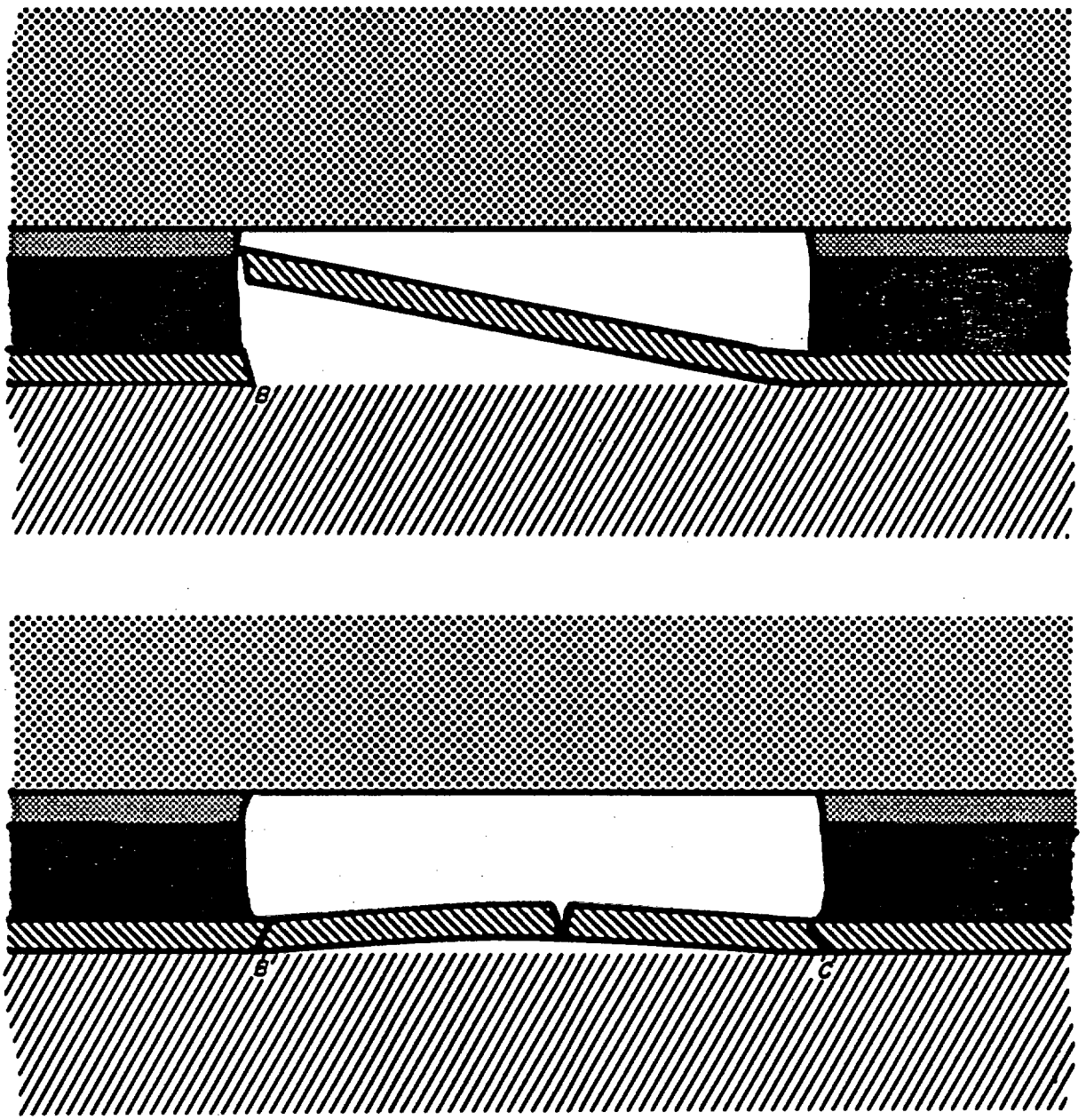

FIGURE 17. - Types of failure.

The analysis that has been presented up to this point has looked at the immediate floor only. In reality, the main floor, as shown in figures 5 and 15, is comprised of sedimentary layers that may also separate and act independently. The analysis has concentrated on the immediate floor because this member has no lateral restrictions and is free to move up into the entry. A stress analysis of a floor member below the immediate floor would require that consideration be given to the lateral load perpendicular to the column. This load would simply be the density of the material multiplied by the distance

between the entry and the layer under investigation. This lateral load on the column can easily be included in the analysis (8).

The method of analysis of the floor heave problem described in this report can be applied to roof members. If the immediate roof of an entry in a coal mine (or any other sedimentary environment) separates along a bedding plane, the majority of the deflection of this member would be due to gravity sag. Further loading of the beam can sometimes be caused by the presence of gas in the roof rocks. Roof bolts tend to hold thin slabs together, forming a beam whose thickness is equal to the length of the roof bolts. The methods by which roof sag magnitudes can be calculated are well known (22, p. 149). The deflection due to gravity sag can then be used to calculate the bending moment that is required in equation 9. For those points on the sagging roof beam at which tension is a maximum, equation 9 can be written in the form

$$\sigma_{max} = -(|\sigma_H| - \sigma_B), \qquad (13)$$

where σ_{max} = stress at the points where the maximum tension will occur,

σ_H = in situ horizontal stress normal to axis of the entry,

and σ_B = stress induced by deflection or bending of the roof beam.

From equation 13 it can be seen that if the in situ horizontal stress is small, the stress at points A and B in figure 18 will be tensile. As the value of σ_H increases, the stress at points A and B will go from tension,

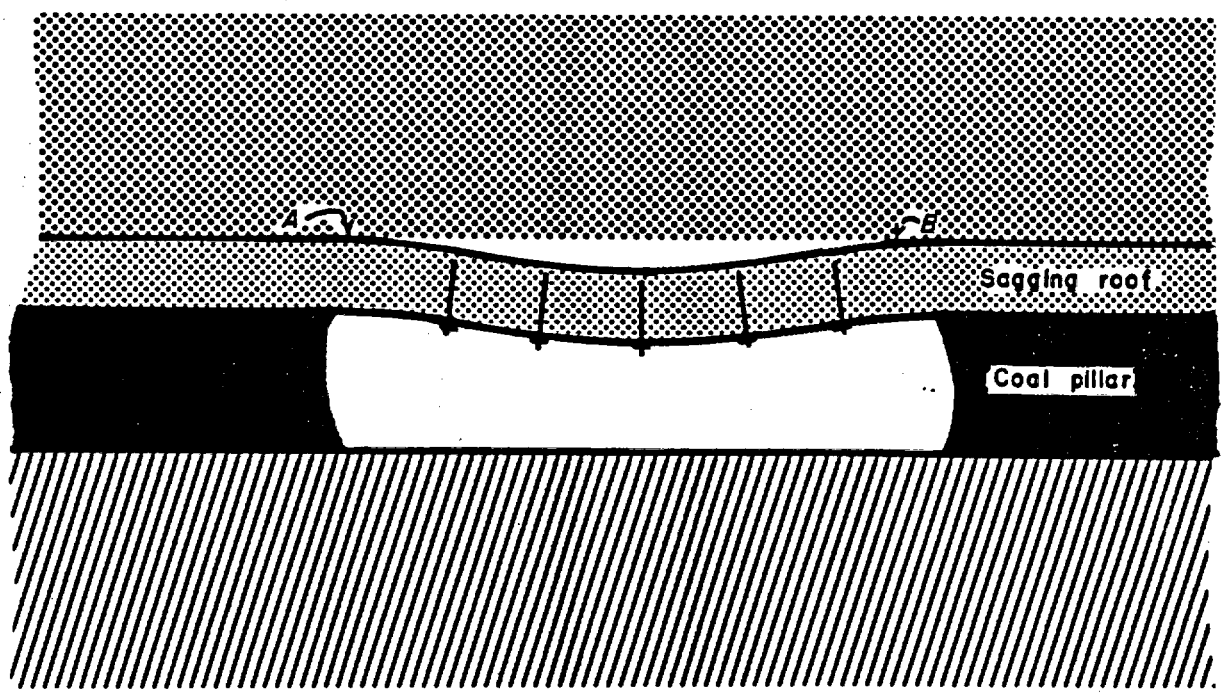

FIGURE 18. - Representation of roof sag.

through zero, to compression. Since rocks are stronger in compression than in tension, compression at points A and B is a more desirable and stable situation. Thus, an excess horizontal stress can add to the structural stability of an opening in certain cases. If the magnitude of the in situ horizontal stress is much larger than that required to force points A and B into compression, increased stability is not assured. Euler buckling of the roof member may occur if the in situ horizontal stress is too large (6).

The use of equation 13 and the previous discussion to assess the stability of roof members is not original with this author (6). It is presented here to emphasize the importance of the concept and to point out that simple beam theory analysis of a mine roof is not complete without some consideration being given to the in situ stress distribution in the plane parallel to the roof.

It is often stated that the most stable underground opening is the opening that has its axis parallel to the direction of maximum normal compressive stress. In general, this statement is true. However, it is possible that under certain conditions, the stability of an opening may be enhanced by mining the opening perpendicular to the maximum horizontal compressive stress, thus forcing all portions of the roof member into compression.

Evidence that the horizontal stress field is affecting beam stresses does exist. This evidence is in the fact that recent stress determinations by the Bureau have shown that the surface stresses at the center of horizontal roof layers are generally in compression, and not in tension as predicted by simple beam theory.

RECOMMENDATIONS FOR MINING

The most obvious solution to the ground control floor heave problem that has been experienced in the Beckley coalbed would be to stress-relieve the immediate floor by cutting a vertical slot (or slots) in the immediate floor member. Such a slot would both relieve stored horizontal strain in the floor and also force the stress down into the contained material in the main floor. The problem with this approach is that the floor is too hard to allow economical cutting with conventional mining equipment. Other considerations preclude stress-relieving the floor by blasting.

It is possible that a high-pressure water jet or jets could be used to cut a vertical slot in the floor. A 2-inch-wide slot cut in the floor, in the manner shown in figure 19, would be more than sufficient to relieve all stored horizontal strain in the floor. The practicality of developing a water-jet-cutting technique to slot the floor will be investigated.

Another solution to the problem would be to reorient the mine in such a way that entries bisect the angles between the maximum and minimum horizontal principal stresses. A reorientation of this type would reduce the normal stress perpendicular to the entries that are not experiencing the majority of the floor heave (N 25° W). However, at the same time, this reorientation would also increase the normal stress perpendicular to those openings in which

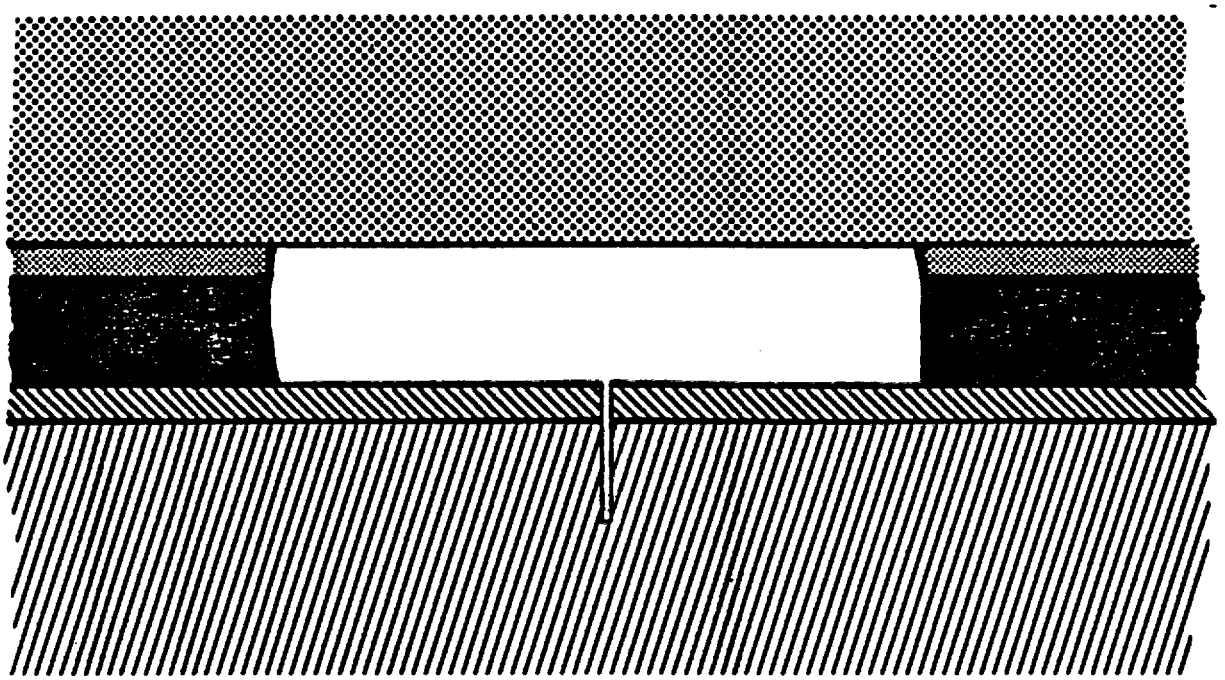

FIGURE 19. - Entry with vertical slot to stress-relieve the floor.

floor heave is a lesser problem. The result would most likely be a situation in which all entries and crosscuts would experience excessive floor heave problems. A mine orientation of 45° to the principal stresses would also put the openings in the coordinate system in which shear stresses in the horizontal plane would be maximized. This situation would not be recommended.

The most rational solution to the mining problems that have been the subject of this investigation is to design an entry and pillar system that deals directly with the problems described. This can be done by driving main entries that will be used for haulage and ventilation in a direction that would be parallel to the direction of maximum compressive horizontal stress. By doing this, the minimum horizontal compressive stress would be acting perpendicular to the entry, thereby reducing the differential creep in the various floor materials. Floor heave in main entries parallel to the maximum stress should be no worse than problems in the existing N 65° E entries. If floor heave in these main entries is intolerable, it may be necessary to stress-relieve the floor by blasting on a limited basis, or to resort to more radical steps, such as bolting the floor in particularly troublesome areas.

Once the main entries are parallel to the maximum compressive stress, the distance between crosscuts should be as large as ventilation requirements will allow. When crosscuts are required, they will be perpendicular to the maximum compressive stress, and thus likely to heave unless preventive measures are taken. Floor heave in the crosscuts can be prevented by reducing the width of the crosscut openings.

The immediate floor in the crosscuts will separate itself from the main floor in the same manner in which it now does. However, if the width of the crosscut is reduced, there will be less axially stored strain available to cause vertical deflection of the floor. If the floor does not deflect as much vertically, the bending moment and resulting stress will be much less. This will result in the reduction of tensile stress at the critical failure points in the floor member.

An example of the effect of reducing the crosscut width is appropriate. If the crosscut width is reduced to 12 feet, the vertical deflection due to the release of stored axial (horizontal) strain in the immediate floor would be 2.869 inches. This value is arrived at by equation 7 with an appropriate value of L'. Solving equation 9 for this new geometry gives the result that the maximum stress at the critical points on the floor member is

$$\sigma_{max} = -(3{,}239 \pm 3{,}713)\ \text{psi}. \qquad (14)$$

The maximum compressive stress would be -6,952 psi. This value is well below the compressive strength of the material involved. The maximum tensile stress at the critical points on the floor member would be 474 psi. Tensile stress of this magnitude is below the tensile strength of the immediate floor, which was determined to be 705 psi. Thus, the floor will deflect vertically, but not fall.

Since the pillars in this recommended design would be longer than present pillar lengths, current extraction efficiency could be maintained by decreasing the width of the pillar. The resulting rectangular pillars could provide the same amount of vertical support as do the present square pillars. The proposed mining plan is shown in figure 20.

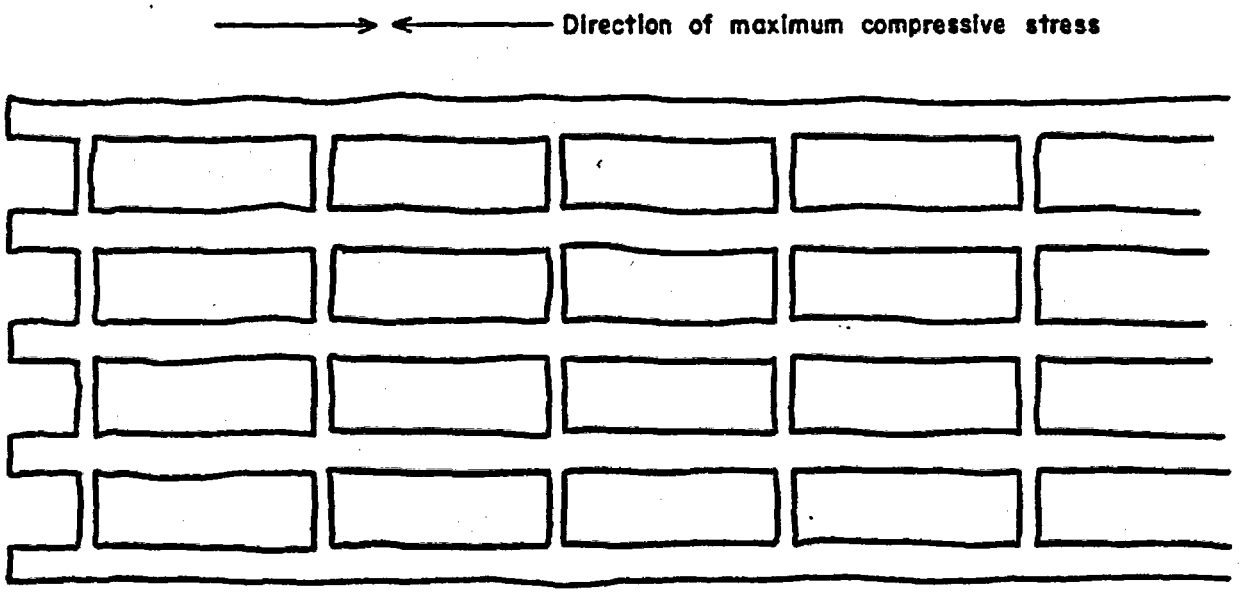

FIGURE 20. - Recommended entry and pillar design.

When permanent entries are required in the direction of minimum horizontal compressive stress, it may be necessary to sacrifice outer entries to shield or stress-relieve inner entries. The effectiveness of this concept, as well as spacing of entries and the mining sequence that would optimize this system, could be determined by experimentation.

SUMMARY

There are probably as many types and causes of floor heave as there are types of roof falls. The investigation and analysis that are described in this report may not apply to those mines experiencing floor heave in which the floor contains significant amount of clay and deformations are of a more plastic nature. However, the floor and roof analysis techniques that are used in this paper may have a wide range of applicability in the mining industry. Although the recommendations for mining that are presented are directed at the floor problems, the suggested orientations and geometries will also enhance roof stability.

As mining is conducted at greater depths in increasingly adverse conditions in the future, traditional mining practices will require modifications in order to be successful. These required modifications cannot be arrived at or discovered by the far-too-expensive and dangerous method of trial and error. Rather, improvements in mining technology and safety must be based on sound engineering principles and the science of rock mechanics. This investigation is an example of how rock mechanics can be used as a tool to understand ground control problems related to mine design as well as to improve the extraction efficiency and the safety conditions associated with an underground mine.

REFERENCES

1. Aggson, J. Report on In Situ Determination of Stresses, Mather Mine, Ishpeming, Michigan. BuMines Progress Report 10006, 1972, 25 pp.; available for consultation at Bureau of Mines Denver Mining Research Center, Denver, Colo.

2. _____. Test Procedures for Nonlinearly Elastic Stress-Relief Overcores. BuMines RI 8251, 1977, 15 pp.

3. Becker, R. M., and V. E. Hooker. Some Anisotropic Considerations in Rock Stress Determination. BuMines RI 6995, 1967, 23 pp.

4. Bickel, D. L., and D. R. Dolinar. In Situ Determination of Stresses, Lakeshore Mine, Casa Grande, Arizona. BuMines Progress Report 10018, 1976, 15 pp.; available for consultation at Bureau of Mines Denver Mining Research Center, Denver, Colo.

5. Durelli, A. J., L. Obert, and V. J. Parks. Stress Required To Initiate Core Discing. Trans. SME, v. 241, 1968, p. 269.

6. Duvall, W. I. General Principles of Underground Opening Design in Competent Rock. Proc. 17th U.S. Symp. on Rock Mechanics, Snowbird, Utah, Aug. 25-27, 1976. University of Utah, Salt Lake City, Utah, 1976, p. 3A1-1.

7. Fitzpatrick, J. Biaxial Device for Determining the Modulus of Elasticity of Stress-Relief Cores. BuMines RI 6128, 1962, 13 pp.

8. Griffel, W. Handbook of Formulas for Stress and Strain. Frederick Ungar Publishing Co., New York, 1976, p. 209.

9. Headlee, A. J., and J. P. Nolting, Jr. Characteristics of Minable Coals of West Virginia. W. Va. Geol. and Econ. Survey, v. 13, 1940, 272 pp.

10. Hooker, V. E., J. R. Aggson, and D. L. Bickel. Improvements in the Three-Component Borehole Deformation Gage and Overcoring Techniques. BuMines RI 7894, 29 pp.

11. _____. Report on In Situ Determination of Stress, Rainier Mesa, Nevada, Test Site. BuMines Internal Report, 1971, 7 pp.; available for consultation at Bureau of Mines Denver Mining Research Center, Denver, Colo.

12. Hooker, V. E., and D. L. Bickel. Overcoring Equipment and Techniques Used in Rock Stress Determination. BuMines IC 8618, 1974, 32 pp.

13. Hooker, V. E., D. L. Bickel, and J. R. Aggson. In Situ Determination of Stresses in Mountainous Topography. BuMines RI 7654, 1972, 19 pp.

14. Hooker, V. E., and C. F. Johnson. Near-Surface Horizontal Stresses Including the Effects of Rock Anisotropy. BuMines RI 7224, 1969, 29 pp.

15. Horino, F. G., and J. R. Aggson. Pillar Failure Analysis and In Situ Stress Determination at the Fletcher Mine, Bunker, Mo. BuMines RI 8278, 1978.

16. Keatley, J. P. Report on the Glen Rogers Mine, Raleigh-Wyoming Mining Company, Glen Rogers, W. Va. W. Va. State Dept. of Mines, April 1929, p. 7.

17. King, P. B., J. Hadley, R. Dietrich, E. Class, J. Rogers, and B. Cooper. Tectonics of the Southern Appalachians. VPI Dept. Geol. Sci., Memoir 1, 1964, 114 pp.

18. Krebs, C. E., and D. D. Teets, Jr. County Reports, Wyoming and McDowell Counties. W. Va. Geol. Survey, 1915, 130 pp.

19. Lotz, C. W. Probable Original Minable Extent of the Bituminous Coal Seams in West Virginia. W. Va. Geol. and Econ. Survey Map, 1970.

20. Obert, L. In Situ Determination of Stress in Rock. Min. Eng., v. 14, August 1962, p. 51.

21. _____. Triaxial Method for Determining the Elastic Constants of Stress Relief Cores. BuMines RI 6490, 1964, 22 pp.

22. Obert, L., and W. I. Duvall. Rock Mechanics and the Design of Structures in Rock. John Wiley & Sons, Inc., New York, 1967, pp. 149, 286, 329, 333.

23. Obert, L., and D. E. Stephenson. Stress Conditions Under Which Core Discing Occurs. Trans. SME, v. 231, 1965, p. 227.

24. Popp, J. T., and C. M. McCulloch. Geological Factors Affecting Methane in the Beckley Coalbed. BuMines RI 8137, 1976, 35 pp.

25. Skinner, E. H., G. G. Waddell, and J. P. Conway. In Situ Determination of Rock Behavior by Overcoring Stress Relief Method, Physical Property Measurements, and Initial Deformation Method. BuMines RI 7962, 1974, 87 pp.

*U.S. GOVERNMENT PRINTING OFFICE: 1978-703-103/6

INT.-BU.OF MINES,PGH.,PA. 22854

PRELIMINARY

REPORT
CASE HISTORY STUDY
HIGH IN SITU STRESSES
UNDERGROUND EXCAVATION

prepared for

Rockwell Hanford Operations
Basalt Waste Isolation Project
Richland, Washington 99352

prepared by

LACHEL HANSEN & Associates, Inc.
P.O. Box 5266
Golden, Colorado 80401

P.O. Box 741
Bellevue, Washington 98009

CASE HISTORY XIII - APATITE - NEPHELINE MINES, KHIBINSKY REGION, USSR

The state of tectonic stress fields in the Apatite-Nepheline Mines of the Khibinský massif on the Kola Peninsula, USSR, was determined through field measurements and observations. Observations of the rock spalling process indicated that rock did not break away from the entire perimeter of a vertical shaft in highly stressed rock, but rather from the north and south walls only. As a result the vertical shafts which had been mined circular in shape became elliptical in cross section (Figure XIII, a).

Also, horizontal openings directed north-south eventually assumed an arch shape (Figures XIII, a and b).

"Failure of the rock around the openings indicates that the stresses are greater than the strength of the rock in these sections. This was confirmed by strain gage and ultrasonic measurements, which showed that at a depth of about 100-150 m the maximum principal horizontal stress was compressive, had a mean azimuth of 100^{o}, and had a magnitude of 570 kgf/cm^2. At some locations around the periphery of the opening, the stresses were equal to the strength of the rock. This was the reason for the observed spalling. The other horizontal principal stress (oriented) at 90 degrees to the major horizontal stress) had an average magnitude of 230 kgf/cm^2.

Horizontal tectonic stresses appear not only in crystalline basement rocks, but beginning at a depth of 2 kilometers in sedimentary rocks as well. Although existing equipment cannot as yet perform the required measurements in deep tectonic and geologic prospecting boreholes, the so-called over pressured or anomalously high stratal pressures observed in oil and gas deposits in moving tectonically active zones on the continents and continental shelves throughout the world are evidence of tectonic stresses. Whereas the normal stratal pressure is equivalent to the hydrostatic head of stratal water from the surface of the earth down to the depth of the deposit, anomalously high stratal pressures are sometimes several times the hydrostatic head. Studies have reported that at depths of over 4.5 km over pressured oil and gas deposits appear almost everywhere and extend throughout deep oil and gas-bearing regions in moving zones of the crust, the so-called Alpine geosynclinal zones and tectonically active plate areas. They arise and exist under the influence of intensive contemporary tectonic processes which deform relatively tight deposits. These deformations

must result from tectonic stresses related to contemporary movements of the crust.

"In the case of a non-hydrostatic distribution of stresses, visual examination allows us to determine whether the greatest principal compressive stress is near vertical or horizontal (possible only for large tectonic forces). This is determined by visual examination of unsupported vertical openings: shafts, raises, winzes and ore passes. If the stability of the rock is the same around the entire perimeter of vertical openings, the maximum compressive stress is vertical. If the maximum principal compressive stress is horizontal, brittle fracture of the rock will occur in the walls of vertical openings. The direction of the maximum principal stress can be determined from the fracturing directions."(54)

A diagram and photograph of an opening illustrating such local fractures are shown in Figure XIII-2.

"If the maximum principal compressive stress acts in a horizontal direction, circular horizontal openings, e.g., a circular room near a drift, may be examined visually to determine the approximate azimuth of this direction. In openings oriented in the same direction as the maximum compressive stress, roof rock is little damaged, or not damaged at all. The greatest damage to the roof rock is seen in openings oriented perpendicular to the maximum principal stress direction. [see Figure XIII-3]

Visual examination may yield an approximate quantitative estimate of the stresses present. If, for example, brittle fracture and spalling occurs in an opening the stress in the rock mass (in the corresponding direction) is at least 1/4 the compressive strength of the rock σ_c. If, when a borehole is drilled to some distance away from the surface of the opening (at least half its transverse dimension), the core which is withdrawn fails by disking, the maximum compressive stress in the rock mass is at least half of the compressive strength σ_c of the rock. The greater the stress, the more intensive is the disking process.

The next stage in the system of observations, following visual observation, is the determination of the stress by the ultrasonic method. Characteristic locations are selected in the region of the rock being studied for ultrasonic measurements, and observation stations are set up. These stations are sections of the opening in which holes are drilled for subsequent measurement (at least three holes in each of three mutually perpendicular directions). Dead end drifts are convenient for such

measurements."(54)

Typical layouts for observation stations for ultrasonic measurements are shown in Figure XIII-4.

"If the previous stages of study, e.g., visual observation, indicate the probable direction of the maximum principal compressive stress, it is best to drill the boreholes in directions parallel and perpendicular to it..."

"...Ultrasonic measurements usually yield an approximate estimate of the stresses present. In addition, however, the rate at which such determinations can be made, makes it possible to perform measurements at many points, thereby revealing the degree of variability of the stress field. For more precise measurements, the stress relief method is used in the final stages of study. Measurements are made in at least two boreholes (one oriented in each of the principal stress directions as determined by the preceding analysis). Measurements are usually performed in a third borehole oriented in the direction of the third principal stress for control purposes.

When determining the field stresses, the measurements are usually located outside the zone of influence of both the openings from which the measurements are performed, as well as all other openings. Individual dead end horizontal drifts and narrow rooms are the most convenient for such measurements.

Statistical methods are used in summarizing the stress magnitudes and directions obtained from the ultrasonic and stress relief techniques."(54)

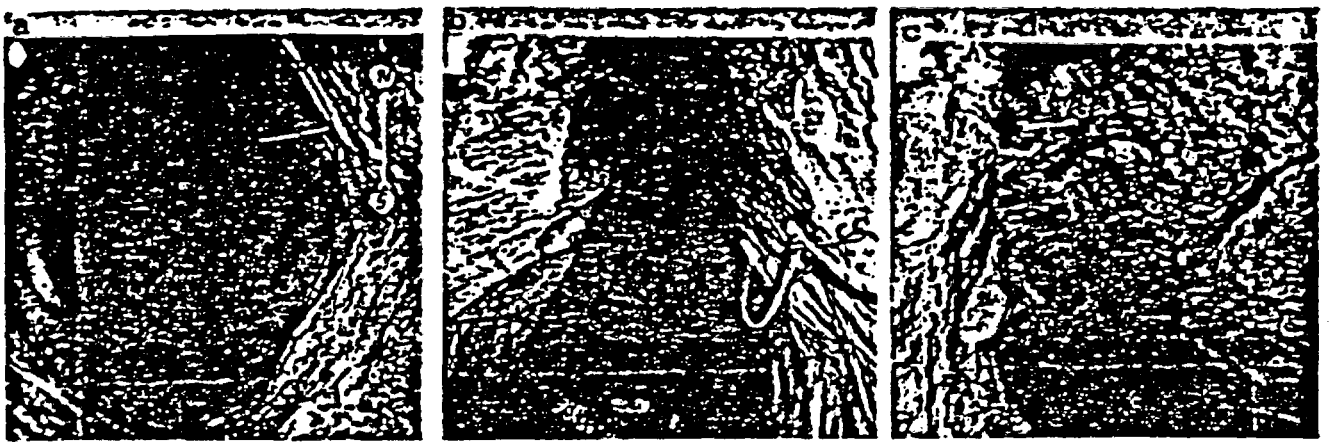

Change in cross-sectional shape of openings east-west in apatite-nepheline mines of the Khibinskiy massiv as a result of tectonic stresses. a - spalling and separation of rock from northern and southern walls of a vertical shaft; as a result, what was initially a circular shaft takes on an elliptical cross section; b - a horizontal working oriented north-south, rock falls from the roof producing an arched shape; c - nature of fracture of roof rock.

FIGURE XIII-1

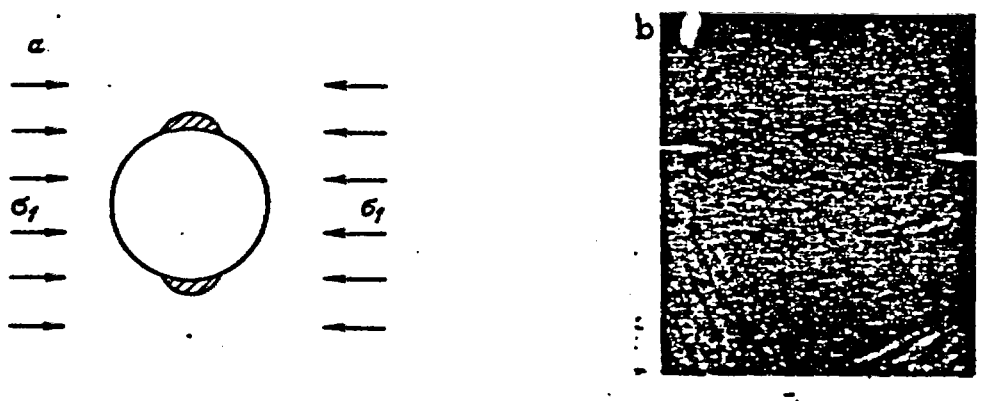

Orientation of zones of brittle fracture (shaded areas) of rock in the cross section of a vertical opening and its relationship to the direction of the greatest principal compressive horizontal stress (2); an example of fracture of the walls of a raise (b).

FIGURE XIII-2

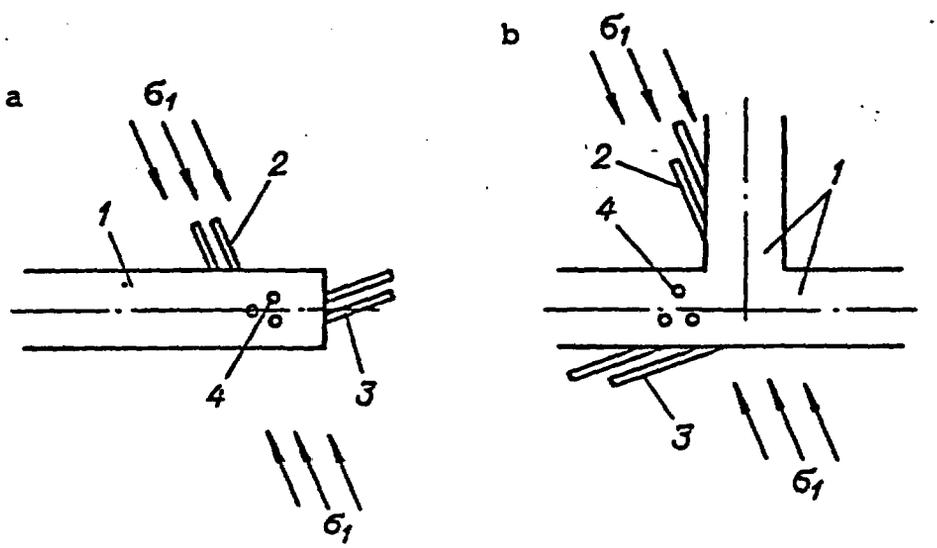

Typical diagrams of observation stations for ultrasonic measurements. a - dead end; b - two perpendicular drifts. 1 - plan of drift; 2 - boreholes in walls parallel to presumed direction of stress σ_1; 3 - boreholes in wall perpendicular to assumed direction of stress σ_1; 4 - holes in roof.

FIGURE XIII-4

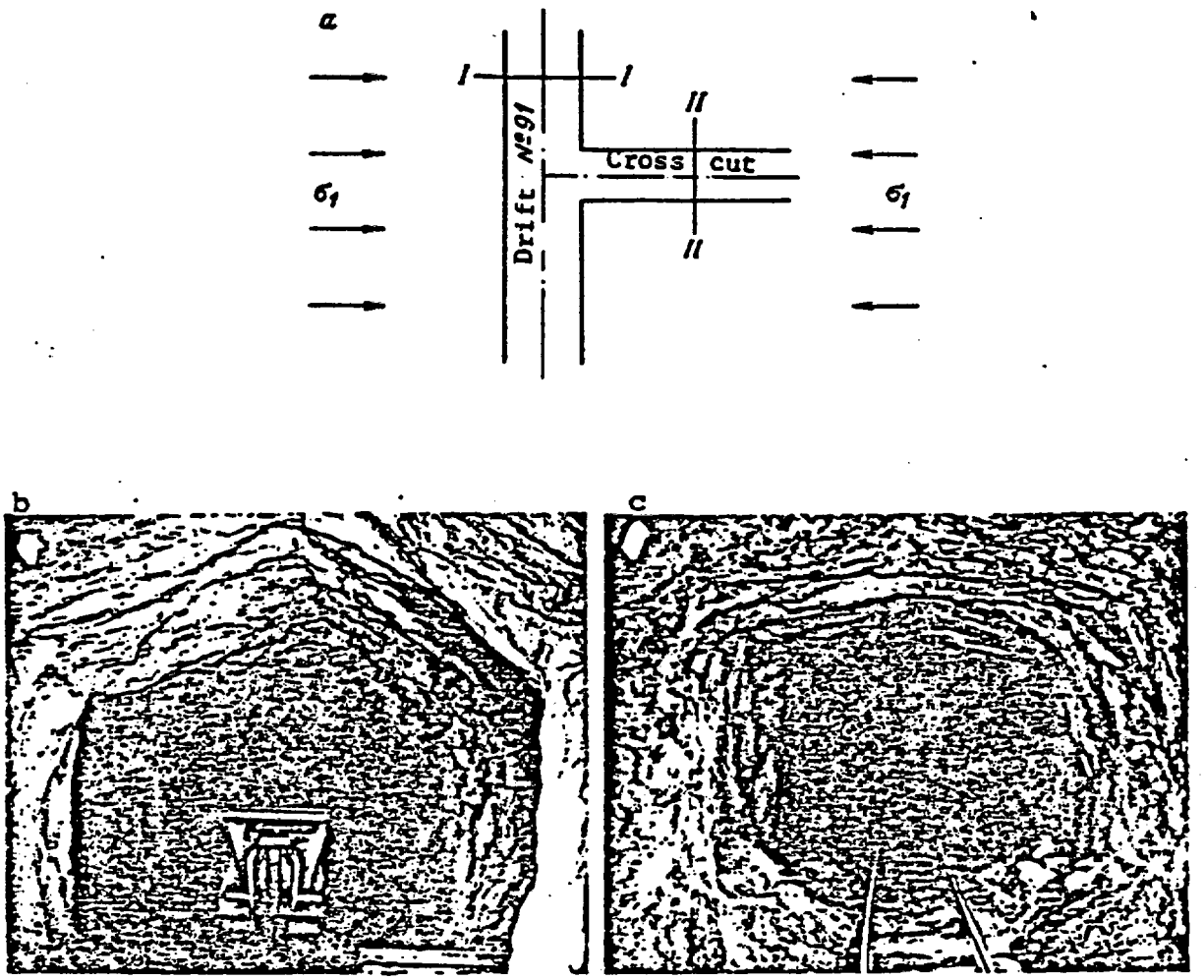

Variation in behavior of rock in the roof of horizontal workings as a function of their orientation relative to stress σ_1 ("Vitimskiy" mine of the "Mamslyuda" group). a - diagram of location of openings; b - longitudinal axis of opening perpendicular to direction of σ_1 (cross section I-I); c - direction of σ_1 along axis of opening (cross section II-II).

FIGURE XIII-3

Report of Investigations 8435

Shaft Design in the Coeur d'Alene Mining District, Idaho--Results of In Situ Stress and Physical Property Measurements

By Michael J. Beus and Samuel S. M. Chan

UNITED STATES DEPARTMENT OF THE INTERIOR
Cecil D. Andrus, Secretary

BUREAU OF MINES
Lindsay D. Norman, Acting Director

This publication has been cataloged as follows:

Beus, Michael J

Shaft design in the Coeur d'Alene mining district, Idaho.

(Report of investigations)
Bibliography: p. 34-38.
Supt. of Docs. no.: I 28.23:8435.

1. Mine shafts. 2. Mines and mineral resources—Idaho—Coeur d' Alene. I. Chan, Samuel S. M., joint author. II. Title. III. Series: United States. Bureau of Mines. Report of investigations ; 8435.

TN23.U43 [TN283] 622'.08s [622'.25'0979691] 79-607065

CONTENTS

ILLUSTRATIONS

ILLUSTRATIONS—Continued

TABLES

SHAFT DESIGN IN THE COEUR d'ALENE MINING DISTRICT, IDAHO–RESULTS OF IN SITU STRESS AND PHYSICAL PROPERTY MEASUREMENTS

by

Michael J. Beus[1] and Samuel S. M. Chan[1]

ABSTRACT

This Bureau of Mines report describes field investigations conducted in the Coeur d'Alene mining district of Idaho to obtain data on rock stress and physical properties. The resulting information has been utilized as input to detailed finite-element analyses to establish structural design criteria for deep-vein mine shafts.

Measurement techniques include the Council for Scientific and Industrial Research biaxial and triaxial strain cells, the U.S. Geological Survey solid-inclusion probe, and the Colorado School of Mines dilatometer. Physical property testing was conducted in the laboratory on core obtained from each test site. Limited in situ physical property tests were also conducted. Reasonable success was obtained with the CSIR equipment, which was considered the most suitable for stress measurement in the study area.

Test sites ranged in depth from 1,200 to 7,700 feet and are described in detail. The stress data were reduced by least-squares linear regression techniques to enable prediction of vertical and horizontal stresses to 7,500 feet. Ratios between the horizontal stresses as utilized for shaft design varied considerably, and a hydrostatic condition is the exception, based on Bureau measurements. Physical properties also varied widely, due to the complex geologic structure.

Analyses of the data in terms of the tectonic history of the area show reasonable correlation. Data from previous rock mechanics investigations from the Coeur d'Alene district were also compiled and presented as part of this report to justify any generalizations regarding stress conditions and physical properties of the district as a whole.

INTRODUCTION

The Coeur d'Alene mining district in Shoshone County, northern Idaho, is the major silver-producing area in the Nation. All major mines in the district have advanced to great depths and are served mainly by vertical

[1]Mining engineer, Spokane Research Center, Bureau of Mines, Spokane, Wash.

shafts for access, emergency escapeway, materials handling, and ventilation purposes. Currently, all shafts in the district have rectangular cross sections and most are supported by timber sets, a design based on 90 years' experience and proven adequacy. As the mines get deeper, many difficulties are anticipated in continuing shaft sinking. The repair work in existing shafts is extensive, especially when major geologic structural discontinuities or highly stressed zones at depth are intercepted. It could, therefore, be advantageous to use rock mechanics to establish preconstruction design guidelines to enhance the structural stability of shafts.

Rock mechanics investigations on opening and support design in the Coeur d'Alene mining district have been conducted by the Bureau of Mines for the past 10 years (1-3, 5-7, 17, 43, 49-50).[2] In situ stress determinations by the overcoring method indicate that the horizontal stress is always higher than the vertical stress in the district. The measured vertical stress may also deviate slightly from a theoretical stress based on overburden calculations. No correlation has been attempted on the relation of measured stresses to geologic and structural features, tectonic history, rock type, or proximity to disturbed ground. Based on previous measurements, the stress field in the district is nonuniform and complex, and in situ stress measurement is extremely difficult.

Most of the physical properties of mine rock from the district have been determined in the laboratory. Quartzites or argilleceous quartzites and some diabase have been studied because of the availability of intact specimens. Rock strength and elastic properties have a wide range of values. Factors such as mineral content, bedding, joints and fractures, and testing variables affect the strength and computed elastic values for the rock.

Deformation of rock masses around mine openings has been measured by several investigators using either closure measurements or the tunnel stress relaxation (TSR) technique (3, 49-50). The rate of deformation is indicative of the stability of the openings and is strongly influenced by opening size and geometry, orientation of the opening with respect to bedding planes, and ground stress. Also, there is generally higher deformation in the horizontal direction than in the vertical, supporting findings from in situ stress measurements. Conventional closure measurements cannot determine the initial elastic deformation that occurs immediately upon excavation.

Little information is available on the specific application of the results of rock mechanics field studies to shaft design in deep, vein-type mines. Karwoski's paper (25), based on previous idealized studies, speculated on the behavior of rock around shafts of different design. He emphasized that basic rock mechanics field data and design guidelines are needed before the sinking of a shaft. Sophisticated numerical methods are available for structural analysis and design. However, numerical analysis needs to be augmented by more accurate input data, including measured stresses and deformation, rock property's support characteristics, and construction variables. This is

[2]Underlined numbers in parentheses refer to items in the bibliography preceding the appendix.

particularly important where traditional design assumptions regarding the direction, magnitude, and nature of applied loads are not applicable.

There are several investigative stages in this project, as follows:

1. The collection of in situ stress data from various depths in mines of the district and pertinent geologic information, and the laboratory and field determination of physical properties of the rock masses.

2. The sinking of circular and rectangular half-scale test shafts, and the monitoring of deformation around the two test shafts.

3. The use of the finite-element method (FEM), together with data obtained from the previous and follow-on work, to predict shaft stability under various conditions.

4. Monitoring of full-scale, existing shafts and establishing baseline data.

5. Construction of full-scale, improved-design, test shafts.

The first phase involved test sites in four mines: August 1973 through the spring of 1975 in the Sunshine mine, in the Star mine and the Caladay shaft station from the spring of 1975 to the fall of 1976, and finally, in the fall of 1977, the in situ stress measurement in the Lucky Friday mine. The second phase began in January 1976 and ended in August 1976, the entire work being carried out in the Caladay shaft station. The third phase is continuing on an intermittent basis. The scope of this report includes the determination of in situ stresses and physical properties of rocks and rock masses in test sites at four mines in the district.

One objective of this report is to dispel some of the uncertainty concerning the stresses to be encountered in typical deep mines in vein-type deposits with steeply dipping strata. This study should be suitable for use both as a source of information for mine operators and ground control engineers, and as design input for structural analysis of shaft and support designs. However, the data presented in this report are not to be construed as complete, but only representative of the Bureau of Mines efforts to date.

ACKNOWLEDGMENTS

The authors appreciate the cooperation given by Callahan Mining Corp., Hecla Mining Co., and Sunshine Mining Co., in providing test sites, labor, and equipment throughout the field tests.

The authors also wish to thank W. H. Luwes of the Republic of South Africa for the CSIR[3] equipment; Daniel Sanders, Fred Kimball, Mike Allen, Jan Patricio, Doug Tesarik, and Bill Vilwock, all of the U.S. Bureau of Mines,

[3]Reference to specific trade names or manufacturers does not imply endorsement by the Bureau of Mines.

for their field and computer assistance; and Jon Langstaff, ground control engineer, Hecla Mining Co., for his special interest and support given to the project.

GEOLOGY AND MINING OF THE DISTRICT

The Coeur d'Alene mining district is situated in the Coeur d'Alene Mountains of Shoshone County, Idaho, between the Montana State line and longitude 116°17', and between latitudes 47°26'15" and 47°33'45". The district is hilly with high peaks ranging from 6,000 to 7,000 feet and a regional relief of 3,000 to 4,000 feet (22). The main stream in the area is the South Fork of the Coeur d'Alene River. Figure 1 shows the district and the mines where the test sites for this investigation are located.

The rocks in the district consist of Precambrian metamorphics of the Belt Supergroup with a maximum thickness reported in excess of 40,000 feet (22).

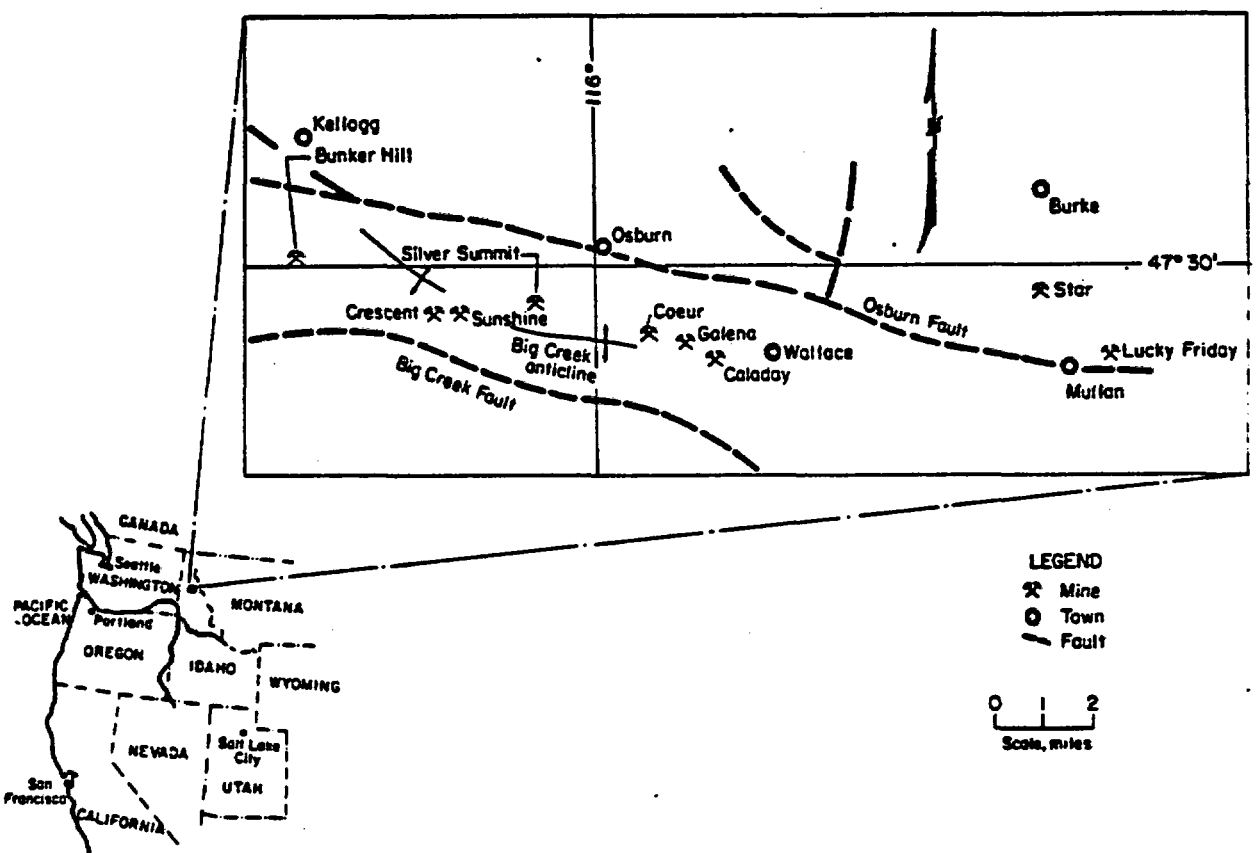

FIGURE 1. - The Coeur d'Alene mining district.

Mineralization occurs mainly in the St. Regis and Revett formations. St. Regis is geologically younger than the Revett formation; both consist mainly of interbedded, fine-grained quartzite and argillite, and dip steeply with frequent overturned beds. There are also Cretaceous igneous, intrusive rocks in the district, occurring as monzonitic stocks with numerous diabase and lamprophyre dikes.

The dominant structural feature is the Osburn fault, which strikes west-northwest and has extensive displacement. There are many smaller faults in the district north and south of the Osburn fault. Most of the faults on the south side are either branches of the main fault or strike nearly parallel to it and dip steeply to the south. Faults that occur on the north side strike toward the north-south direction. The major fold in the district is the Big Creek anticline south of the Osburn fault (fig. 1).

Most major mines in the district are located within a few miles of the Osburn fault or its branches. The mineral deposits occur as steeply dipping veins containing silver-bearing tetrahedrite, galena, and sphalerite. The main mining method is horizontal cut-and-fill stoping using conventional drill, blast, and mucking cycles. Hoist and rail haulage are the major means of transportation of ore, rock, and materials. Rock bolting, timbering, and hydraulic sandfilling are the types of ground support. Shafts are mostly vertical, all rectangular of various sizes (30), most with three or four compartments, and are up to 8,000 feet below the ground surface.

IN SITU STRESS MEASUREMENTS

Determining the magnitude and direction of the in situ stress field in rock masses where pertinent underground openings such as shafts are to be located is an important part in the design of stable rock structures. These data are used to establish criteria of failure for stability evaluation. In addition, with knowledge of the direction of the major principal in situ stress and the maximum and minimum horizontal stress ratio, mining engineers can properly orient a shaft and select a favorable shape.

In some cases, in situ stresses may be theoretically calculated, assuming pure overburden gravity loading and an ideal, lateral confining condition without the influence of tectonic activity. Such simplifying assumptions have not been found appropriate to the stress field in the Coeur d'Alene mining district owing to the complex geologic structural pattern and the extensive relief. In situ stress measurements made at various depths throughout the district tend to verify the high magnitude and nonuniform nature of the stress field. Summaries and results of the measurements are described below.

The Council for Scientific and Industrial Research (CSIR) biaxial strain-cell method (27-28) was used for the in situ stress determination in three out of the four test sites mentioned above. During previous investigations in the district (5), other conventional methods had been tried and found to be unsatisfactory. One of the main difficulties in measuring ground stress is intensive fracturing and bedding in the rock formations, which makes it nearly impossible to successfully complete an overcoring operation. Compared with

other in situ stress measurement methods, the CSIR biaxial strain-cell technique requires a minimum volume of overcore. The successful application in the Coeur d'Alene district for ground stress determination was, therefore, considered quite promising.

The CSIR biaxial strain-cell system consists of the strain cell itself, an installation tool and extension rods, a switch box and cable, and a strain indicator. The strain cell is a plastic shell containing an embedded four-element, 45°, strain-gage rosette to measure strain change after stress relief in the rock core by overcoring. To obtain the complete set of three-dimensional stress data, the drilling and overcoring of at least three holes at different angles are required. The rock modulus of elasticity, Poisson's ratio, and a stress concentration factor at the center of the flattened end of the borehole are also required. The borehole is 2-3/8 inches in diameter (BX) and the minimum length of overcore needed to measure valid stress relief is 2 inches. Figure 2 shows the setup of the CSIR biaxial strain-cell unit.

The U.S. Geological Survey's (USGS) solid-inclusion probes (32) were used in a test site in the Sunshine mine. The gage consists of three-element, strain-gage rosettes mounted orthogonally on the surface of an aluminum ball. The ball itself is embedded approximately in the center of a 3-inch-size (NX) epoxy cylinder gage body. Strain changes are measured by first installing the gage in the NX-size borehole and then overcoring with a 8-inch-diameter overcoring bit. The advantage of this method is that the three-dimensional stress field can be determined with a set of measurements taken at one location in a single borehole.

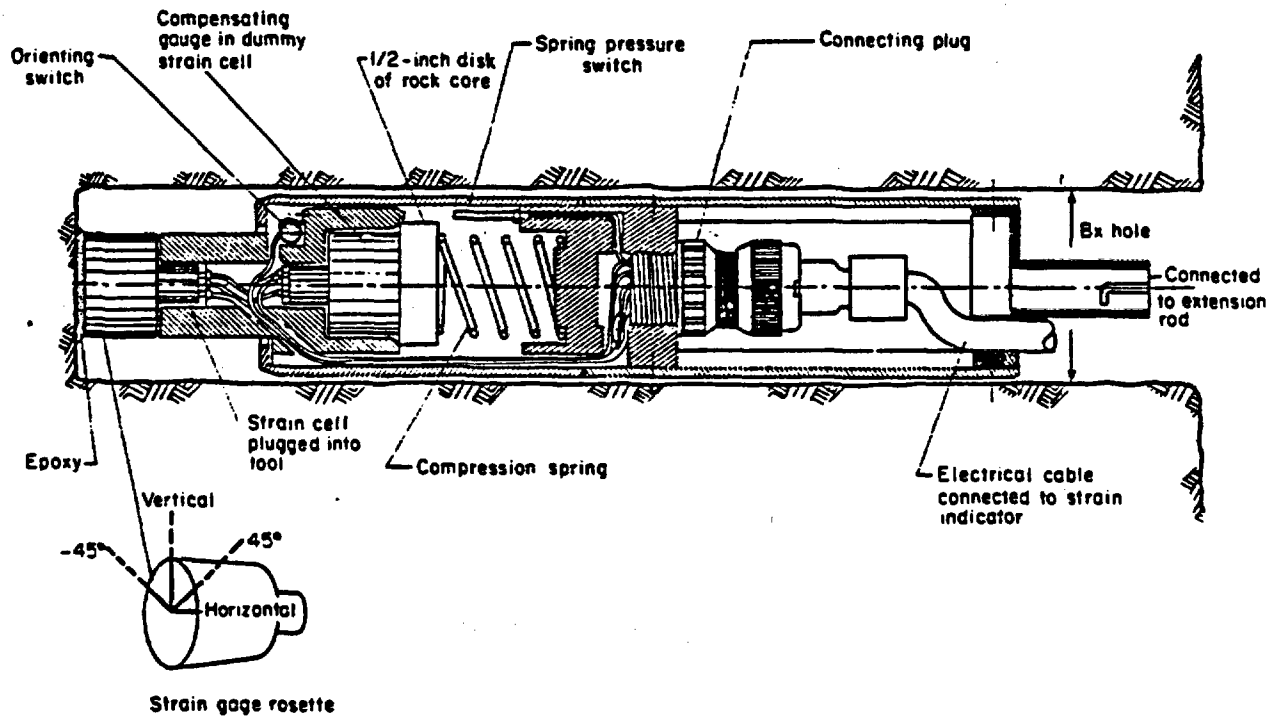

FIGURE 2. - The CSIR biaxial strain-cell setup in a borehole before overcoring.

The four test sites for the in situ stress measurement are, in order of depth, the shaft station of the Caladay project (1,220 feet deep), the 4250 level of the Lucky Friday mine (4,250 feet), the 4800 level of the Sunshine mine (4,800 feet), and the 7300 level (7,340 feet) of the Star mine.

The Caladay Shaft Station

The Caladay project is located on the south side of the Osburn fault, 1 mile west of Wallace. There was a main adit, several short crosscuts, a shaft station, and its related excavations in the project at the time of investigation. The work was done under a cooperative agreement with the Callahan Mining Corp. The information derived from the investigation was to be used for structural design guidelines before and during the sinking stages of a proposed rectangular shaft.

The test site for the in situ stress determination is approximately 5,000 feet inside the portal of the main adit and is situated roughly 200 feet northeast of the shaft station. The site is within steeply dipping (65° to 70° N) argillaceous quartzite of the St. Regis formation striking northwest at 45°. Figure 3 shows the opening geometry, the location of the test site, the simplified geologic structures, and the orientation of the three overcoring holes. The total overburden at the test site is about 1,220 feet, and the site lies about 300 feet above the adjacent valley floor. There is no excavation between the test site and the ground surface.

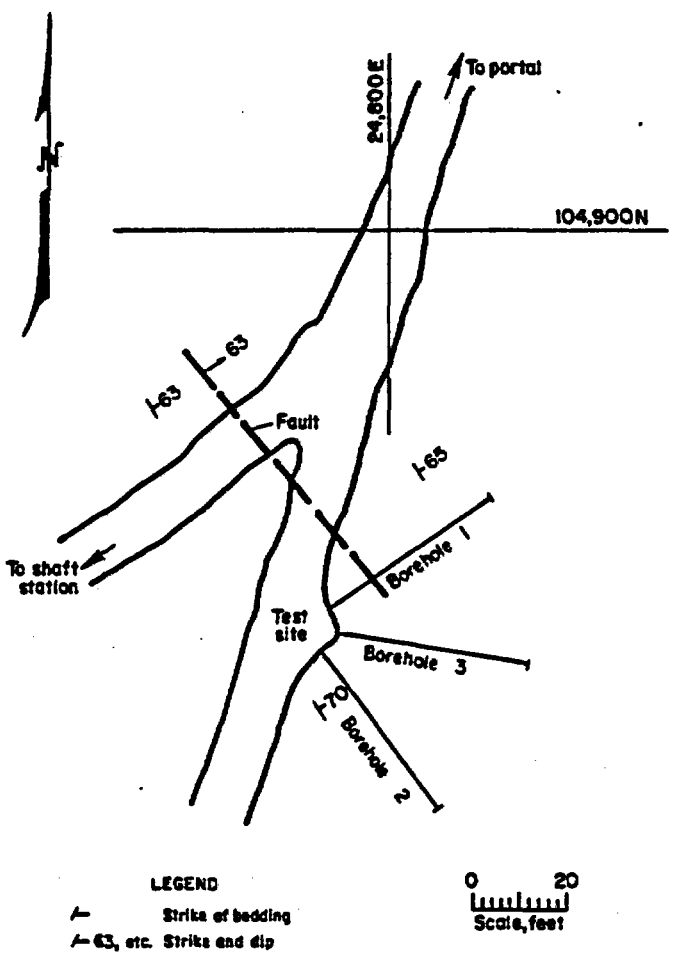

FIGURE 3. - Test site for in situ stress near the Caladay shaft station.

For the in situ stress measurement, the CSIR biaxial strain-cell method was employed. Three horizontal BX holes were drilled at the test site. The depth of each hole was approximately 40 feet, and the axes of the holes were oriented 45° to each other (figs. 3-4). Figure 4 illustrates coplanar setup of the three drill holes and the orientation of the strain-gage

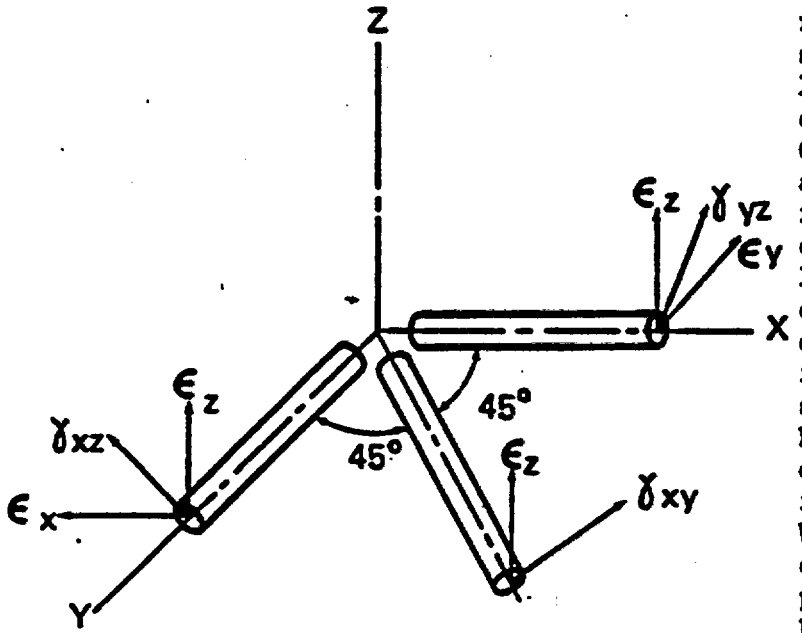

FIGURE 4. - Layout of borehole to obtain required stress data for three-dimensional solution of in situ stress.

rosettes of the biaxial strain cells for the calculation of the three-dimensional stresses. A Chicago Pneumatic CP65 portable diamond drill was used for all drilling, driven by compressed air from mine air lines. Eight biaxial strain cells were installed and overcored in each borehole for a total of 24 tests. As shown in figure 3, borehole No. 1 cuts across the bedding and intersects a small fault at a depth of 15 feet. Water ran out of this hole constantly during testing, presumably from the fault. Drill cores from this hole were generally less than 2 inches long because of the bedding separation and only two out of eight strain cells were successfully overcored. Drill hole No. 2 was drilled parallel to the bedding, and long, competent cores were obtained. The overcoring in this hole was 75 percent successful; that is, only two out of eight tests were unsuccessful. Borehole No. 3 was drilled between boreholes No. 1 and No. 2 at 45°, and, again, fairly competent cores were obtained. Physical properties of the rock were determined both in the laboratory and in the field with a Colorado School of Mines (CSM) dilatometer. Input strain and physical property data were as follows:

Strain, 10^{-6} in/in:	
Normal strain in x direction (ϵ_x).....	34
Normal strain in y direction (ϵ_y).....	60
Normal strain in z direction (ϵ_z).....	133
Shear strain in xy plane (γ_{xy}).....	65
Shear strain in yz plane (γ_{yz}).....	100
Shear strain in zx plane (γ_{zx}).....	137
Modulus of elasticity (E), lb/in^2.....	10 x 10^6
Poisson's ration (μ).....	0.26
Stress concentration factor (S.C.F.).....	1.25

Table 1 shows the in situ free-field stresses at the Caladay project.

The vertical stress is almost exactly what would be expected from the theoretical calculation of overburden using an average weight density of 170 lb/ft^3. The ratio between principal stresses in the horizontal plane is 1.56, which indicates a nonuniform field and is significant for the selection of shape for mine shafts. The ratio of the maximum horizontal stress

to the vertical stress is 0.88, which suggests mainly a condition of lateral confinement for the horizontal stress field.

TABLE 1. - In situ free-field[1] stresses at the Caladay project

Stress (σ), lb/in^2	Bearing	Plunge
Principal stresses:		
σ_1 = 1,854	S 80° E	54°
σ_2 = 960	S 44° W	20°
σ_3 = 696	N 31° W	29°
Secondary principal stresses, horizontal plane:		
σ_{H_1} = 1,280	N 87° E	-
σ_{H_2} = 820	S 3° E	-
Vertical stress:		
σ_V = 1,450	-	-

[1]Calculated from data obtained beyond the area of influence of the immediate opening; that is, at a distance approximately equal to two opening diameters.

The Lucky Friday Mine

The Lucky Friday mine, owned and operated by Hecla Mining Co., lies just north of the Osburn fault and is located about 1 mile east of Mullan (fig. 1). The ore deposits, similar to the others in the district, occur as steeply dipping veins and extend from or near the surface to unknown depths. The veins have also been cut and offset by the numerous faults that occur between two major faults—the White Ledge fault on the north side, and the Osburn fault zone to the south of the mine. Besides the faulting, a system of several small folds combined with a larger anticline and syncline strikes generally east-west to southeasterly through the mine. Rocks in the Lucky Friday mine are St. Regis in the upper part of the mine and Revett quartzite in the lower portion. The contact zone of the two formations is located at about the 1800 level. Figure 5 shows the general geologic features and the main vein. It also shows the location of two shafts currently serving the mine.

Shaft No. 1 is the original shaft, which was sunk from the adit at an elevation of 3,365 feet to the 2000 level. Shaft No. 2, 325 feet south of shaft No. 1, extending from the surface to the lowest working level, is the main hoisting shaft at present. Both shafts are rectangular and are supported by timber sets and rock bolts. The rock opening in the lower portion of the new shaft is about 13 by 26 feet. An investigation (17) during the extension of the new shaft around the 4660 level in 1974 indicated a closure of 16 inches across the short axis of the shaft over a period of 6 months. Most of the closure occurred during the last 2 months of measurement (17, p. 4), and a problem of long-term stability and less-than-favorable

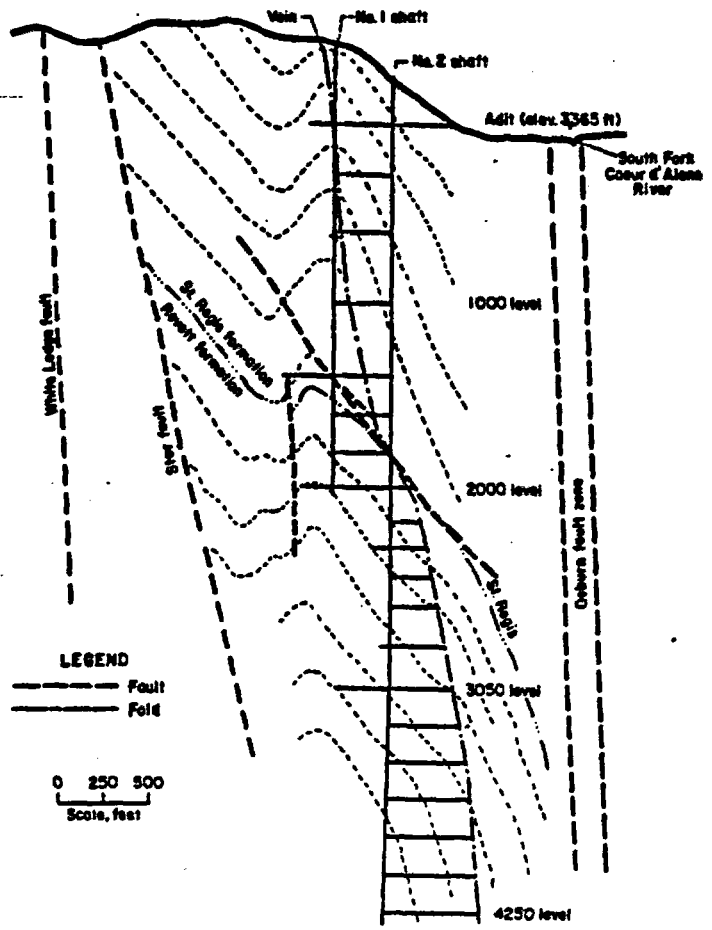

FIGURE 5. - Lucky Friday mine—a generalized section looking east.

orientation of the shaft with respect to the direction of major principal stresses were suspected by the Hecla engineering staff. Hecla Mining Co. was planning to sink a new shaft from the 4450 level downward. To assist in determining a relationship between shaft closure and the shaft orientation with respect to the direction of the ground stresses, the Bureau conducted further shaft-related investigations in the Lucky Friday mine, including in situ stress measurement work described as follows.

The stress measurement was first taken at a spot near the proposed shaft site on the 4450 level using the CSIR biaxial strain cells. The drill used in the Caladay project was employed in this investigation. A hole was drilled to a depth of 30 feet and several unsuccessful attempts were made to obtain meaningful strain data. Intensive fracturing in the rock and unusually large amounts of water flowing into the borehole through the fractures were the main causes of failure. Changing direction of the boreholes did not remedy the situation and the site was abandoned.

A second site was selected in which stress measurement was subsequently carried out successfully. This test site was located on the 4250 level and is between the main shaft and the projection of the proposed shaft site. Figure 6 shows the location of the test site, the bearing of the test holes, and the simplified geology. The site is in the Revett quartzite and at the end of a small anticline plunging southeasterly, as shown in figure 6. Three holes were drilled 45° apart in a coplanar pattern. The depths were approximately 35 feet for hole No. 1 and less than 30 feet for hole Nos. 2 and 3. Eight biaxial strain cells were installed and overcored in each borehole making a total of 24 tests. Water flowing into the boreholes through fractures was again a problem during testing, causing some high fluctuations in some of the strain readings. Physical properties of the rock were determined entirely in the laboratory.

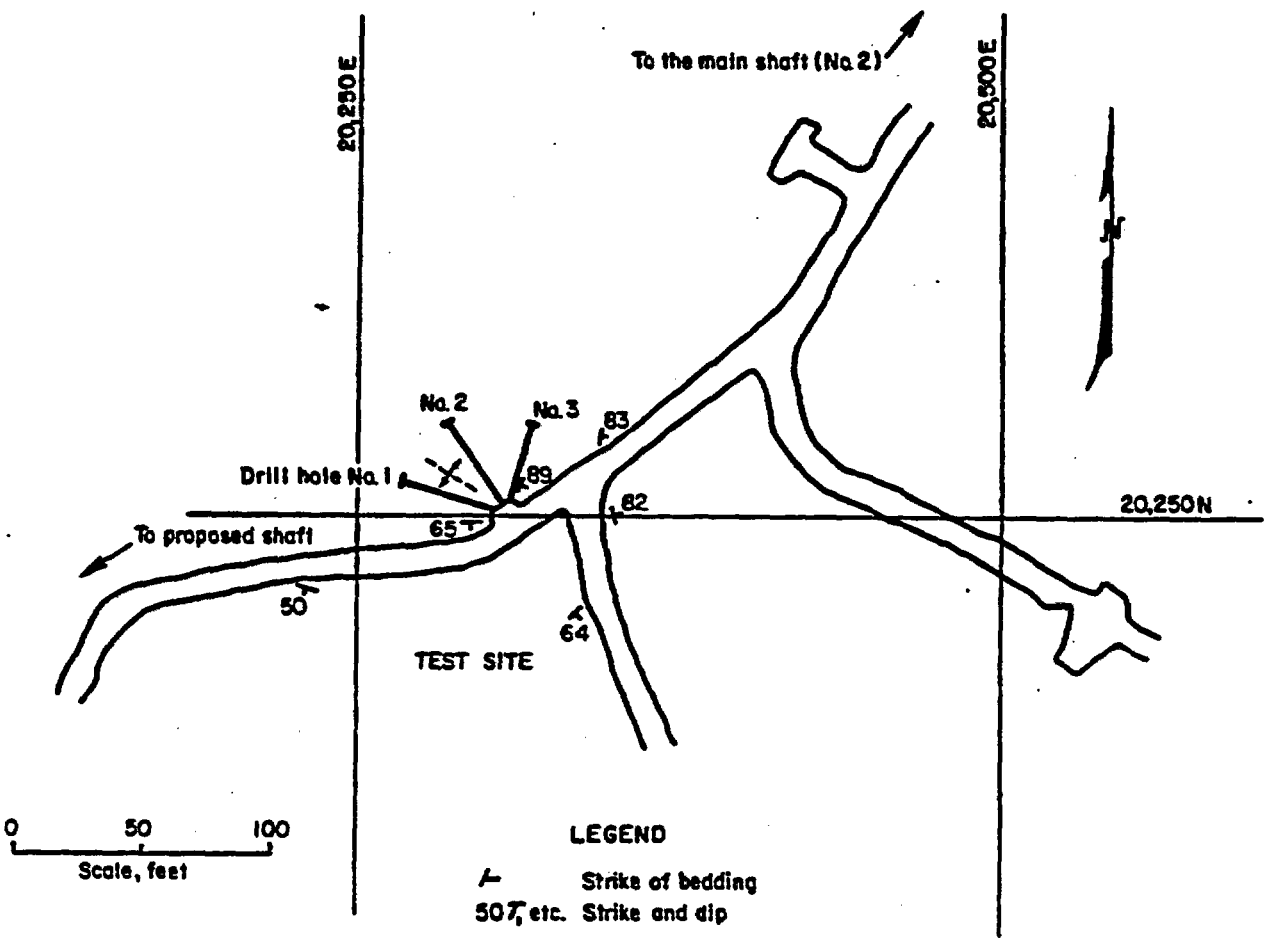

FIGURE 6. - In situ stress measurement test site in the Lucky Friday mine, 4250 level.

The principal stresses at the Lucky Friday site were calculated based on the following input parameters:

Strain, 9 x 10^{-6} in/in:	
ϵ_x	854
ϵ_y	1,080
ϵ_z	308
γ_{xy}	500
γ_{yz}	787
γ_{zx}	787
E, lb/in^2	7.5 x 10^6
μ	.18
S.C.F.	1.25

Table 2 shows the principal stresses determined at the Lucky Friday mine.

The vertical stress is 95 percent of the theoretical value of 5,017 lb/in^2 from overburden computations. The ratio of the maximum horizontal stress to the vertical stress is 1.99, suggesting the presence of tectonic influence in addition to the lateral confinement.

TABLE 2. - In situ free-field[1] stresses at 4250 level, Lucky Friday mine

Stress, lb/in^2	Bearing	Plunge
Principal stresses:		
σ_1 = 10,770	N 37° W	29°
σ_2 = 6,788	N 56° E	3°
σ_3 = 3,460	S 20° E	61°
Secondary principal stresses, horizontal plane:		
σ_{H_1} = 9,518	N 40° W	-
σ_{H_2} = 6,729	N 50° E	-
Vertical stress:		
σ_v = 4,772	-	-

[1]Calculated from data obtained beyond the area of influence of the immediate opening: that is, at a distance approximately equal to two opening diameters.

In connection with the in situ stress measurement work, Allen (1) measured the orientation of some 80 joints along the main haulage and some crosscuts of the 4250 level of the Lucky Friday mine and selected three groups of stress systems that were best fitted to the mapped joint patterns plotted with conventional stereographic projection. One of the three stress systems that might have caused the joint patterns indicates the direction of the major principal stress to be N 30° W, which is almost identical to the findings from the CSIR biaxial strain-cell measurements.

According to Jon Langstaff of Hecla Mining Co., measurements of deformation occurring in a 7-foot-diameter raise bore also were made by Hecla Mining Co. ground control personnel from the 3050 level to the 4250 level. An average of measurement on eight sections throughout the length of the opening indicates that the axis of maximum strain in the raise bore near the 4250 level was N 30° E, implying that the direction of the major principal stress that caused the main deformation was N 60° W. These findings correlate reasonably well with the results of both the CSIR biaxial strain cell and the joint mapping.

The Sunshine Mine

The Sunshine mine lies on the south side of the Osburn fault and is about 3 miles west of the town of Osburn. The ore deposits of the mine occur as steeply dipping siderite veins containing silver-bearing tetrahedrite and galena, similar to the deposits that occur in the other mines in the district. Lithologically, the mine is within the Wallace, St. Regis, and Revett formations, with Revett quartzite being the predominant rock in the lower portion of the mine. Structurally, the mine is located on the north limb of the Big Creek anticline, which is bounded by the Osburn fault on the north and the Big Creek fault on the south. The axis of the anticline and the strike of the faults approximately parallel each other at a trend of N 80° W for several miles (fig. 1).

The horizontal cut-and-fill method is the main mining method used in the Sunshine mine. Rock bolting and timbering are the major types of ground support. The main entry to the underground workings of the mine is the Jewell shaft, which is a rectangular, four-compartment shaft extending from the ground surface to the 3700 level. The long axis of the rectangular cross section of the shaft is oriented roughly at right angles to the strike of the bedding. Figure 7 is an east-west section of the Sunshine mine showing the surface topography, the main shafts, and levels. It also shows the location of the test site for the in situ measurements.

The Sunshine Mining Co. was the first district operator to cooperate with the Bureau for the specific purpose of conducting rock mechanics research to establish shaft-design criteria. The testing for the in situ stress and physical property measurements was conducted at the site of a possible future shaft on the 4800 level, which is in the medium-thick-bedded, fine-grained, Revett quartzite on the west side of the 12 south crosscut. The bedding in the test site and its vicinity strike approximately N 80° W and dip between 75° and 85°, overturned to the south. The joint orientation parallels that of the bedding but dips steeply to the north. Figure 8 is a simplified geologic sketch of the test site, showing essentially the geology described above.

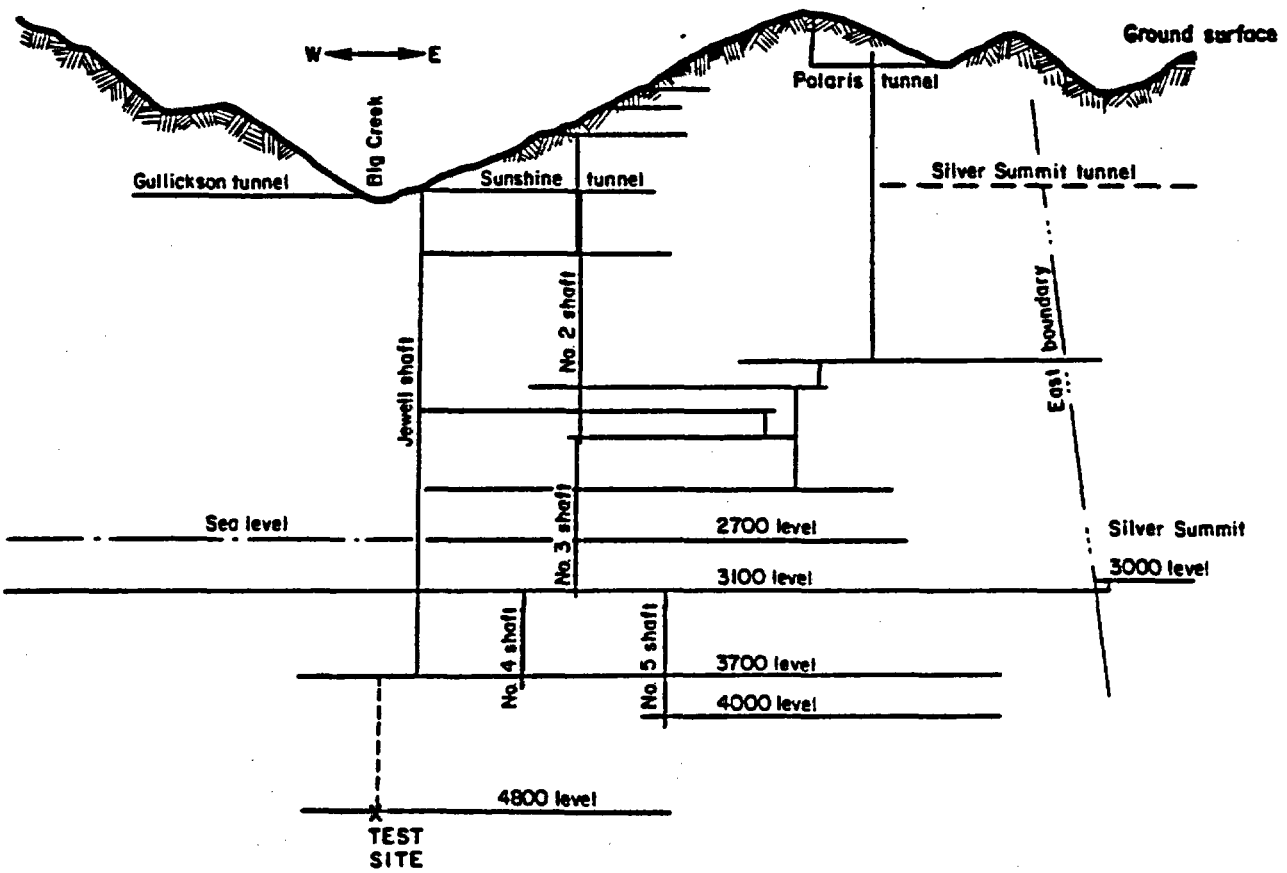

FIGURE 7. - East-west section of the Sunshine mine showing the location of the test site.

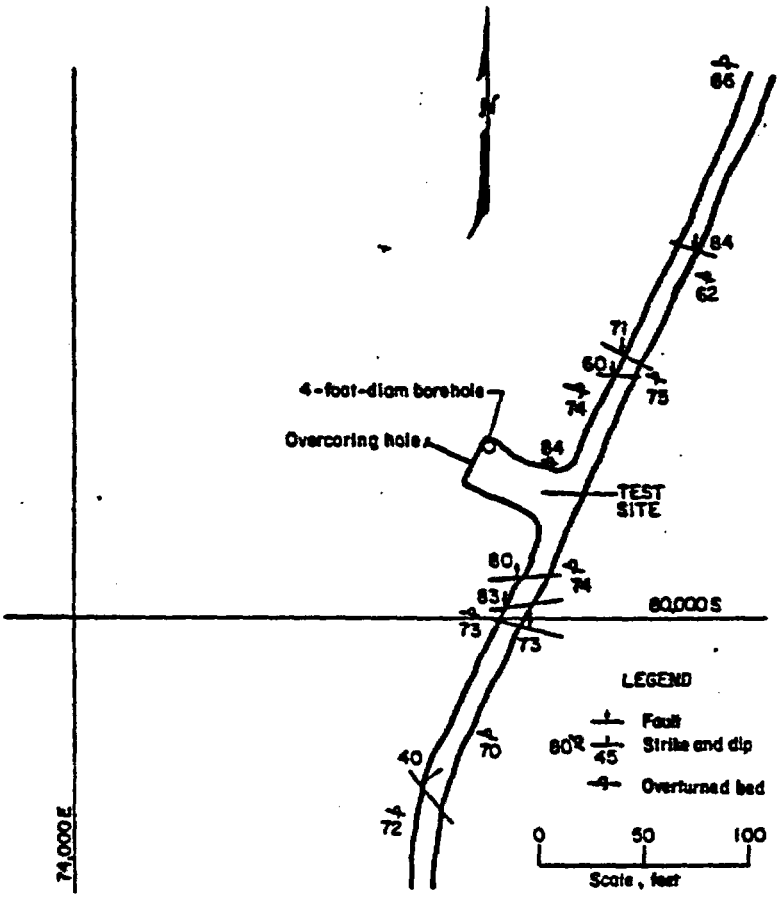

FIGURE 8. - Geology at the test site on the 4800 level of the Sunshine mine.

For in situ stress determination, two tests were made using the USGS solid-inclusion gages at 16- and 18-foot depths of the same overcoring hole shown in figure 8. These depths were predetermined to be sections of competent rock and beyond the influence of the immediate opening. The overcoring operation went smoothly during these two tests, but the calculated vertical stress was considerably lower than anticipated from a gravity-loaded mass at this depth. A finite-element study, together with the subsequent cutaway view of the overcores, shows that epoxy voids running the length of both gages decreased the vertical strain sensitivity by a factor of about 2.5. Table 3 shows the results after application of this correction factor. The vertical stress is slightly higher than the maximum horizontal stress at this site, and the stress ratios in the horizontal plane as determined from these measurements are 1.8 and 3.5 for the two tests. The maximum horizontal stress was oriented roughly parallel to the strike of the bedding, averaging N 80° E. Additional measurements attempts were unsuccessful because of technical difficulties and inability to obtain a sufficient core length.

TABLE 3. - In situ free-field[1] stresses at 4800 level, Sunshine mine

Probe No.	Depth, ft.	Secondary principal stresses	Magnitude, lb/in^2	Bearing	Ratio of horizontal stresses ($\sigma_{H_1}/\sigma_{H_2}$)
A-19	18	Horizontal (σ_{H_1})	5,625	N 88° E	3.5
		Horizontal (σ_{H_2})	1,630	N 02° W	
		Vertical (σ_V)	6,547	-	-
A-22	16	Horizontal (σ_{H_1})	7,224	N 75° E	1.8
		Horizontal (σ_{H_2})	4,006	N 15° W	
		Vertical (σ_V)	7,426	-	-

[1]Calculated from data obtained beyond the area of influence of the immediate opening; that is, at a distance equal approximately to two opening diameters.

Observation of a vertical, 4-foot-diameter raise bore (fig. 8) at the test site verified the horizontal stress ratio obtained by measurement. The lower portion of the raise had spalled into an elliptical shape with the major axis perpendicular to the bedding at approximately N 10° E. Figure 9 is a photograph of the raise borehole looking up from the 4800 level, showing the elliptical shape of the opening. This normally occurs in a biaxial field with the large, compressive stress acting normal to the major axis (28). In this

FIGURE 9. - The 4-foot-diameter raise bore at the Sunshine mine, 4800-level test site showing the elliptical shape. The near-vertical bedding planes are from left to right across the photo.

case, failure in shear was evident along favorably oriented bedding planes of weakness. Evidence of core disking also was obtained from holes drilled normal to the bedding, suggesting a major stress direction compatible with the observed shear failure and actual measurement.

The Star Mine

In conjunction with shaft design and a separate Bureau destressing and rockburst control project, and in cooperation with Hecla Mining Co., overcoring stress relief using the CSIR biaxial strain cells was conducted to determine the in situ ground stress in the east lateral drift of the 7300 level of the Star mine (fig. 1). The Star mine is one of the deepest operations in the Coeur d'Alene mining district. The ore veins dip steeply, and the lower portion of the mine, which is described as very hard, brittle quartzite (22) is within the Revett formation. Previous attempts at in situ stress determination in this mine using other methods, such as Bureau borehole deformation gages, triaxial strain cells, and University of Wisconsin hydraulic fracturing,

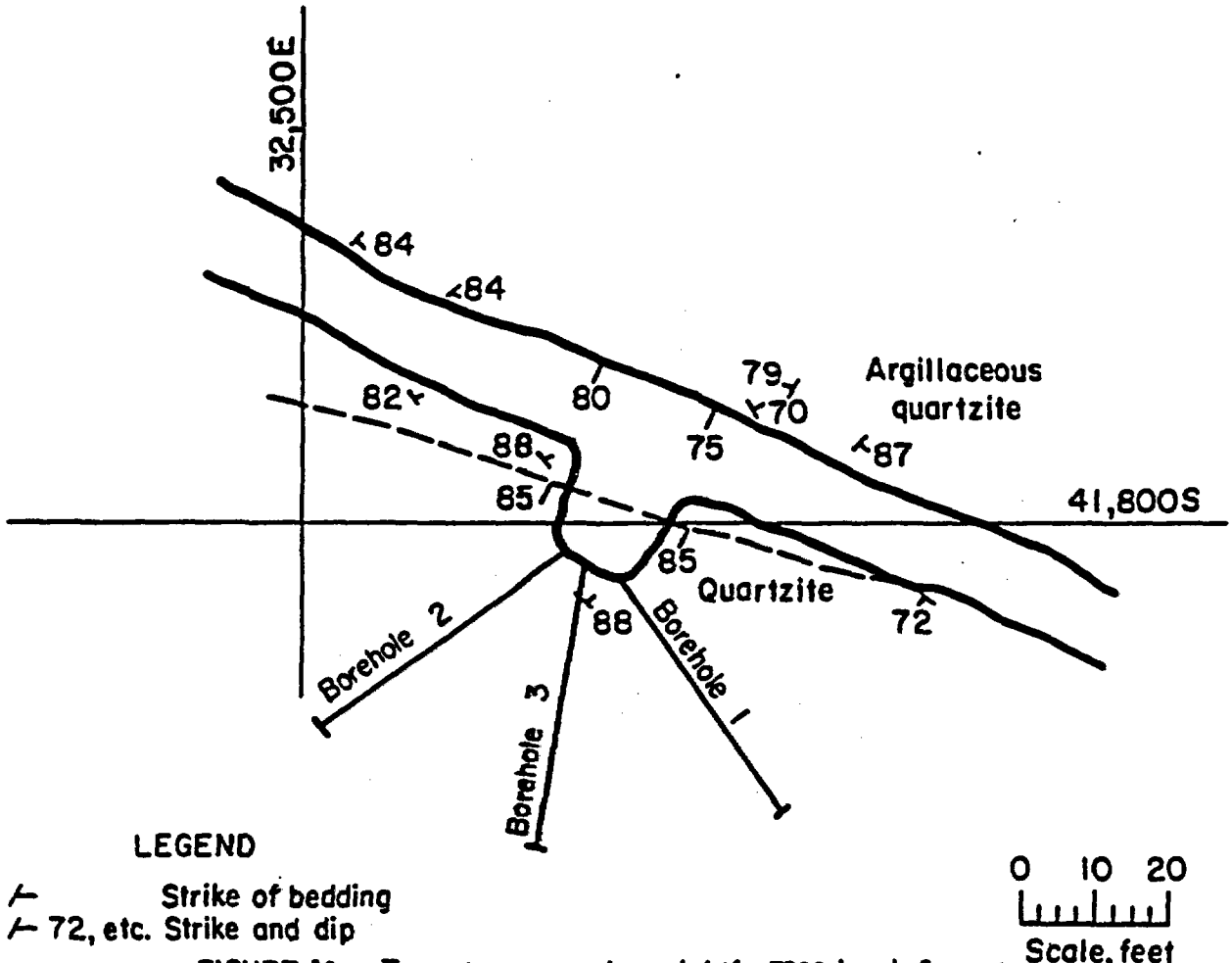

FIGURE 10. - Test site on east lateral drift, 7300 level, Star mine.

were somewhat unsuccessful owing to numerous natural and induced fractures and bedding planes in the rock mass. The biaxial strain-cell method offered the most promise.

At the test site, three horizontal, BX-size holes were drilled 40° apart in a coplanar manner, and CSIR biaxial strain cells were installed and overcored. The depth, approximately 40 feet, and bearing of each borehole and the simplified geology of the test site are shown in figure 10. Since the CSIR biaxial strain-cell method requires relatively short overcores, satisfactory data were obtained despite the many geologic discontinuities.

Physical properties were determined by laboratory testing. These values were used for the stress calculation as shown in table 4, together with a stress concentration factor of 1.25 at the bottom of the BX hole, as was determined from a previous finite-element study.

The three-dimensional principal stresses were then computed using the average strain readings from accepted overcores along with the modulus and stress concentration factors, listed below:

Strain, 10^{-6} in/in:	
ϵ_x	303
ϵ_y	785
ϵ_z	306
γ_{xy}	388
γ_{yz}	407
γ_{zx}	398
E, lb/in^2	9.26×10^6
μ	0.29
S.C.F.	1.25

Average variation of the strain readings resulting from the Star mine field measurement was 47 percent, ranging from 29 percent for normal strain in the y direction to 77 percent for shear strain on the yz plane. (See fig. 4 for orientation of strain planes.) Results of the three-dimensional stress computations (table 4) show the major principal stress alined roughly parallel to the strike of the bedding of the rock formations at S 12° E, plunging at about 28°. The bedding is vertical, and strike varies 20° on either side north at this location. The hypothetical vertical stress from a purely gravitational load, using an average weight density of 170 lb/ft^3 at a depth of 7,340 feet below the ground surface, should be 8,600 lb/in^2. The measured vertical stress is, therefore, about 15 percent lower than that of the theoretical value. There is no single explanation for this deviation, but the complexity of the work mass and inherent measurement error are suspected to be major contributors. Gresseth (18) previously concluded that the maximum ground force during the most recent period of deformation acted horizontally in a general north-south direction, verifying the direction of the major principal stress determined by the present investigation in the Star mine.

TABLE 4. - In situ free-field[1] stresses at the east lateral drift 7300 level, Star mine

Stress, lb/in^2	Bearing	Plunge
Principal stresses:		
σ_1 = 11,033	S 12° E	28°
σ_2 = 7,422	N 84° W	33°
σ_3 = 6,133	N 54° E	45°
Secondary principal stresses, horizontal plane:		
σ_{H_1} = 10,428	S 16° E	-
σ_{H_2} = 6,875	N 74° E	-
Vertical stress:		
σ_V = 7,285	-	-

[1]Calculated from data obtained beyond the area of influence of the immediate opening; that is, at a distance approximately equal to two opening diameters.

GENERAL TREATMENT OF FIELD DATA

Although the success of the CSIR biaxial strain-cell field operations in the Coeur d'Alene district was as high as 50 percent in some cases (6), and most strain readings from redundant gages seemed to agree with each other within a reasonable range, there still existed extremely high or low outlying values in many cases. These might have been caused by high stress concentration in the vicinity of small fractures, partially stress-relieved rocks in a shear zone, or by the presence of moisture and/or poor bonding. Data obtained beyond the area of influence of the immediate opening were utilized in the calculation of the free field stress. Data were rejected if there was a poor epoxy-rock bond, inferior rock surface preparation, insufficient core length, or visible surface fracture. About 50 percent of the data obtained beyond two opening diameters were considered acceptable according to these criteria. Comparisons were often made with the standard deviations of small groups of data obtained from the same zones, usually from the same drill hole. The strain ellipses were calculated by combining readings from different gages to determine the best-fit stress tensor and to eliminate the extreme outliers. No statistical treatment was done on the data from the USGS solid-inclusion gages because of insufficient field data.

Correlation of Tectonic Activity

Figure 11 shows the direction of compressive forces determined at the four test sites in the Coeur d'Alene mining district. They are N 87° E at the Caladay project, N 40° W at the Lucky Friday mine, N 75° E at the Sunshine mine, and S 16° E at the Star mine. Generally, the ground forces at the first three locations are acting at a small angle or nearly parallel to the Osburn fault. According to a popular hypothesis of tectonic evolution of the Coeur d'Alene mining district (22, p. 133), there were three stages in the development of the tectonic setting of the district. In the first stage,

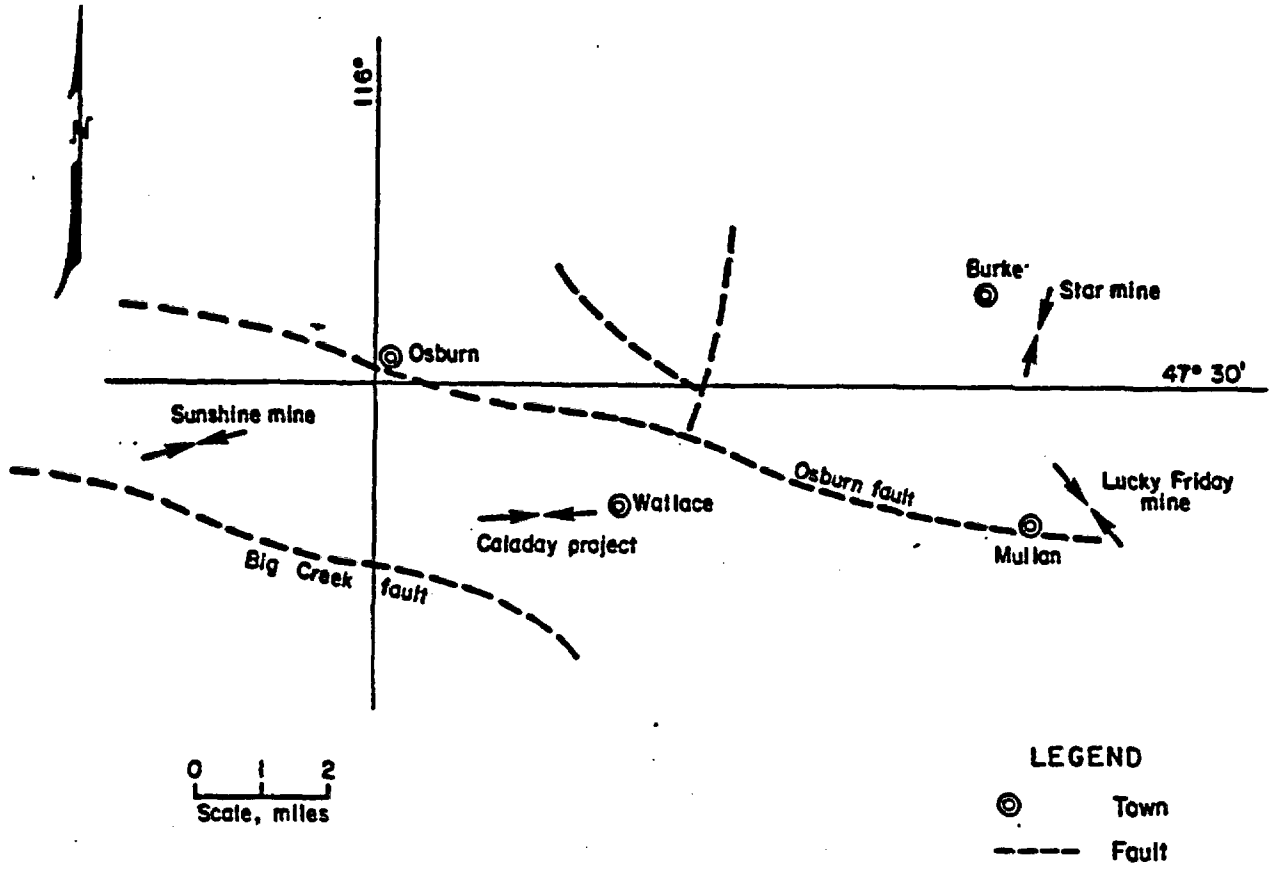

FIGURE 11. - Direction of maximum horizontal compressive force determined at the four test sites in the Coeur d'Alene mining district.

during Precambrian time, a strong, horizontal, compressive force occurred in the generally northeast-southwest direction, forming a series of anticlines, synclines, and some faults with their axes parallel to each other as shown in figure 12A. In the second stage, the regional ground force was reoriented to a somewhat east-west direction, the Osburn fault and its branches were formed, and the existing folds and faults were offset as shown in figure 12B. The third state consisted of Cretaceous igneous intrusions, mineralization, and the formation of veins that added to the complexity of the structural pattern of the district.

Comparing figure 11 carefully with figure 12, some similarities may be observed. First, the direction of maximum horizontal forces occurring near the Osburn fault generally alines with the direction of the ground force at the second stage shown in figure 12B. Second, the ground stress direction determined in the Star mine, which is a further distance from the Osburn fault, is also roughly parallel to the direction of the ground force of the first stage of tectonic development in the district. In general, the in situ stress measurements carried out in the present investigation agree with field evidence found by structural mapping of previous investigators (18), and the data correlate reasonably well with the regional tectonic activity, past and

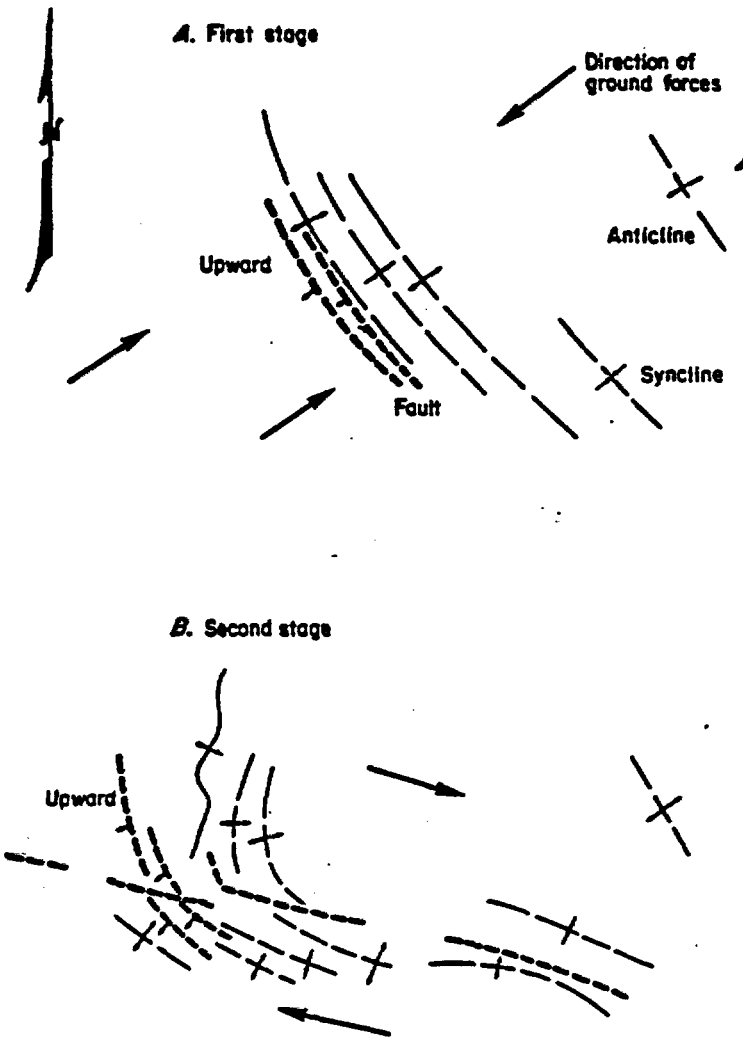

FIGURE 12. - Assumed stages in the development of the tectonic setting of the Coeur d'Alene mining district.

present, although minor local modifications are expected from the effects of mining.

Summary of Previous and Current Investigations

Table 5 summarizes, to the authors' knowledge, all of the three-dimensional, in situ stress data available for the Coeur d'Alene mining district from 1967 to 1977. Table 5 indicates that most of the major principal stresses plunge gently in a near-horizontal attitude. Table 6 lists the principal stress ratios with respect to depths. It shows that the ratios of major principal stress to minor principal stress range from 3.18 at the Sunshine mine to 1.25 at the Crescent mine, averaging 2.37. This indicates that nonhydrostatic conditions prevail, and tectonic influence is likely. The stress ratio, however, does not seem to increase with depth.

The in situ stress information was further resolved for vertical and horizontal stresses, which are listed in table 7 in the order of increasing depth of overburden. The data are also plotted as linear curves in figures 13 and 14 to show the stress-depth relationship.

Table 7 reveals that the horizontal stress in the district is generally greater than vertical stress beyond intermediate depths and is nearly the same or slightly lower than vertical stress at shallow depth. The average ratio of σ_{H_1}/σ_V is 1.54 with a mixiumum of 2.37 in the Galena mine and a minimum of 0.88 in the Caladay shaft station. The ratio of maximum to minimum horizontal stress, $\sigma_{H_1}/\sigma_{H_2}$, ranges from 1.25 in the Cresent mine to 2.73 in in the Silver Summit mine, averaging 1.66 among the seven mines. The ratio between horizontal stresses is most useful for establishing shaft design, particularly the optimum shape.

TABLE 5. - Principal stresses determined in the Coeur d'Alene mining district, 1967-77

Test site	Major			Intermediate			Minor			Investigation
	Magnitude, lb/in^2	Bearing	Plunge	Magnitude, lb/in^2	Bearing	Plunge	Magnitude, lb/in^2	Bearing	Plunge	
3400 level, Galena mine.	13,000	N 45° W	0°	11,010	S 45° W	-30°	7,000	N 45° E	-30°	Ageton, 1967.
3300 level, Crescent mine.	7,380	N 27° W	-2°	6,550	N 63.6° E	16.5°	6,250	N 56.1° E	73.4°	Skinner, Waddell, Conway, 1969.
4000 level, Silver Summit mine.	15,240	N 24.7° E	14.9°	8,220	N 5.2° W	-73°	5,440	N 67.5° W	8.1°	Chan, 1970.
4800 level, Sunshine mine.	5,310	N 41.1° E	16.9°	4,350	N 67.8° W	22.5°	1.670	S 0° E	63.3°	Beus and Chan, 1973.
7300 level, Star mine.	11,030	N 12° E	28°	7,434	N 84° W	33°	6,130	N 54° E	45°	Chan and Beus, 1975.
Shaft station, Caladay project.	1,860	S 80° E	54°	960	S 44° W	20°	700	N 31° W	29°	Chan and Beus, 1976.
4250 level, Lucky Friday mine.	10,770	N 37° W	-37.6°	6,790	N 56° E	-3.2°	3,470	S 20° E	-61.4°	Allen, Chan, Beus, 1977.

TABLE 6. - Principal stress ratio determined in the Coeur d'Alene mining district

Mine	Principal stress ratio (σ_1/σ_2)	Depth of test site, ft
Sunshine	3.18	4,800
Lucky Friday	3.11	4,250
Silver Summit	2.80	5,500
Caladay	2.65	1,220
Galena	1.85	4,000
Star	1.78	7,340
Crescent	1.25	5,300

TABLE 7. - Vertical and horizontal stresses, Coeur d'Alene mining district

Test site	Overburden, ft	Vertical stress (σ_V), lb/in^2	Maximum horizontal stress (σ_{H_1}), lb/in^2	Minimum horizontal stress (σ_{H_2}), lb/in^2	Ratio of σ_{H_1} to σ_V	Ratio of σ_{H_1} to σ_{H_2}
Shaft station, Caladay project	1,220	1,450	1,280	820	0.88	1.56
3400 level, Galena mine	4,000	5,500	13,000	9,540	2.37	1.36
4250 level, Lucky Friday mine	4,250	4,770	9,520	6,730	2.00	1.42
4800 level, Sunshine mine	4,800	7,420	7,220	4,000	.97	1.81
3300 level, Crescent mine	5,300	6,300	7,830	6,280	1.24	1.25
4000 level, Silver Summit mine	5,500	7,870	14,720	5,390	1.87	2.73
7300 level, Star mine	7,340	7,280	10,430	6,880	1.43	1.52

Both vertical stress and maximum horizontal stress tend to increase with depth in the district. There are unavoidably some local variations caused by the local geological conditions, mining activities, and inherent errors of the measurements. Figure 13 illustrates a linear relation between the vertical stresses and the overburden depths in the district. Since different methods and various investigators were involved, three curves were plotted according to the methods used. Least-squares regression analysis was employed assuming a linear relation. Curve A shows a stress-depth relation of $\sigma_V = 435 + 0.952h$, where σ_V is the vertical stress, in pounds per square inch, and h is the depth of overburden, in feet. This curve is based on the CSIR biaxial strain-cell data obtained from this investigation. Curve B, $\sigma_V = 928 + 1.052h$, is based on data from all seven mines using various in situ measurement methods. Curve C, $\sigma_V = 1{,}104 + 1.157h$, was plotted using data other than those obtained with the CSIR method. Both the slope of the curves and their extrapolated values at ground surface of the three curves are comparable. This may

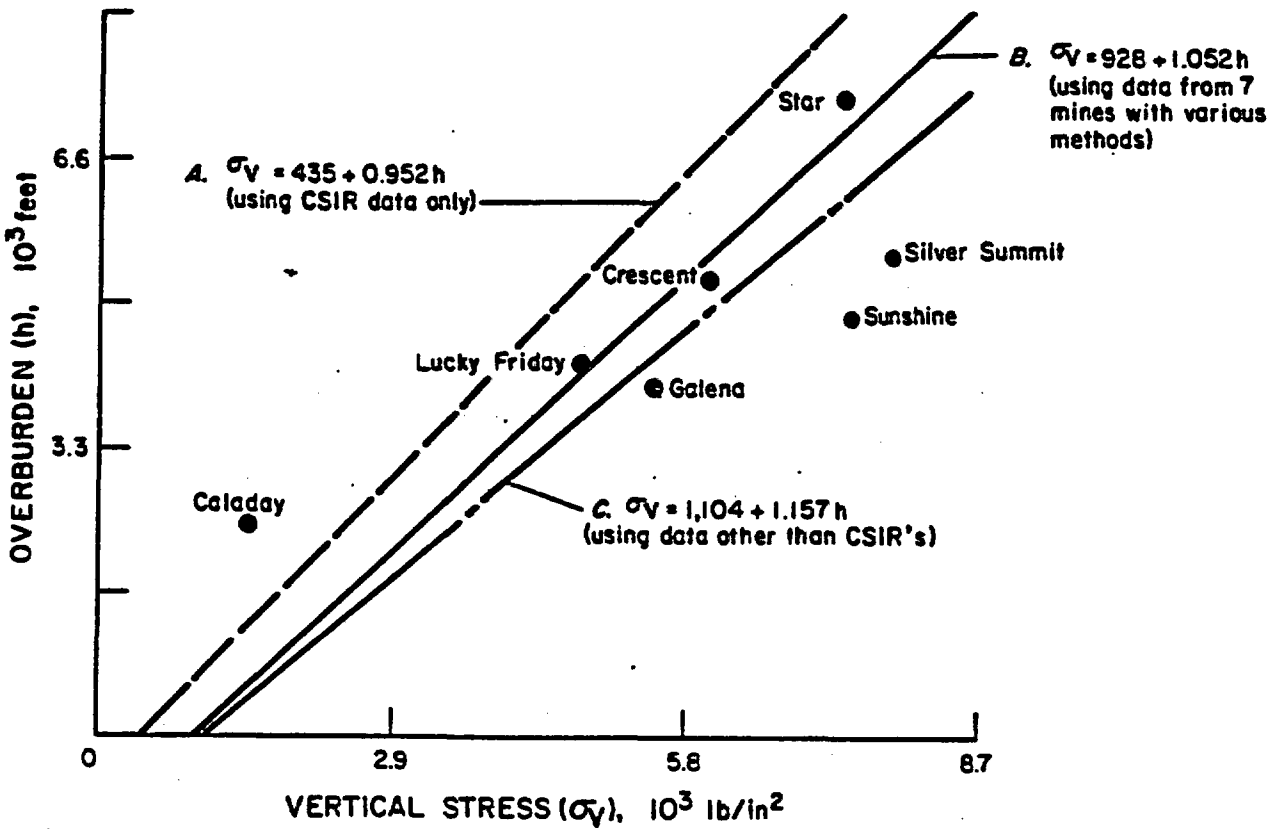

FIGURE 13. - Relations between vertical stress and overburden depth in the selected mines of the Coeur d'Alene mining district.

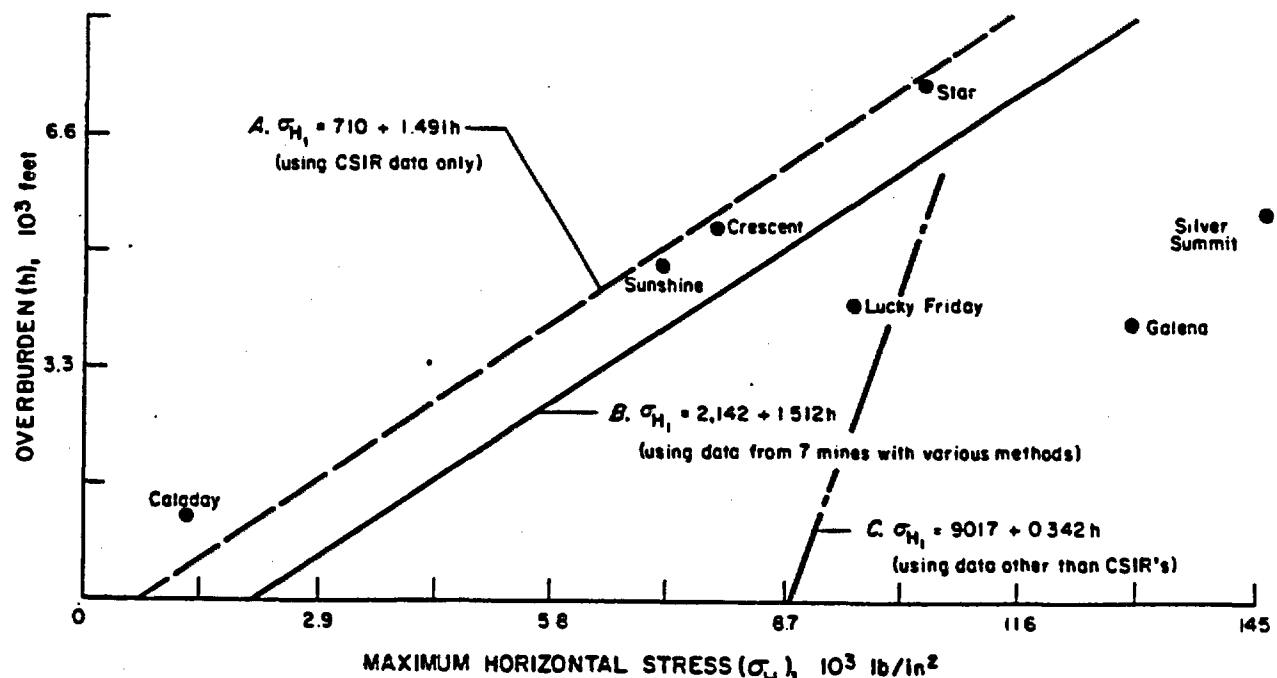

FIGURE 14. - Increase of horizontal stress with depth in the Coeur d'Alene mining district.

indicate a measure of the relative reliability among the methods used. Curve A has a minimum stress value at zero depth below ground surface, indicating that the results obtained from the CSIR biaxial strain cells might be more reliable. In the same manner, figure 14 shows the increase of horizontal stress as depth increases in the Coeur d'Alene district. Curve A, $\sigma_{H_1} = 710 + 1.491h$, deviates from curve B, $\sigma_{H_1} = 2{,}142 + 1.512h$, mainly in the initial stress value at zero depth. The maximum horizontal stress, σ_{H_1}, in curve C, $\sigma_{H_1} = 9{,}017 + 0.342h$, is greatly different from that of the others. This is mainly due to the high values of the maximum horizontal stresses that exist in the Galena and Silver Summit mines. The high value of the computed horizontal stress near surface is an indication of either experimental errors, an excessive amount of lateral tectonic force that exists in the area, or a combination of these factors.

Application of the In Situ Stress Data to Shaft Design

The main approach to shaft design in this project is the use of the finite-element method (FEM) to analyze the stability of the rock structure around shafts. The in situ stress data determined from the field operations are used as applied loads to the boundaries of the FEM models, together with the physical properties of the rocks, forming the major input parameters for the structural analyses. Following are the primary applications of the data to FEM analysis:

1. Vertical and maximum and minimum horizontal stresses determined from individual test sites are applied directly to the boundaries of a three-dimensional FEM model as applied loads.

2. Maximum and minimum horizontal stresses determined from individual test sites are applied directly to the boundaries of two-dimensional FEM models as applied loads.

3. Shear and normal stresses are applied as loads to the boundaries of the models, if necessary.

4. Curve A or B of figure 14 may be used as working curves to obtain maximum horizontal stress at the desired depth of overburden where stress levels are unknown and/or measurement is not practical. The minimum horizontal stress may then be computed using the appropriate stress ratio, $\sigma_{H_1}/\sigma_{H_2}$.

5. The maximum horizontal-to-vertical stress ratio, σ_H/σ_{V_1}, in table 7 can be used as a guide to compute the maximum horizontal stress from the theoretically calculated vertical stress based on gravity load only; then the minimum horizontal stress based on the stress ratios, $\sigma_{H_1}/\sigma_{H_2}$, listed in table 7 can be computed.

PHYSICAL PROPERTIES OF ROCKS IN THE DISTRICT

Physical properties, especially the strength and elastic parameters of rocks, were required as input to the finite-element models for structural analysis. There are four major methods for determining physical properties of rocks and rock masses.

1. Geophysical methods to determine dynamic and static rock properties; that is, electrical resistivity and seismic techniques.

2. Large-scale in situ testing such as pressure chamber and radial jacking tests.

3. Small-scale in situ borehole testing such as uniaxial borehole jack and borehole dilatometer tests.

4. Laboratory testing of rock samples with various standardized techniques.

Because of time and budget limitations, only the last two methods were employed for this investigation.

Determination of In Situ Modulus of Deformation

The in situ moduli of deformation of some Revett and St. Regis quartzites were determined in the Caladay, Sunshine, and Star mines by the use of

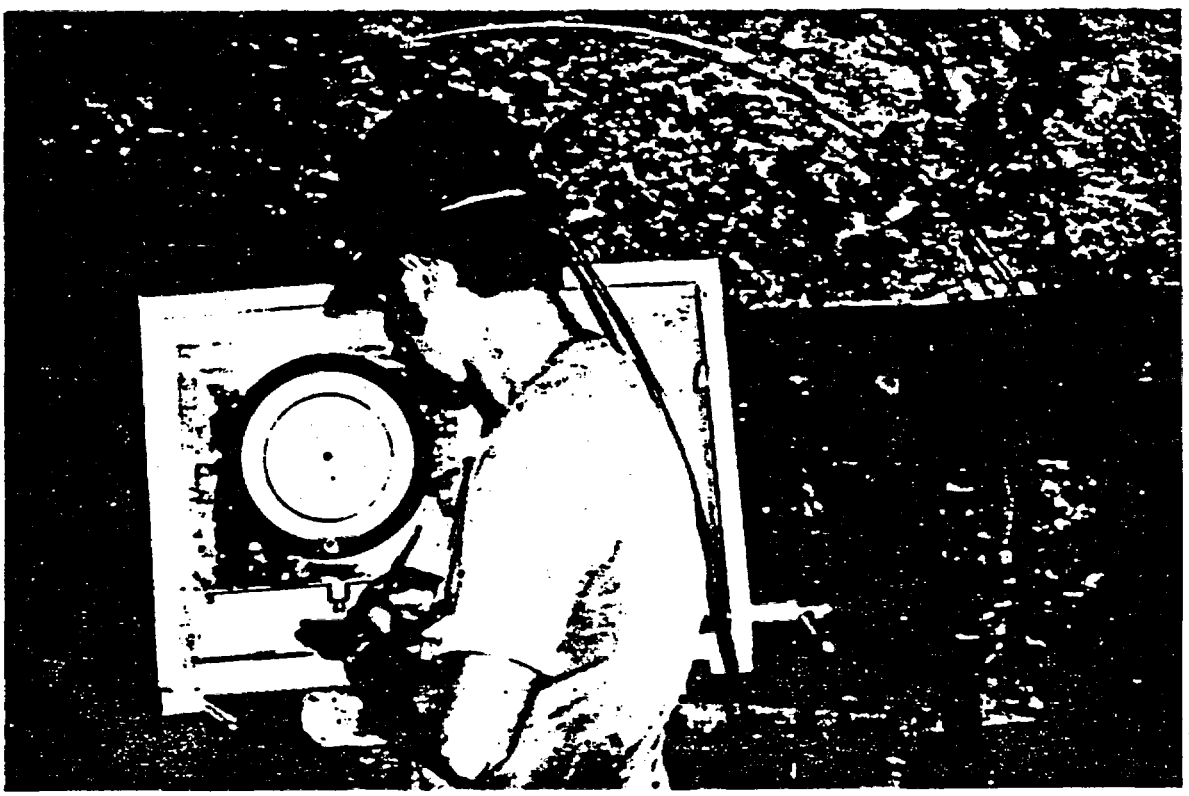

FIGURE 15. - The Colorado School of Mines borehole dilatometer.

CMS borehole dilatometer during the same periods of the in situ stress measurement for this investigation.

The four basic components of the CSM dilatometer system (23, 38) are the polymeric cells that fits EX hole size, a waterbase fluid, a hydraulic pressure generator, and a Bourdon pressure gage (fig. 15). The polymeric cell is made of an adiprene-moca mixture, a plastic selected for its flexibility and ease of fabrication. A screw-type, hydraulic-pressure generator is hand-cranked to displace a specific amount of fluid. The volume change is recorded as the number of turns of the pump handle. Modulus of deformation is obtained by mathematically comparing the pressure-volume relationship of a material of known physical properties with that of the rock mass. The basic assumption is that the calibration material, expanded by an internal radial force under similar conditions to the rock mass, will respond in an analogous fashion. The shear modulus is first computed. With a known or assumed Poisson's ratio, the modulus of deformation is finally calculated (23, 38).

Field operations were conducted at the in situ stress measurement sites of the Caladay, Sunshine, and Star mines. Three EX holes, each approximately 20 feet deep, were drilled in three different directions so that the axis of each hole was parallel, perpendicular, or at 45° to the bedding. The drill cores were carefully logged to inspect the general condition of the rock mass. A Lennox stratascope with a panoramic view window was used to observe and log the fracture conditions in the walls of the hole. This observation was necessary because open fractures in the borehole would cause the cell membrane of the CSM dilatometer to rupture. The cell had to be placed within competent rock sections to obtain successful test. After the cell was properly placed at a certain depth of the borehole, it would be loaded or expanded in steps until the maximum pressure capacity was reached; meanwhile, the number of pump turns (that is, the volume of fluid change) would be recorded. Unloading or contraction was then begun and recorded. The expansion yielded the compression modulus which was utilized as the modulus of deformation.

The results of the CSM dilatometer tests in the three mines are summarized and listed in table 8. These data indicate that there are directional variations of modulus of deformation of the rock mass. The results of the CSM dilatometer tests are comparable with those that were determined in the laboratory and are considered more realistic than those obtained by NX uniaxial jacking tests (5, pp. 57-67). The one major disadvantage of this technique is its incapability to include major discontinuities in the rock volume being tested.

Rock Strength and Elastic Parameters From Laboratory Testing

BX- and NX-size diamond drill cores were tested for their compressive, tensile, and shear strengths, moduli of elasticity, and Poisson's ratios in the laboratory according to ASTM recommended standard procedures. The results of these tests are listed in tables 9 through 13.

TABLE 8. - In situ Modulus of deformation of quartzite

Mine	EX hole No.	Number of tests	Angle to bedding	Rock type	Poisson's ratio	Mean modulus of deformation, E x 10^6 lb/in^2	Standard deviation	Calibration material
Sunshine	E1	3	90°	Revett-St. Regis quartzite.	0.25	10.00	1.42	Aluminum.
	E2	3	0°	....do.....	.25	9.90	1.19	Do.
	E3	6	Vertical	....do.....	.25	6.33	2.76	Do.
Star....	E1	3	90°	St. Regis..	.25	7.01	2.67	Aluminum.
	E2	3	0°	....do.....	.25	11.11	2.70	Do.
	E3	12	45°	....do.....	.25	9.78	3.57	Do.
Caladay.	E1	3	90°	St. Regis quartzite.	.25	7.01	2.67	Titanium.
	E2	2	45°	....do.....	.25	2.60	.71	Do.
	E3	10	0°	....do.....	.25	9.60	2.18	Do.

Table 9 lists the overall average unconfined compressive strength of the quartzite samples taken from the four test sites. The strength of the rocks ranges from a low outlier of 12,608 lb/in^2 in the Sunshine mine to as high as 44,916 lb/in^2 in the Lucky Friday rocks. Difference in mineral contents from sample to sample, especially the amount of argillaceous materials, and existence of microfractures, fractures, beddings, and other planes of weakness are the major causes of the wide variation in the rock strength.

TABLE 9. - Unconfined compressive strength of quartzite

Mine	Number of samples	Mean value, lb/in^2	Standard deviation, lb/in^2	95 percent confidence interval, lb/in^2	Coefficient of variation
Caladay.....	30	18,275	4,993	16,411 to 26,139	27
Lucky Friday	6	44,916	5,530	39,392 to 50,440	12
Sunshine....	31	23,036	3,513	21,748 to 24,325	15
Star.....	13	20,613	1,237	20,140 to 21,086	6

Table 10 lists the results of the flexural, direct, and indirect Brazilian tensile tests. The tensile strengths of the rocks from the four test sites, again, vary widely, ranging from 1,710 lb/in^2 in the Lucky Friday rocks to 7,252 lb/in^2 (flexural) in the Sunshine samples. The wide spectrum in tensile values was expected because different testing methods were involved. Judging from the coefficients of variation, the indirect tensile tests produced the most reliable data.

Table 11 shows the mean values of the unconfined, tangent modulus of elasticity of quartzite samples taken from the four test sites. Although there were variations when comparing from sample to sample, the mean values differ very little from each other. There is only a 23-percent deviation from the minimum value of 8.10 x 10^6 lb/in^2 in the Lucky Friday rocks to the maximum value of 10.4 x 10^6 lb/in^2 in the Sunshine mine samples. There is also very little difference between these laboratory-determined values and those determined in situ with the CSM dilatometer (table 8).

PHYSICAL PROPERTIES OF ROCKS IN THE DISTRICT

Physical properties, especially the strength and elastic parameters of rocks, were required as input to the finite-element models for structural analysis. There are four major methods for determining physical properties of rocks and rock masses.

1. Geophysical methods to determine dynamic and static rock properties; that is, electrical resistivity and seismic techniques.

2. Large-scale in situ testing such as pressure chamber and radial jacking tests.

3. Small-scale in situ borehole testing such as uniaxial borehole jack and borehole dilatometer tests.

4. Laboratory testing of rock samples with various standardized techniques.

Because of time and budget limitations, only the last two methods were employed for this investigation.

Determination of In Situ Modulus of Deformation

The in situ moduli of deformation of some Revett and St. Regis quartzites were determined in the Caladay, Sunshine, and Star mines by the use of

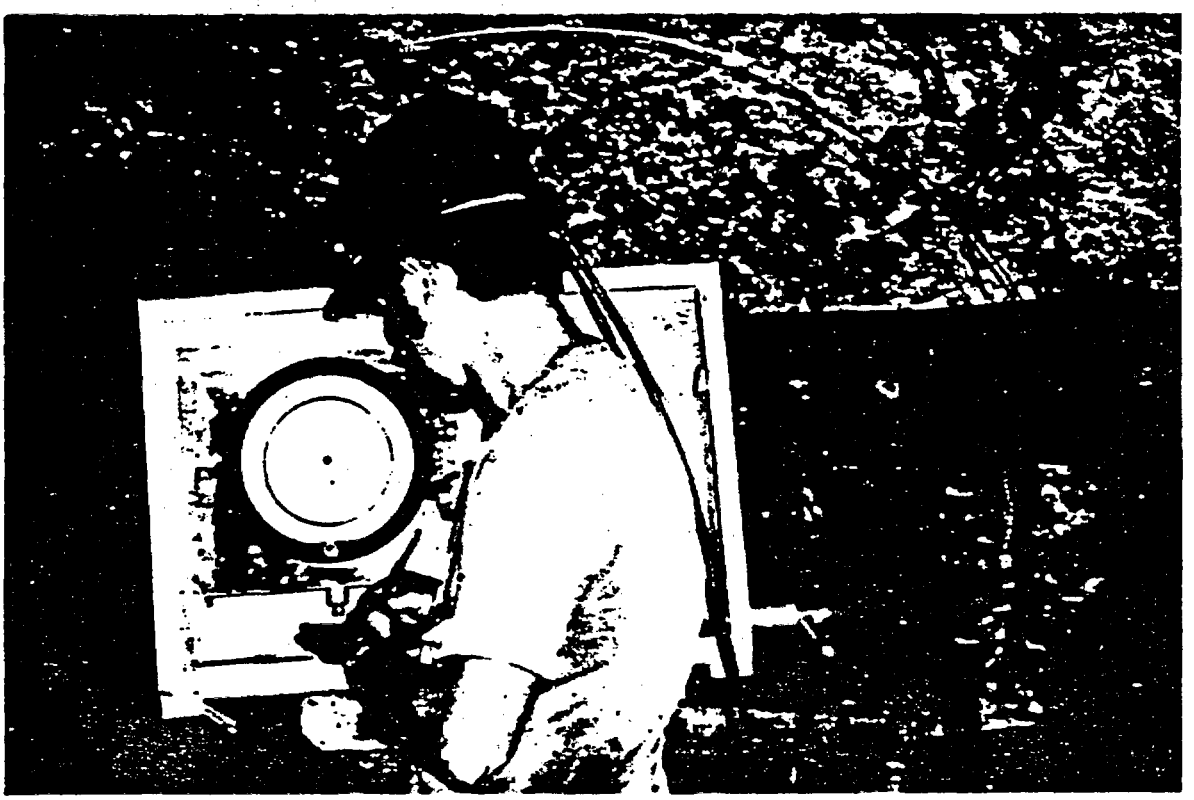

FIGURE 15. - The Colorado School of Mines borehole dilatometer.

TABLE 10. - Tensile strength of quartzite

Mine	Number of samples	Mean value, lb/in^2	Standard deviation, lb/in^2	95 percent confidence interval, lb/in^2	Coefficient of variation
Caladay.....	11 (direct)	1,754	353	1,517 to 1,991	20
	7 (indirect)	2,220	292	1,950 to 2,490	13
Lucky Friday..	41 (indirect)	1,710	446	1,573 to 1,847	26
Sunshine.....	20 (difect)	2,619	690	2,295 to 2,942	26
	14 (flexural)	7,252	1,772	6,228 to 8,275	24
Star.....	11 (indirect)	3,496	321	3,305 to 3,687	9

TABLE 11. - Modulus of elasticity of quartzite (unconfined, tangent)

Mine	Number of samples	Mean value, 10^6 lb/in^2	Standard deviation, lb/in^2	95 percent confidence interval, 10^6 lb/in^2	Coefficient of variation
Caladay.....	11	9.57	0.284	9.36 to 9.80	3
Lucky Friday....	13	8.10	.750	7.65 to 8.50	9
Sunshine.....	16	10.54	1.390	9.80 to 11.20	13
Star.....	14	9.26	1.482	8.49 to 10.04	16

Poisson's ratios of rock samples taken from all four test sites show uniform values—0.205 for the Caladay, 0.25 for Lucky Friday rocks, 0.260 for the Sunshine mine, and 0.290 for the Star mine samples (table 12).

TABLE 12. - Poisson's ratio of quartzite

Mine	Number of samples	Mean value	Standard deviation	95 percent confidence interval	Coefficient of variation
Caladay.....	11	0.205	0.048	0.172 to 0.237	24
Lucky Friday.....	9	.25	.070	.152 to .258	34
Sunshine.....	13	.260	.070	.222 to .306	27
Star.....	11	.290	.075	.245 to .335	26

The rocks from all four mines deformed very elastically under either uniaxial or triaxial loads. This was illustrated from the linear stress-strain curves shown in figures 16 and 17. Most of the competent rock samples burst violently at failure during the tests in the laboratory, indicating the brittle nature and the capacity for elastic strain energy storage in the rocks.

Table 13 lists all triaxial testing data for the Revett and St. Regis quartzites in three of the four mines. These data are used to find indirect shear strength of the mine rocks. Mohr envelopes plotted with these data are also used to determine failure according to Mohr-Coulomb criteria. Figure 18 shows the equation of a Mohr envelope using data from table 13 to obtain a linear fit of St. Regis quartzite from the Caladay project. A parabolic fit might also be appropriate to establish the Mohr envelope as shown in figure 19.

TABLE 13. - Triaxial testing data for quartzite

Confining stress, lb/in^2	Number of samples	Mean value of axial stress, lb/in^2	Standard deviation, lb/in^2	95 percent confidence interval, lb/in^2	Coefficient of variation
CALADAY PROJECT[1]					
500	7	23,919	6,936	17,504 to 30,333	29
1,000	6	29,224	6,762	22,127 to 36,322	23
1,500	7	34,263	4,531	30,073 to 38,454	13
3,000	7	41,995	5,977	36,468 to 47,523	14
6,000	6	48,606	6,293	42,000 to 55,211	13
SUNSHINE MINE[2]					
400	2	13,193	1,470	11,156 to 15,230	11
800	2	13,893	224	13,583 to 14,203	2
1,600	2	17,022	2,097	14,116 to 19,928	12
3,000	2	30,882	7,353	20,690 to 41,074	24
6,000	4	33,036	12,848	20,445 to 45,627	39
12,000	3	40,220	9,374	29,612 to 50,827	23
STAR MINE					
400	4	42,560	12,768	30,047 to 55,072	30
800	4	44,914	8,534	36,550 to 53,277	19
1,600	1	54,157	-	-	-
3,200	4	45,687	2,284	43,449 to 47,925	5

[1]Cohesion = 2,836 lb/in^2; internal friction angle = 52.2°.
[2]Cohesion = 3,300 lb/in^2; internal friction angle = 50°.

For comparison purposes, a table summarizing most of the previously determined main physical properties of mine rocks from the Coeur d'Alene mining district is included as an appendix. The data were obtained mainly from a research grant report (5) and several interim technical reports by the Bureau. These data correlated closely to the findings of the present investigation. The strength parameters have a wide range depending upon many factors, and the elastic parameters are relatively uniform. However, both Poisson's ratio and the modulus of elasticity may vary with change in confining conditions; normally, Poisson's ratio decreases and the modulus of elasticity increases when confining pressure increases (5, pp. 80-81).

Preliminary laboratory work on creep testing using a spring-loaded, rigid testing frame was done on two St. Regis quartzite samples from the Caladay test site for a period of about 5 months. The first sample was loaded parallel to the bedding at a value of roughly 75 percent of the unconfined compressive strength, and a creep rate of 0.115×10^{-5} in/hr was obtained. The second sample was loaded perpendicular to the bedding, and a creep rate of 0.175×10^{-5} in/hr was recorded. Previously, in situ creep rates of rock masses around a tunnel in the Silver Summit mine were calculated from closure data. The mean values from measurement of seven stations were averaged, and a creep rate of 4.08×10^{-5} in/hr in a direction approximately parallel to the direction of the in situ major principal stress at that test site was determined (5, pp. 34-35). This rate is 23 times greater than the maximum value

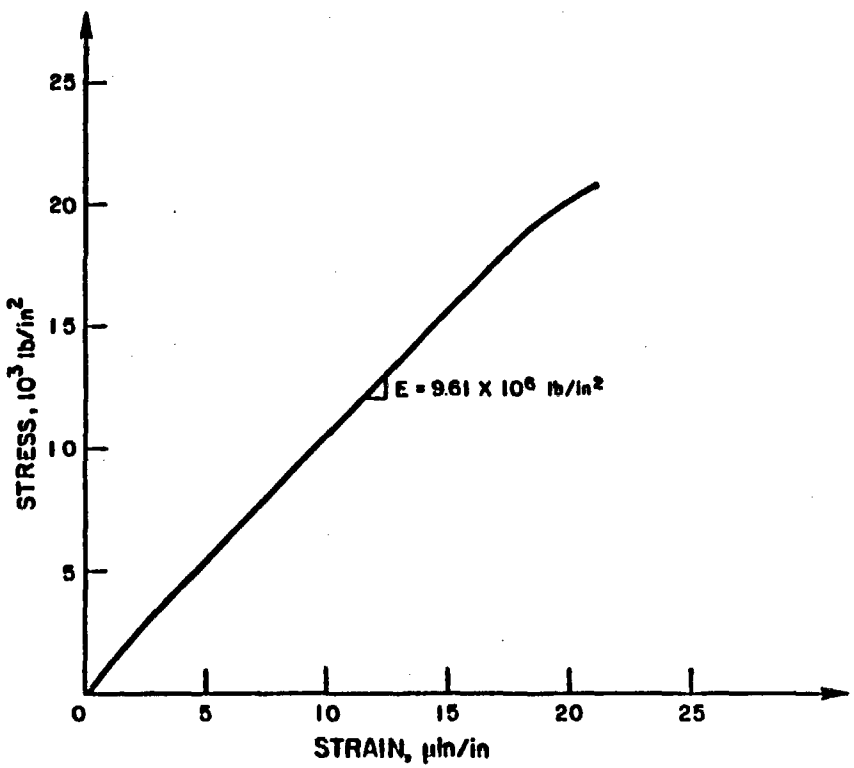

FIGURE 16. - Typical stress-strain curve, NXCU size, unconfined test, St. Regis quartzite, Caladay project.

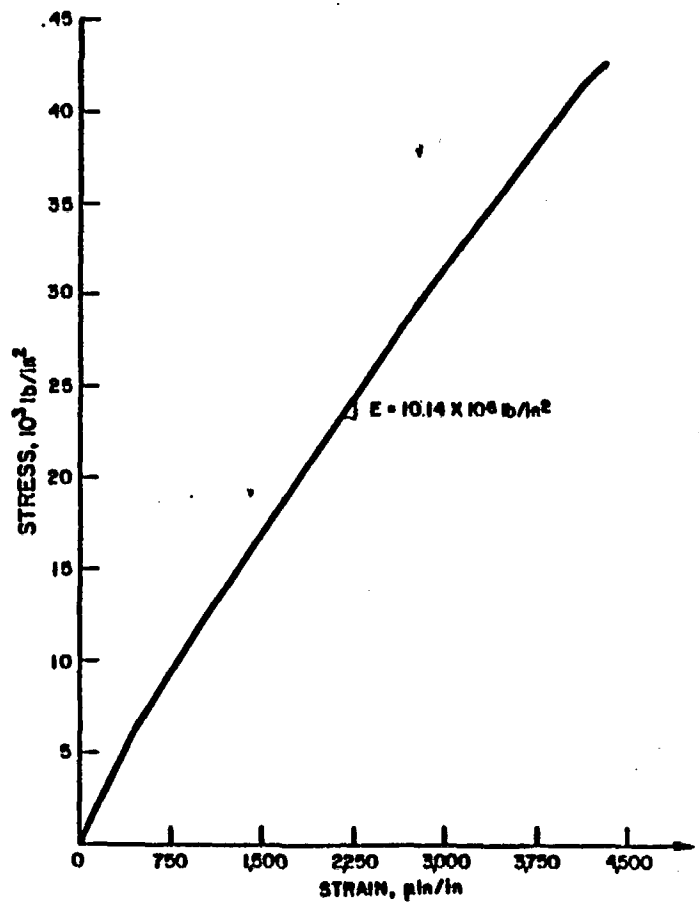

FIGURE 17. - Triaxial stress-strain curve, NXCU size, 3,000-lb/in^2 confining stress, St. Regis quartzite, Caladay project.

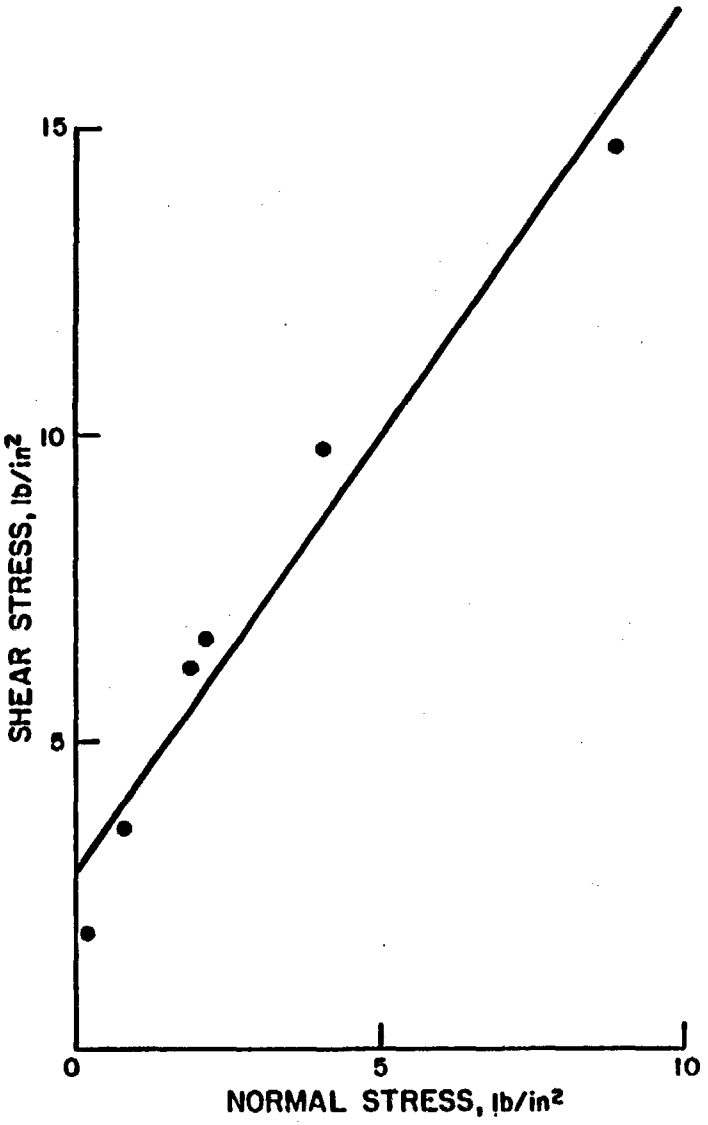

FIGURE 18. - Mohr envelope, linear fit, St. Regis quartzite, Caladay project. Equation for the curve is $\tau = 2{,}836 + \sigma \tan 52.2°$.

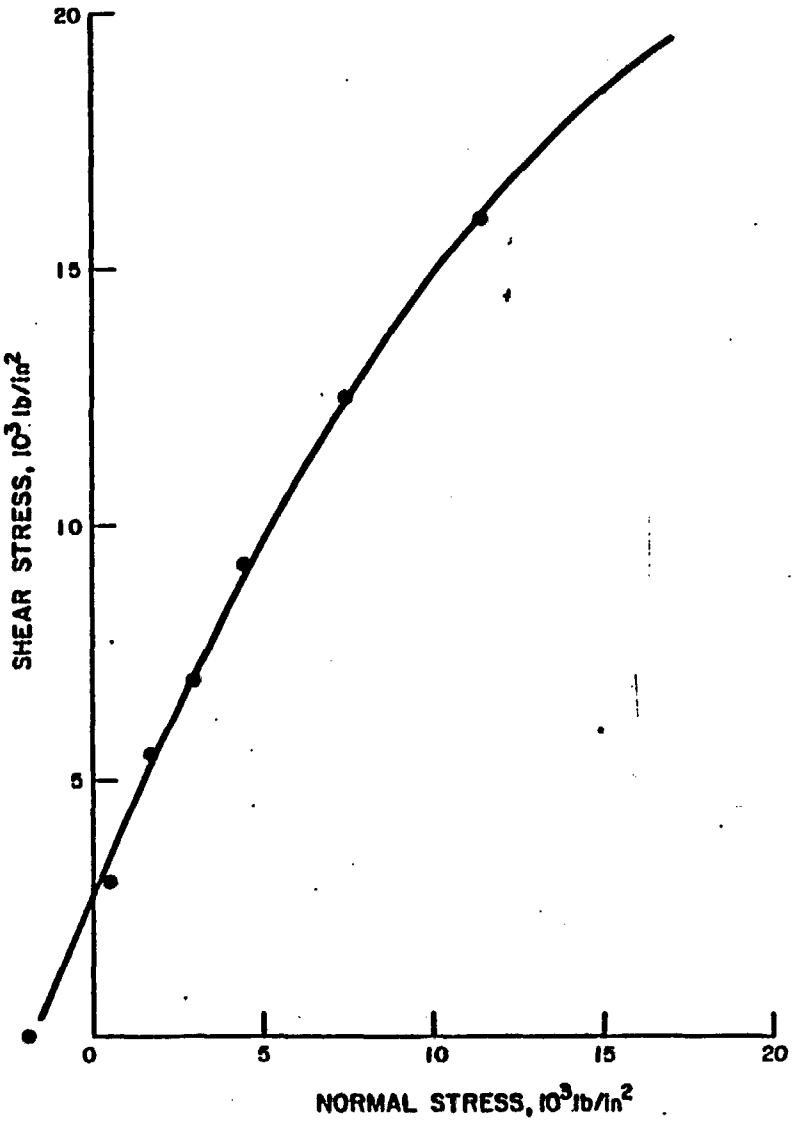

FIGURE 19. - Mohr envelope, tangent point, parabolic fit, St. Regis quartzite, Caladay project. Equation for the curve is $\tau = 2{,}813 + 1.519\,\sigma - (3.181 \times 10^{-5})\sigma^2$.

of the Caladay rock samples determined in the laboratory. A reasonable explanation is that there is more fracture expansion in the rock mass than in the small rock sample.

Once the creep rate is determined, the strain rate of the rock may be computed, and the coefficient of viscosity of the rock (that is, the ratio of the stress to the strain rate), may also be estimated. In the case of the Caladay rock, for example, the maximum creep rate is 1.43×10^{-5} in/hr and the strain rate is, therefore, 5.0×10^{-5} in/in/hr; if the load is in the order of 1×10^{3} lb/in^2 or 1×10^{4} lb/in^2, the coefficient of viscosity would be in the order of 1×10^{-2} or 1×10^{-1} lb-hr/in^2.

Summing up the findings of the physical properties of the mine rocks in the Coeur d'Alene mining district, it is obvious that (1) the rocks are hard, brittle, and deform elastically; (2) the strength of the rocks and rock masses are highly variable depending upon the mineral content, fracturing, and interlayering conditions; (3) the elastic parameters of the rocks are variable but are less influenced by the above-mentioned factors and conditions and are more easily affected by the degree of confinement; and (4) the rocks and rock masses in the district do creep but at small rates of deformation.

Application of Physical Properties of Rocks to Shaft Design

The physical properties of rocks determined for this investigation were used mainly as input data to the finite-element models for structural analysis. For models assuming elastic deformation only, Poisson's ratio and modulus of elasticity were used. For viscoelastic deformation, the coefficient of viscosity was also needed. In addition, the general shape of the creep curve was useful to determine whether the Maxwell or Kelvin creep model was appropriate. For plastic analysis, rock strength, cohesion, and internal friction angle are also required.

CONCLUSIONS

Based on the results of field measurement and laboratory testing, the following conclusions are made concerning the establishment of structural design guidelines for deep shafts in the Coeur d'Alene mining district of northern Idaho. Many of these conclusions may also be applied to deep, hard rock mines of other mining districts having similar geologic conditions.

1. In situ ground stress is one of the most important factors that affect shaft stability. Some field determination of the three-dimensional in situ stresses at shaft sites must be made to properly assess the magnitude and orientation of the stresses. For vertical shafts, the influence of the horizontal stress components is most significant.

2. In the Coeur d'Alene mining district where ground pressure is high and the rock is brittle, the CSIR biaxial strain-cell method has been found to be the most suitable method for obtaining three-dimensional in situ ground stress because the method requires a minimal volume of overcore.

3. The following equations, derived empirically from the in situ stress measurements in the district by means of the CSIR biaxial strain-cell method, may be used to estimate the vertical stress and the maximum horizontal stress at any point between depths of 1,200 and 7,500 feet.

$$\sigma_V = 435 + 0.952h \quad (1)$$

$$\sigma_H = 710 + 1.491h \quad (2)$$

where σ_V = the vertical stress, in lb/in^2

σ_H = the maximum horizontal stress, in lb/in^2

and h = the overburden depth above the test site, in feet.

4. The value of applied stress ratio affects to a certain extent the magnitude of stress concentration in the rock and supporting structures around shaft openings and, therefore, the stability of the shafts. The ratio of the maximum horizontal stress to the vertical stress in the district ranges from 0.88 near the shaft station of the Caladay project under 1,220 feet of overburden, to 2.37 in the 3400 level of the Galena mine under 4,000 feet of overburden. The ratio of the maximum horizontal stress to the minimum horizontal stress in the district ranges from 1.25 in the 3300 level of the Crescent mine under 5,300 feet of overburden, to 2.73 in the 4000 level of the Silver Summit mine with 5,500 feet of overburden above the test site. An exact hydrostatic pressure condition does not seem prevalent in the Coeur d'Alene mining district. In more than 70 percent of the test sites, the horizontal stress is higher than the vertical stress. This is attributed to residual and tectonic stresses.

5. The physical properties of rocks in the district vary widely. Since most of the physical property measurements were conducted in the laboratory using competent quartzite samples, the actual physical properties of the rock masses, especially the rock strength, would vary even more, considering the influence of interbedded argillite and complex geologic structures. Unfortunately, time and budget limitations restrict large-scale in situ physical property testing.

6. As indicated from the stress-strain curves of the rock samples that were tested, most of the quartzites from the district deform either entirely elastically or with a very short period of plastic deformation. Once plastic yielding occurs, the rock may be considered as entering a stage of instability.

7. Even though only a very limited amount of work has been done on rock creep in the district, evidence indicates that the quartzite in the district has minimal creep. Therefore, analysis of short-term elastic stability resulting from the initial elastic strain is more practical than a long-term viscoelastic analysis.

BIBLIOGRAPHY

1. Allen, M. D., S. S. M. Chan, and M. J. Beus. Correlation of In Situ Stress Measurement and Geologic Mapping in the Lucky Friday Mine, Mullan, Idaho. Proc. 16th Ann. Symp. Eng. Geol. and Soils Eng., Boise, Idaho, 1978, pp. 1-22.

2. Beus, M. J., and S. S. M. Chan. Preliminary Structural Design for Deep Shafts in the Coeur d'Alene District, Idaho. Pres. at Ann. Meeting, AIME, Las Vegas, Nev., Feb. 22-26, 1976, Preprint 76-AM-15, 24 pp.

3. Beus, M. J., E. L. Phillips, and G. G. Waddell. Instrument To Measure the Initial Deformation of Rock Around Underground Openings. BuMines RI 8275, 1978, 40 pp.

4. Bucky, P. B. Fundamental Considerations in Block Caving. Q. Colo. School of Mines, v. 51, No. 3, 1956, pp. 127-143.

5. Chan, S. S. M. A Case Study of In Situ Rock Deformation Behavior for the Design of Ground Support System. BuMines Open File Rept. 44-73, 1972, 130 pp.; available for reference at Bureau of Mines facilities in Pittsburgh, Pa., Denver, Colo., Spokane, Wash., and Twin Cities, Minn.; at the Central Library, U.S. Department of the Interior, Washington, D.C.; and from the National Technical Information Service, Springfield, Va., PB 221 880/AS.

6. Chan, S. S. M., and M. J. Beus. Ground Stress Determination in the Coeur d'Alene District Using the CSIR Technique. Proc. Pacific Northwest Metals and Miner. Conf., AIME, Coeur d'Alene, Idaho, 1976, pp. 1-16; available for reference at Bureau of Mines Library, Spokane, Wash.

7. _____. Interpretation of In Situ Deformational Behavior of a Rectangular Test Shaft Using Finite Element Method. Proc. Internat. Symp. on Field Measurement in Rock Mechanics (pub. as Field Measurements in Rock Mechanics, ed. by K. Kovari). A. S. Balkema, Rotterdam, v. 2, 1977, pp. 889-903.

8. Coates, D. F. Shafts, Drifts, and Tunnels. Ch. in Rock Mechanics Principles. Dept. of Energy, Mines and Resources, Ottawa, Canada, Mines Branch Monograph 874, 1970, pp. 3-1 to 3-42.

9. Coates, D. F., and Y. S. Yu. Three-Dimensional Stress Distributions Around a Cylindrical Hole and Anchor. Proc. 2d Cong. Internat. Soc. Rock Mechanics, Belgrade, v. 3, 1970, pp. 175-180.

10. Cornish, E. Vertical Shafts. Colo. School of Mines Miner. Ind. Bull., v. 10, No. 5, September 1967, 23 pp.

11. Dravo Corp. Analysis of Large-Scale Non-Coal Underground Mining Methods. BuMines Open File Rept. 36-74, 1974, pp. 176-268; available for reference at Bureau of Mines facilities at Pittsburgh, Pa., Denver, Colo., Twin Cities, Minn., and Spokane, Wash.; at the Central Library, U.S. Department of the Interior, Washington, D.C.; and from the National Technical Information Service, Springfield, Va.,PB 234 555/AS.

12. Durelli, A. J. Applied Stress Analysis. Prentice-Hall, Inc., Englewood Cliffs, N.J., 1967, 180 pp.

13. Duvall, W. I. General Principles of Underground Opening Design in Competent Rock. Proc. 17th U.S. Symp. on Rock Mechanics, Snowbird, Utah, Aug. 25-27, 1976 (pub. as Site Characterization, ed. by W. S. Brown, S. J. Green, and W. A. Hustrulid). University of Utah, Salt Lake City, Utah, 1976, pp. 3A1-1 to 3A1-11.

14. Ewing, R. D., and E. M. Raney. User's Guide for a Computer Program for Analytical Modeling of Rock Structure Interaction. Final Rept., BuMines Contract No. Ho262020, 1976, 95 pp.; available from the National Technical Information Service, Springfield, Va., AD 761648-AD 761650.

15. Galanka, J. Problems of Shaft Sinking in Poland. Proc. Symp. on Shaft Sinking and Tunneling, Inst. Min. Eng., London, 1960, pp. 369-380.

16. Gnirk, P. F., and R. E. Johnson. The Deformational Behavior of a Circular Mine Shaft Situated in a Viscoelastic Medium Under Hydrostatic Stress. Proc. 6th Symp. Rock Mechanics, Univ. Mo., Rolla, Mo., 1964, pp. 231-258.

17. Gooch, A. E., and J. P. Conway. Field Measurements and Corresponding Finite-Element Analysis of Closure During Shaft Sinking at the Lucky Friday Mine. BuMines RI 8193, 1976, 19 pp.

18. Gresseth, E. W. Determination of Principal Stress Directions Through an Analysis of Rock Joint and Fracture Orientations, Star Mine, Burke, Idaho. BuMines RI 6413, 1964, 41 pp.

19. Hast, N. The State of Stress in the Upper Part of the Earth's Crust. Eng. Geol., v. 2, No. 1, 1967, pp. 5-17.

20. Herget, G., A. Pahl, and P. Oliver. Ground Stresses Below 3,000 Feet. Proc. 10th Canadian Rock Mech. Symp., Queen's Univ., Kingston, Ontario, 1975, v. 1, pp. 281-307.

21. Hetinyi, M. Handbook of Experimental Stress Analysis. John Wiley & Sons, Inc., New York, 1966, pp. 407-415.

22. Hobbs, S. W., A. B. Griggs, R. E. Wallace, and A. B. Campbell. Geology of the Coeur d'Alene District, Shoshone Country, Idaho. U.S. Geol. Survey Prof. Paper 478, 1965, 139 pp.

23. Hustrulid, W. Development of a Borehole Device To Determine the Modulus of Rigidity of Coal Measure Rocks. BuMines Open File Rept. 12-72, 1971, 119 pp.; available for reference at Bureau of Mines facilities at Denver, Colo., Twin Cities, Minn.; Pittsburgh, Pa., and Spokane, Wash.; at the Central Library, U.S. Department of the Interior, Washington, D.C.; and from the National Technical Information Service, Springfield, Va., PB 209 548/AS.

24. Hynd, J. G. S., and E. Singer. Some Aspects of Circular Concrete-Lined Shaft Sinkings. Proc. Pac. Northwest Met. and Miner. Conf., AIME, Coeur d'Alene, Idaho, 1973, 22 pp.

25. Karwoski, W. J. Deep Shaft Design Parameters. Proc. Pac. Northwest Metals and Miner. Conf., AIME, Coeur d'Alene, Idaho, 1973, 30 pp.

26. Karwoski, W. J., and D. E. Van Dillen. Applications of Bureau of Mines Three-Dimensional Finite Element Computer Code to Large Mine Structural Problems. Proc. 19th U.S. Symp. Rock Mechanics, Univ. Nev., Stateline, Nev., 1978, v. 2, pp. 114-120.

27. Leeman, E. R. The "Doorstopper" and Triaxial Rock Stress Measuring Instrument Developed by the CSIR. J. S. African Inst. Min. and Met., v. 69, 1969, pp. 305-339.

28. _____. The Measurement of Stress in Rock. J. S. African Inst. Min. and Met., v. 65, 1967, pp. 45-144, 254-284.

29. Linder, E. N., and J. A. Halpern. In Situ Stress and Analysis. Proc. 18th U.S. Symp. Rock Mech., Colo. School of Mines, Keystone, Colo., 1977, pp. 4C1-1 to 4C1-7.

30. McWilliams, J. R., and E. G. Erickson. Methods and Costs of Shaft Sinking in the Coeur d'Alene District, Shoshone Country, Idaho. BuMines IC 7961, 1960, 49 pp.

31. Morrison, R. G. K. A Philosophy of Ground Control. Ontario Department of Mines, Toronto, Ontario, Canada, 1976, 182 pp.

32. Nichols, T. G., Jr., J. F. Abel, Jr., and F. T. Lee. A Solid-Inclusion Borehole Probe To Determine Three-Dimensional Stress Changes at a Point in a Rock Mass. U.S. Geol. Survey Bull. 1258-C, 1968, pp. C1-C28.

33. Obert, L., and W. I. Duvall. Rock Mechanics and the Design of Structures in Rock. John Wiley & Sons, Inc., New York, 1967, 360 pp.

34. Obert, L., W. I. Duvall, and R. H. Merrill. Design of Underground Openings in Competent Rock. BuMines Bull. 587, 1960, 36 pp.

35. Obert, L., and D. E. Stephenson. Stress Conditions Under Which Core Disking Occurs. Trans. Soc. Min. Eng., AIME, September 1965, pp. 227-234.

36. Ostrowski, W. J. S. Design Considerations for Modern Shaft Linings. Can. Min. and Met. Bull., October 1972, pp. 58-72.

37. Pariseau, W. G. Estimation of Support Load Requirements for Underground Mining Openings by Computer Simulation of the Mining Sequence. Pres. at Fall Meeting, Soc. Min. Eng., AIME, Salt Lake City, Utah, Sept. 10-12, 1975, SME Preprint 75-AM-358, 36 pp.

38. Patricio, J. G., and M. J. Beus. Determination of In Situ Modulus of Deformation in Hard Rock Mines of the Coeur d'Alene District, Idaho. Proc. 17th U.S. Symp. on Rock Mechanics, Univ. Utah, Salt Lake City, Utah, 1976, pp. 4B9-1 to 4B9-7.

39. Peck, R. B., and D. U. Deere. Shafts and Shaft Linings. Ch. in Some Design Considerations in the Selection of Underground Support Systems. A report by the Univ. Ill. for the Dept. of Transportation, 1969, pp. 78-105; available from the National Technical Information Service, Springfield, Va., PB190 443.

40. Procter and White. Rock Tunneling With Steel Supports. Commercial Shearing and Stamping Co., Youngstown- Ohio, 1946, 282 pp.

41. Raleigh, C. B. Crustal Stress and Global Tectonics. Proc. 3d Internat. Symp. Rock Mech., Nat. Acad. Sci., Denver, Colo., 1974, pp. 593-597.

42. Roberts, A. Geotechnology, An Introductory Test for Students and Engineers. Pergamon Press, Elmsford, N.Y., 1977, 347 pp.

43. Skinner, E. H., G. G. Waddell, and J. P. Conway. In Situ Determination of Rock Behavior by Overcore Stress Relief Method, Physical Property Measurements, and Initial Deformation Method. BuMines RI 7962, 1974, 86 pp.

44. Swaisgoof, J. R., and R. E. Versaw. Geotechnical Investigations for Mine Shafts. Proc. Pac. Northwest Metals and Miner. Cong., AIME, Coeur d'Alene, Idaho, 1973, 18 pp.

45. Timoshenko, S. P., and J. N. Goodier. Theory of Elasticity. McGraw-Hill Book Co., Inc., New York, 3d ed., 1970, pp. 68-71, 80-96.

46. Trollope, D. H. The Stability of Deep Circular Shafts in Hard Rock. Proc. 2d Cong. Internat. Soc. Rock Mech., Belgrade, v. 2, 1970, pp. 669-673.

47. U.S. Army Corps of Engineers. Engineering and Design—Tunnels and Shafts in Rock. Corps of Engineers Draft Man. EM 1110-2-2901, pt. 2, December 1973, 149 pp.

48. Vutukuri, V. S., R. D. Lama, and S. S. Saluja. Handbook on Mechanical Properties of Rocks—Testing Techniques and Results. Trans Tech Publications, Bay Village, Ohio, v. 1, 1974, 280 pp.

49. Waddell, G. G., T. S. Crocker, and E. H. Skinner. Technique of Measuring Initial Deformation Around an Opening--Analysis of Two Raise-Bore Tests. BuMines RI 7505, 1971, 60 pp.

50. Waddell, G. G., and E. L. Phillips (assigned to U.S. Department of the Interior). Stress Relaxation Gage. U.S. Pat. 3,600,938, Aug. 24, 1971.

51. Wilson, J. W. The Protection of Vertical Shafts in Deep Level, Hard-Rock Mines. Proc. 17th U.S. Symp. on Rock Mech., Univ. Utah, Snowbird, Utah, 1976, pp. 3A5-1 to 3A5-12.

52. Zahary, G., and K. Unrug. Reinforced Concrete as a Shaft Lining. Proceedings of the 8th Canadian Rock Mechanics Symposium. Department of Energy, Mines and Resources, Mines Branch, Ottawa, Canada, 1973, pp. 265-282.

APPENDIX.—PHYSICAL PROPERTIES OF COEUR d'ALENE MINE ROCKS FROM PREVIOUS INVESTIGATIONS

Parameter and mine	Rock type	Number of samples	Mean	Standard deviation	Investigator
Unconfined compressive strength, lb/in^2:					
Galena	Revett quartzite	20	32,500	3,700	Chan (5).
Do	Competent quartzite	6	42,020	5,390	Royea.
Do	Incompetent quartzite	23	28,820	10,280	-
Do	Revett quartzite	123	16,760	6,000	Ageton.
Silver Summit	St. Regis quartzite	8	24,750	9,273	Chan (5).
Crescent	Revett quartzite	85	26,851	10,288	Skinner (43).
Bunker Hill	Quartzite	4	23,625	2,020	Conway.
Star	do	13	26,000	8,500	Waddell.
Caladay	St. Regis quartzite	29	17,325	10,178	Smith.
Tensile strength, lb/in^2:					
Galena	Revett quartzite	81	2,400	855	Chan (5).
		50	1,600	720	Ageton.
Silver Summit	St. Regis quartzite	10	3,665	413	Chan (5).
Star	Quartzite	13	1,500	540	Waddell.
Modulus of elasticity, 10^6 lb/in^2:					
Galena	Revett quartzite	20	7.30	1.57	Chan (5).
Do	Quartzite	29	8.8	0.95	Royea.
Do	Revett quartzite	140	6.36	2.01	Ageton.
Silver Summit	St. Regis quartzite	16	6.57	2.65	Chan (5).
Crescent	Revett quartzite	84	7.10	1.50	Skinner (43).
Bunker Hill	Quartzite	4	7.43	0.94	Conway.
Star	do	13	8.5	1.1	Waddell.
Do	Revett quartzite	-	9.0	0.8	Ageton.
Poisson's ratio:					
Galena	Revett quartzite	20	0.27	0.002	Chan (5).
Silver Summit	St. Regis quartzite	8	0.15	0.071	Do.
Dynamic Poisson's ratio:					
Crescent	Revett quartzite	37	0.29	0.086	Skinner (43).
Density, g/cm^3:					
Galena	Revett quartzite	48	2.89	0.15	Chan (5).
Do	do	113	2.88	0.12	Ageton.
Crescent	do	36	2.69	0.018	Skinner (43).
Bunker Hill	Quartzite	4	2.70	0.002	Conway.
Star	do	13	2.68	0.020	Waddell.
Shore hardness:					
Crescent	Revett quartzite	58	81.5	11.3	Skinner (43).
Star	Quartzite	13	72.0	4.7	Waddell.
Triaxial compressive strength, lb/in^2:					
Galena	Revett quartzite	3	38,400	1,500	Chan (5).
		2	46,600	2,000	-
		1	60,900	4,000	-
Silver Summit	St. Regis argillaceous quartzite.	1	24,800	1,000	Do.
		1	25,900	1,000	-
		1	37,200	3,000	-
		1	47,000	4,000	-

☆U.S. GOVERNMENT PRINTING OFFICE: 1980-603-102/59

INT.-BU.OF MINES,PGH.,PA. 24521